Synthesis of Crescent Shaped Heterocyclic Urea-Linked Foldamers

James Mousseau

A Thesis

In

The Department

of

Chemistry and Biochemistry

Presented in Partial Fulfillment of the Requirements
for the Degree of Master of Science (Chemistry) at
Concordia University
Montreal, Quebec, Canada

December 2006

Your file Votre référence
ISBN: 978-0-494-28880-1
Our file Notre référence
ISBN: 978-0-494-28880-1

Abstract

Synthesis of Crescent Shaped Heterocyclic Urea-Linked Foldamers

James Mousseau

Foldamers are oligomers or polymers that have well-defined conformations in solution. The synthesis of tunable, heterocyclic, urea-linked foldamers is described. The curvatures of the foldamers can be altered by varying the heterocylic diazine (pyrazine, pyrimidine, pyridazine) or the non-heterocyclic (tolyl, *o*-xylyl, *m*-xylyl) aromatic units. Foldamers comprised of three to five aromatic groups were synthesized. Folding of these oligomers is driven by the restricted rotation along the urea bonds linking the aromatic units. This restricted rotation is caused by the additive effects of non-covalent interactions, particularly intramolecular hydrogen bonding between the urea hydrogen and the heterocyclic nitrogen atoms and steric interaction between the urea carbonyl and the toluene or xylene methyl groups. These foldamers were characterized using NMR, MALDI-TOF-MS, and FTIR. To the best of our knowledge, these are the first urea-based foldamers where curvature of the macromolecule can be easily controlled by varying either the heterocyclic or non-heterocyclic aromatic segments.

Acknowlegement

I would like to express my unending gratitude to my supervisor, Dr. Louis Cuccia for his guidance, support, encouragement, patience, and friendship for a fulfilling graduate study experience. I am thankful to Dr. Heidi Muchall and Dr. Sébastien Robidoux for agreeing to serve on my research committee and for their insightful comments. Many thanks are given to Liyan Xing, Nathalie Tang, Neenah Navasero, Angela Saverinuthu, Johnston Hoang, Elodie Siband, and Carolin Madwar for their scientific contribution which is the foundation of the work presented herein. I would like to further thank Dr. Robidoux, as well as Dr. Chris Wilds and Dr. Paul Xia, for their guidance with NMR; Dr. Ann English for giving me access to the MS facilities and to Alain Tessier for offering much help; and to Dr. Rolf Schmidt for assistance with the FTIR spectroscopy. The comments made by Dr. Schmidt and Marta Kocun have been invaluable in the preparation of this thesis. I would like to give my thanks to the former and current members of the Cuccia lab for their insight, patience, and most importantly, friendship: Liyan, Marta, Monica, Rolf, Chris, Aylin, Johnston, Carolin, Elodie, Sharon, Wendy, Anna, Daniel, Jacinthe, Joséphine, Jesse, and Natalie. I also acknowledge the assistance from my fellow graduates, the administration, and staff in this department. The assistance provided by Maria Ciaramella, Donna Gordon and Lisa Montesano is much appreciated. Last but not least, I thank my beautiful wife, family, and friends for their unconditional love, understanding, and support.

Dedicated to Melissa

Table of Contents

List of Figures

List of Schemes

List of abbreviations

bm: broad multiplet

CDI: *N,N'*-carbonyldiimidazole

DIEA: diisopropylethylamine

DMSO: dimethylsulfoxide

DNA: deoxyribonucleic acid

eq.: equivalence

FTIR: Fourier transform infrared spectroscopy

h: hour

HPLC: high performance liquid chromatography

KI: potassium iodide

MALDI-TOF: matrix assisted laser desorption ionization-time-of-flight

min.: minutes

mmol: millimole

mL: milliliter

m.p.: melting point

ms: millisecond

MS: mass spectrometry

MSTFA: *N*-Methyl-*N*-(trimethylsilyl)-trifluoroacetamide

NMR: nuclear magnetic resonance

NOE: nucleur overhauser effect

NOESY: nuclear overhauser effect spectroscopy

ppm: parts per million

psi: pounds per square inch

R_f: retention factor

r.t.: room temperature

TDI: tolylene-2,6-diisocyanate

TEA: triethylamine

THF: tetrahydrofuran

TLC: thin layer chromatography

tRNA: trasnfer ribonucleic acid

1. Introduction

1.1. Overview

Foldamers are a remarkable class of oligomeric compounds. They play a vital role in all aspects of life[1]. Foldamers play this role by catalyzing an incalculable number of reactions in our bodies every second. These molecules maintain the delicate balance of ion concentrations inside and outside cells[2], and encode vital information to allow life to proceed and progress[3]. Put quite simply, life as we know it would not exist without these macromolecules.

The term foldamer has been defined as any oligomer or polymer with a strong tendency to adopt a specific compact conformation in solution[4-6]. These conformations are stabilized by the additive effects of weak, non-covalent interactions[4,5]. The cooperativity of these interactions is widely observed in Nature[3,7] and is an inspiration for the design of artificial folding systems.

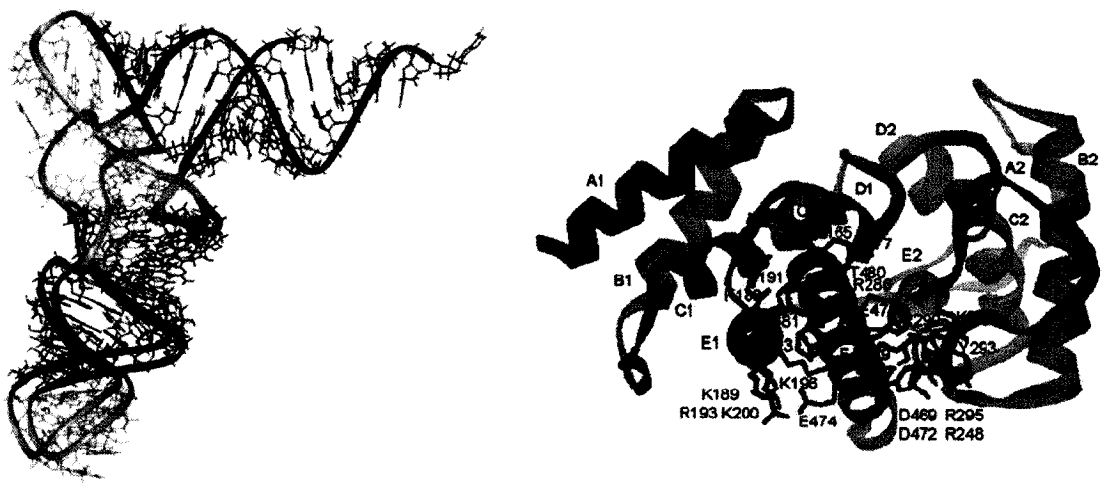

Figure 1-1 tRNA and simplex virion16 protein; examples of natural foldamers.

Examples of natural foldamers include RNA[8], where oligomeric ribonucleic acids adopt specific conformations required for their function (Figure 1-1). These conformations are stabilized by intramolecular hydrogen bonding, π-π stacking, steric interactions, and solvophobic effects[4]. These weak interactions provide enough enthalpy to overcome the loss of entropy resulting from the formation of stable, compact, relatively rigid structures. Perhaps the best examples of natural foldamers are proteins[5]. Again, there are a series of non-covalent interactions that allow proteins to fold into well defined structures. Proteins contain both α-helical and β-sheet domains that are compact structures held together by non-covalent interactions. In α-helical domains the peptide strand forms a right-handed helix that is stabilized by hydrogen bonding between the amide hydrogen and the carbonyl oxygen of an amino acid four residues earlier[7]. This gives a helix that is 5.4 Å wide with a translation of 1.5 Å per residue. The helix is further stabilized by a macroscopic dipole as all the dipoles of the residues are aligned in a head-to-tail fashion[9]. β-Sheets occur when two parallel amino acid strands form hydrogen bond interactions between the carbonyl oxygen and the amide hydrogen[7]. Like α-helices, β-sheets are also directional and can run either parallel or anti-parallel. They are also rarely extended and usually exhibit a slight twist due to the chirality of the amino acid side chains[7]. β-Sheets are more stable than α-helices due to the higher number of non-covalent interactions present (one hydrogen bond every residue *vs.* one every fourth residue). Well-defined secondary structures of proteins further interact non-covalently to form distinct tertiary and quaternary structures[10-13]. This is nicely shown in the herpes simplex virion protein 16 illustrated in Figure 1-1. This protein contains two strong activation regions that can either cooperatively or independently initiate transcription[10].

Interactions in natural foldamers are not limited to intramolecular interactions. The double helical conformation of DNA involves both intra- and intermolecular non-covalent interactions between two oligonucleotide strands[4]. Double helical strands are then packaged through inter-molecular interactions *via* binding with histones[3]. Histones spool DNA and form higher order chromatin strands that further complex into chromosomes. Folding is so efficient that two meters of DNA can be compacted into a single chromosome[3].

Nature's examples of foldamers can be quite complex and in most cases cannot be easily reproduced in the laboratory[4,14]. Even with the plethora of tools available to modern synthetic chemists, we cannot mimic the efficiency nor the complexity observed in Nature. As a result, there has been much interest in the last decade focused on preparing simple, abiotic foldamers[4,6]. Some of the challenges in preparing unnatural foldamers include: *i*) ease of synthesis, *ii*) folding stability, *iii*) tunability of shape, and *iv*) the ability to change folded conformations[14]. The first challenge is self explanatory as a general desire in organic chemistry is the facile synthesis of compounds in high yields. The second challenge, based on the definition of a foldamer, is evident; in order to study a foldamer it must remain in a relatively stable folded state. The third challenge may not be clear to one unfamiliar with foldamer chemistry. Tunability is the capacity to alter monomeric units in order to vary the shape of the foldamer. This has wide implications in that systems can be tailor made to study specific phenomena or create specific functionalities to mimic natural foldamers. The fourth challenge is perhaps the most interesting feature with regards to designing functional foldamers. Oligonucleotides and proteins are able to undergo changes in conformation in order to function properly[15,16].

This does not necessarily mean that their global folding is unstable, only that it is flexible. Therefore, in order to create functional foldamers, it is important to have reversible folding to allow changes in conformation[17]. Both tunability and flexibility are highlighted in Figure 1-2. The cartoon depicts an aromatic oligoamide molecular apple peel where the cavity size is tuned by varying the aromatic monomer units. These systems have also been shown to be able to unwind and reversibly encapsulate single water molecules[17].

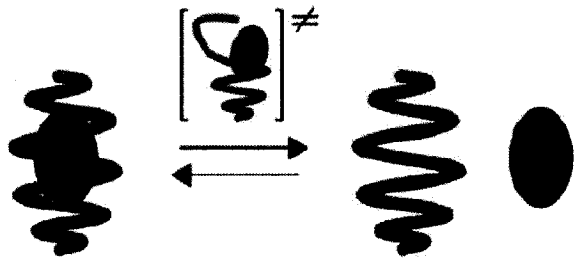

Figure 1-2 Example of a molecular apple peel. This foldamer exhibits tunability by varying the diameter of the helix. The folding is reversible allowing the encapsulation of small molecules. Figure reproduced with permission[17].

One of the goals of foldamer chemistry is to mimic Nature with simpler systems in order to eventually better understand Nature[4]. By better understanding Nature we can then in turn ameliorate our ability to mimic it[18,19]. This has a wide range of potential applications[20]. Natural peptides are known to make poor drugs due to their susceptibility to degradation in the gastrointestinal (GI) tract by proteosomes[20]. With synthetic foldamers it may be possible to prepare compounds that are more resistant to degradation while increasing the specificity to a desired target[20]. In addition, by preparing synthetic foldamers we can obtain novel compounds that may have unique properties useful for potential applications in materials science. Although foldamer research is still in its

infancy, complex molecules with interesting functions and properties have already been prepared[20].

Nature has a limited number of backbones at her disposal in preparing a vast number of diverse foldamers. However, synthetic chemists have available to them a wide range of backbones on which to scaffold their system designs[4]. With this in mind, one can easily assume that the number and complexity of foldamers that can be prepared synthetically should far exceed those found in Nature. Some of the more common backbones reported in the literature include those based on imine, amide, and urea linkages.

1.2. Classes of Foldamers

1.2.1. Solvophobic Effects

There are a variety of ways to induce folding in oligomers. Clearly the method chosen to induce folding will influence the molecular design. One such method to control the conformation of foldamers is by taking advantage of solvophobic effects as pioneered by Moore and co-workers[21-24]. Foldamer **1** (Figure 1-3) is a *meta* substituted phenylene ethynylene oligomer that folds as a result of interactions between the side chains and the solvent in which the oligomer is dissolved. The typical design involves using relatively polar side chains connected to the phenyl ring. When the oligomer is dissolved in a polar solvent, such as acetonitrile, it folds to maximize interactions between the polar side chains and the solvent[21]. This simultaneously creates a non-polar cavity that minimizes the unfavourable interactions of the non-polar phenyl backbone and the polar solvent.

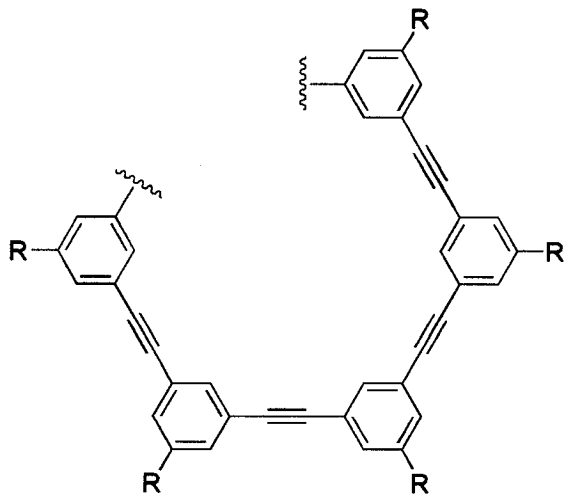

1

Figure 1-3 Phenylene ethynylene foldamer.

Another group to take advantage of solvophobic effects for folding is led by Brent Iverson. Folding in his system is induced by interactions between electron poor 1,4,5,8-naphthalenetetracarboxylic diimide (**2**) and electron rich dialkoxynaphthalene (**3**) groups (Figure 1-4)[25-27]. These aromatic groups are tethered together by flexible linkers containing pendant carboxylic acid groups. Folding is promoted when the system is dissolved in aqueous solutions. The donor and acceptor groups stack on top of each other as a result of favourable aromatic stacking, again minimizing interactions between the non-polar aromatic groups and the polar solvent, while maximizing solvent interactions with the polar side chains, in this case the carboxylic acid groups of the linker[26].

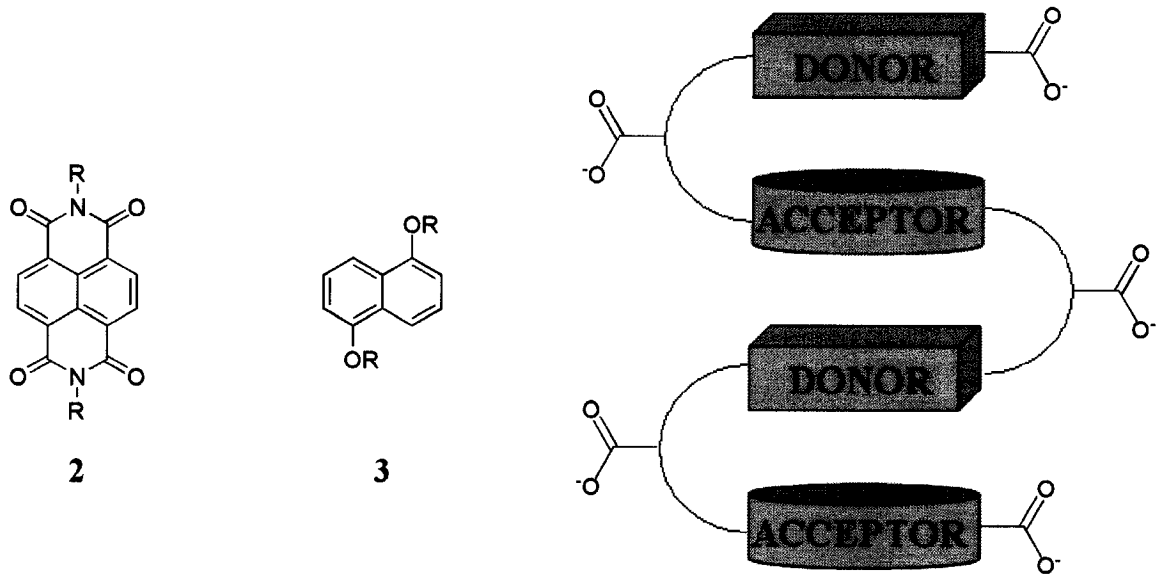

Figure 1-4 Iverson's 1,5-dialkoxynaphthalene (**2**) and 1,4,5,8-napthlenetetracarboxylic dimidine (**3**) based foldamer.

1.2.2. Unnatural Peptides

Other examples of well defined folding interactions have been demonstrated using unnatural peptides. Over the past few years there has been growing interest in preparing unnatural oligomers with increased *in vivo* stability that are similar to biopolymers[28]. Aside from their resistance to proteolytic degradation, both the β- and γ-peptide derivatives are of interest due to the fact that they form unusually stable helices for short chain lengths. This enables them to act as good scaffolds for the creation of biologically active molecules[29,30]. Some of the backbones that have been used include β-peptides, γ-peptides, peptoids and *N,N'*-linked oligoureas. An example of a foldamer constructed from β-petides is oligomer **4** in Figure 1-5 prepared by Gellman and co-workers[30]. β-Peptides containing as few as six amide residues can form stable 14-helices that are stabilized by two N-H··O=C hydrogen bonds. These helices contain three residues per

turn and have a pitch of 5 Å[30]. Similarly to α-peptides, β-peptides can adopt other secondary structures, including sheets and turns[31]. However, the folding of β-peptides into tertiary structures has been limited due to the difficulty in the synthesis of long chains by either solid or solution phase chemistry. Oligomer **5** in Figure 1-5 is a foldamer prepared by Guichard and co-workers that uses *N,N'*-linked oligoureas that are analogous to γ-peptides (*i.e.* two extra carbon atoms in the backbone) except that the $^{\alpha}C$ of the corresponding γ-peptide is replaced by a nitrogen atom. Similar to natural peptides, folding is induced by interactions between the carbonyl oxygen of the urea linkage and, in this example, the urea hydrogen two residues away[31,32,29] . These urea oligomers have been shown to adopt stable helical conformations at room temperature with 2.5 residues per helical turn, giving a 14-helix, that unfolds as the temperature is increased[29].

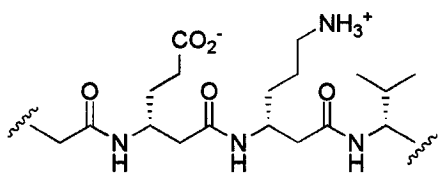

4

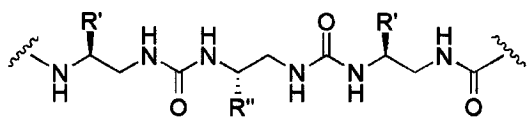

5

Figure 1-5 Examples of unnatural pepide-like foldamers. Oligomer **4** is a β-peptide and oligomer **5** is an example of an *N,N'*-linked oligourea.

1.2.3. Restricted Rotation

1.2.3.1. Overview

Our principle interest lies in foldamers where conformation is determined by restricted rotation. In these systems free rotation along a certain bond is limited due to non-covalent interactions. Although rotation is restricted in the earlier examples

described by Gellman and Guichard, the overall folding is due to long range interactions. Herein we will focus on short range interactions between adjacent monomeric units. An example of such a system is given in Figure 1-6. In this example, the oligo-pyridine/pyrimidine strand prepared by Lehn and co-workers is locked into a helical conformation despite the possibility of rotation around the single bonds linking the heterocyclic units (highlighted in green)[33]. The conformation is fixed due to several intra-molecular forces. The first of these interactions is the favourable antiparallel dipole-dipole arrangement between monomeric units in conformation **6a** (Figure 1-6). In this conformation, the dipoles are oriented in opposite directions, as indicated by the green arrows, giving an attractive force otherwise known as a negative potential[9]. On the other hand, the dipoles are relatively parallel in conformation **6b**, giving a repulsive force (positive potential)[9]. The second interaction is a weak C-H··N hydrogen bond between the heterocyclic nitrogen and the *ortho* hydrogen on the neighbouring ring shown in red in conformation **6a**. This interaction is not present in conformation **6b**. In addition, there are unfavourable steric interactions between the *ortho* hydrogen atoms in conformation **6b**[33].

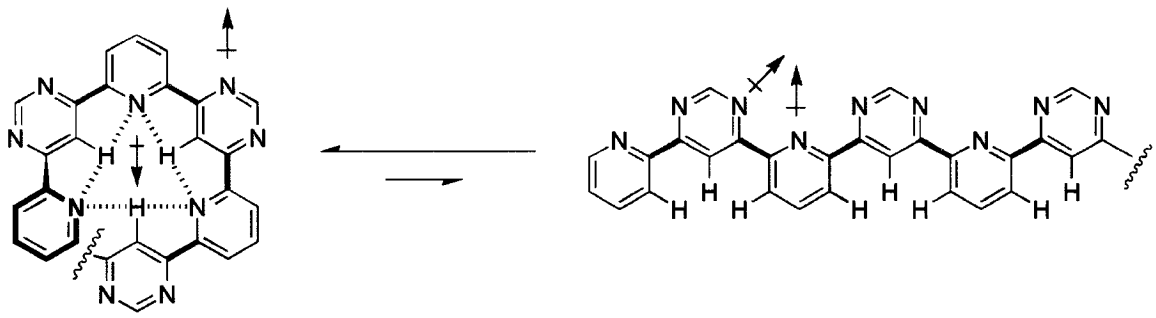

6a **6b**

Figure 1-6 Restricted rotation in Lehn's oligo-pyridine/pyrimidine molecular strand. Rotation around the bonds linking the pyridine and pyrimidine rings is restricted due to the preferred *transoid* arrangement of the nitrogen dipoles, C-H··N hydrogen bonding, and steric interactions. The bonds with restricted rotation are highlighted in green.

Though this example illustrates how restricted rotation can be used to direct folding in oligomers, our interest lies in using hydrogen bonding as the principal driving force in the determination of the most desired foldamer conformation. Hydrogen bond interactions take place between a polarized D-H bond, where D is considered to be the donor atom, and the polarized non-bonding orbitals of an acceptor atom[9]. Therefore it can be said that the hydrogen bond is primarily a dipole-dipole interaction, except that these interactions bring the donor hydrogen and acceptor atom closer than the sum of their van der Waals radii, and because of this they can be classified as weak bonds[9]. Since dipole-dipole interactions are directional, and hydrogen bonds contain many of the same characteristics of dipole-dipole interactions, they too are directional. As shown in **7a** (Figure 1-7) the acceptor and donor are aligned in a head-to-tail fashion, giving an N-H··O bond angle of 180° [9]. This maximizes the polarizing interactions of the donor and the acceptor, allowing for a relatively strong hydrogen bond compared to example **7b** where the b6nd angle is 120° [9]. Although there still is the possibility of interactions in **7b**, the strength of the hydrogen bond is dependant on the polarizing ability of the donor and

acceptor groups and moderate hydrogen bond strengths can vary from 8 to 30 kJ/mol[9]. It should be noted that even the weakest hydrogen bond can aid in restricting the rotation in foldamer conformations, especially if several of these interactions are incorporated into the overall system. This is in keeping with the general theme of foldamers which utilize the additive effects of non-covalent interactions to induce the final most stable conformation. As hydrogen bonding interactions are relatively strong and directional, it is easy to envision the interest in using them to restrict the rotation of bonds in various foldamers.

7a (180°) **7b** (120°)

Figure 1-7 Directionality of hydrogen bonding interactions. Bonds are stronger when the N-H··O bond angle is 180°.

1.2.3.2. Imine Linkage

There are many ways to induce folding in oligomeric systems. Likewise, there are many ways to control folding using restricted rotation, and more specifically rotation restricted primarily by hydrogen bonding. One method is to use hydrogen bonding in conjunction with imine linkages as demonstrated by MacLachlan and co-workers[34,35]. As illustrated in Figure 1-8, a series of trimeric compounds were prepared to investigate the properties of keto-enamine isomerization in Schiff base macrocyles[35]. Compounds **8a** and **9a** can readily tautomerize to **8b** and **9b**. In these trimers rotation about the green highlighted sp^3 bonds is restricted due to intramolecular hydrogen bonding. In trimers **8a** and **9a** the hydrogen bonding occurs between the hydroxyl hydrogen of the aromatic moiety and the non-bonding electrons of the enamine nitrogen. In trimers **8b** and **9b** the

intramolecular bonding is between the amine hydrogen and the keto oxygen as demonstrated through ^{1}H NMR and x-ray crystallography[35]. The hydrogen bonding interactions are expected to be stronger in **8a** and **9a** compared to **8b** and **9b**. However the keto tautomer is more stable than the enamine tautomer, and therefore tautomers **8b** and **9b** are predominantly observed. Due to the restricted rotation *via* hydrogen bonding, there is a high degree of preorganisation within these molecules. If the addition of monomeric units to either end of these molecules were to occur, they would be expected to adopt a helical conformation. This helps explain why the oligomer readily macrocyclizes into compound **10a** as macrocycles can be thought as helical foldamers containing a single turn, with the terminal ends bound together. Macrocycle **10a** readily tautomerizes to **10b**. These macrocyclic systems are of interest due to their polar cavities that are able to coordinate water molecules[34], as well as cations such as Na^{+} and NH_4^{+}[35].

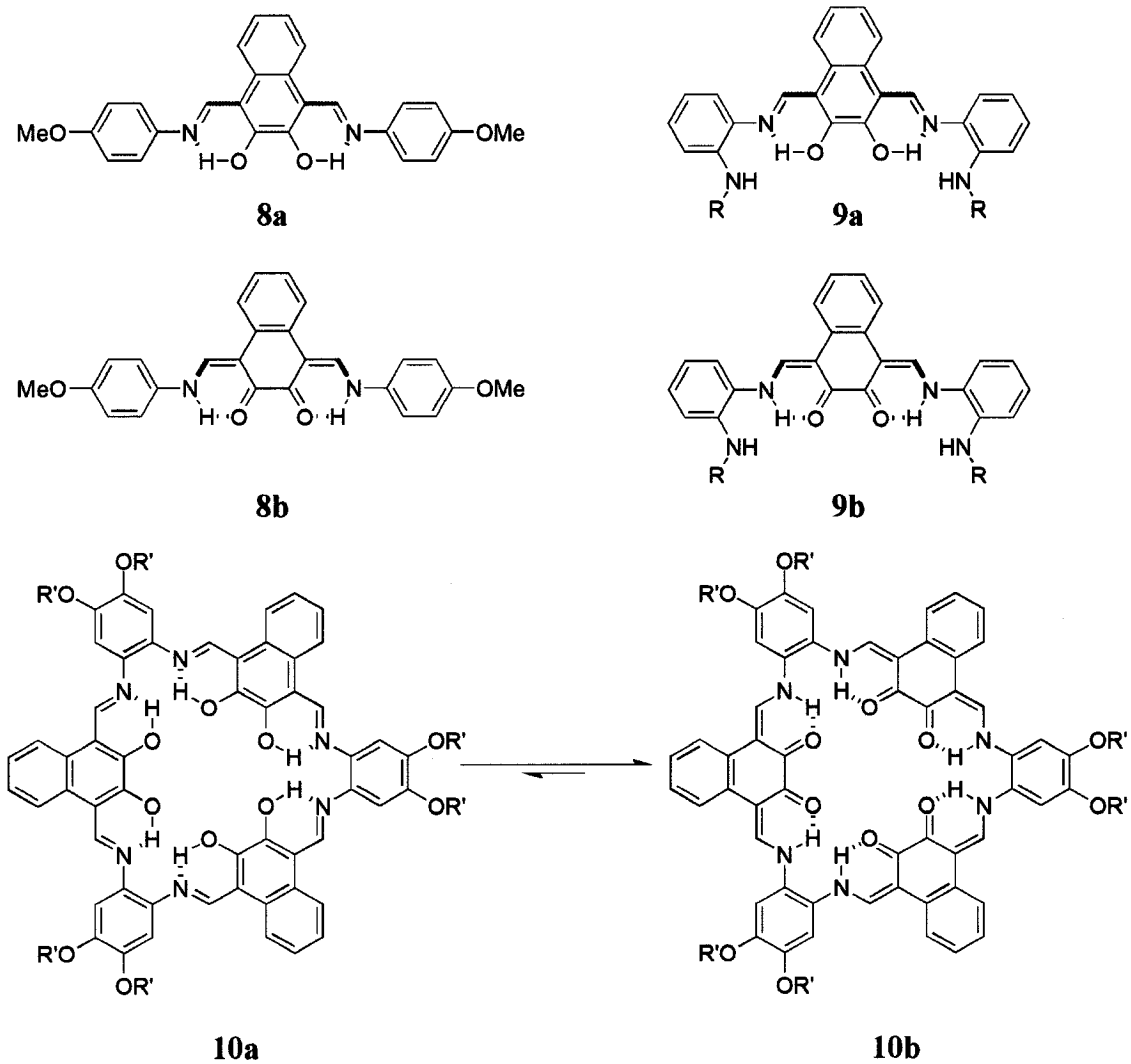

Figure 1-8 Examples of restricted rotation in keto-enamine trimers and macrocycles. The bonds with restricted rotation are highlighted in green.

1.2.3.3. Amide Linkage

Perhaps the best example of a linkage capable of inducing folding *via* hydrogen bond mediated restricted rotation is the amide group. Amide linkages are of interest due to their planarity and their ability to hydrogen bond[16]. They are interesting since the amide bond is ubiquitous throughout Nature. Examples of abiotic foldamers that

incorporate amide linkages have been prepared by Li and co-workers. As seen in foldamer **11** (Figure 1-9), this system utilizes three-centered hydrogen bonds in the interior of the foldamer to direct folding[11]. The hydrogen bonding was observed by both x-ray crystallography and ^{1}H NMR. The crystal structure of the dimer (two aromatic units) showed the hydrogen bond distance for the five-membered ring to be 2.17 Å and the six-membered ring to be 1.98 Å with bond angles of 112.4° and 141.2°, respectively[11]. These distances were small enough for hydrogen bonding and were confirmed *via* ^{1}H NMR (amide protons are at approximately 10 ppm)[11]. Furthermore NOE contacts were observed between the amide and central methoxy proton, and not between the amide and *ortho* benzyl protons. Based on these observations it was concluded that hydrogen bonding is restricting the rotation of the bonds highlighted in green in Figure 1-9. Because of this locked conformation, these molecules can bind alkylated ammonium ions, which was observed using fluorescence and NMR experiments[11].

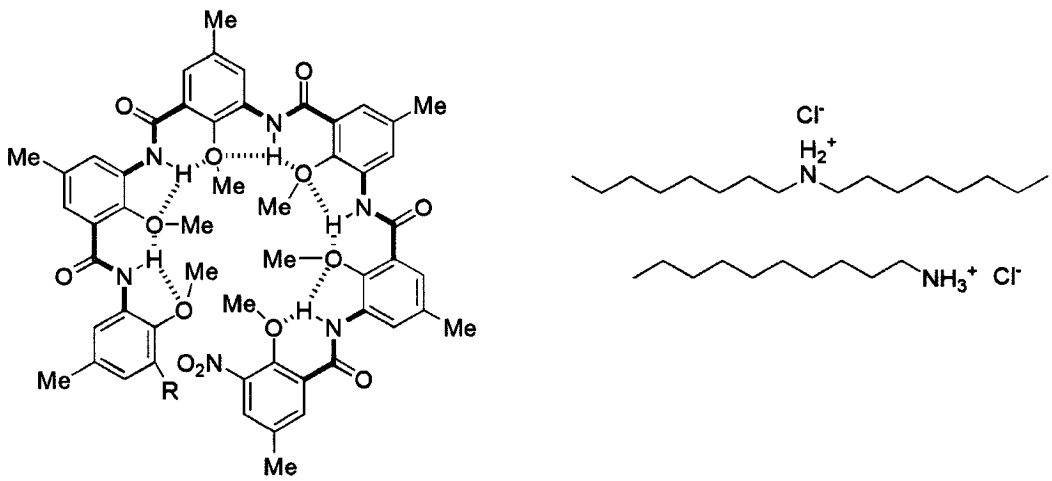

11

Figure 1-9 Li's amide based foldamers. In this example, a three-center hydrogen bond is formed in the center of the foldamer. This foldamer is capable of bonding alkylated ammonium ions such as those shown next to **11**. The bonds with restricted rotation are highlighted in green.

Gong and co-workers have also used three-point hydrogen bonds to restrict rotation and direct folding in oligoamide foldamers[36-38]. Unlike Li's foldamers, hydrogen bonding takes place on the periphery of their oligomers. In foldamer **12** (Figure 1-10), bonding takes place between the amide hydrogen and the ether oxygen of the side chains. The three-center bond creates both *pseudo* five- and six-membered rings as observed in Li's system. ^{1}H NMR shows the amide peak at approximately 10 ppm, again indicative of hydrogen bonding[36-38]. Furthermore, NOESY experiments also confirmed the crescent-shaped conformation as there were observed NOE contacts between the amide proton and the side chain methoxy protons. More strikingly, when oligomers with full helical turns were prepared, NOE contacts were also observed between the overlapping aromatic groups[37]. These observations help demonstrate conformational control using restricted rotation by hydrogen bonding.

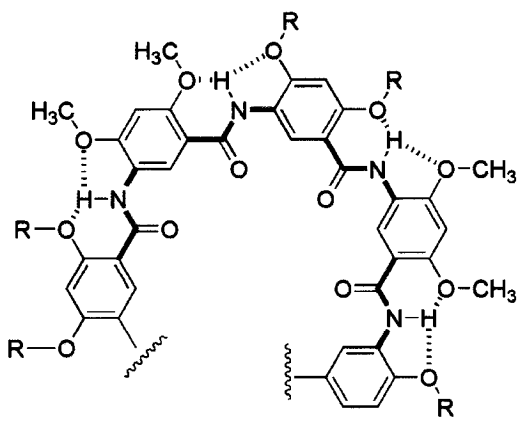

R = *n*-$C_{10}H_{21}$

12

Figure 1-10 Example of three-point hydrogen bond centers utilized in Gong's foldamers. Hydrogen bonding occurs on the periphery of the foldamer. The bonds with restricted rotation are highlighted in green.

Heterocyclic nitrogen atoms have the ability to direct hydrogen bonding and restrict rotation. Hamilton and co-workers have developed a series of oligoanthranilamide foldamers (**13**) where the aromatic groups alternate between heterocyclic pyridyl and non-heterocyclic phenyl monomers[39,40]. As in the two previously described systems, a three-point hydrogen bond center is observed where the hydrogen bonding occurs between the amide hydrogen, the pyridine nitrogen and the adjacent amide carbonyl oxygen. Again, this restricts the rotation of the bonds shown in green in Figure 1-11. The amide proton exhibits a chemical shift at approximately 11 ppm, indicative of hydrogen bonding interactions[40]. X-ray crystallography determined the N-H··N bond lengths to be 2.02 Å and the N-H··O bond length was 1.82 Å[39]. This agrees with the folded conformation depicted in Figure 1-11 as the amide hydrogen is closer to the oxygen than to the nitrogen (six-membered ring *vs.* five-membered ring). The foldamer was prepared with two full helical turns and NOE contacts were observed between overlapping phenyl groups. As the aromatic groups are overlapping, π-π stacking was observed as anisotropic effects in ^{1}H NMR where aromatic protons were shifted downfield by 0.5 to 1.0 ppm[40]. These stacking interactions help to further stabilize the helical conformation.

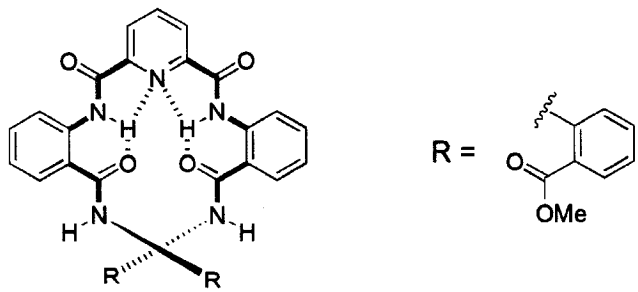

13

Figure 1-11 Hamilton's amide-based foldamers illustrating hydrogen bonding to form a helical conformation. The bonds with restricted rotation are highlighted in green.

Aromatic oligoamide foldamers composed of only aromatic heterocyclic monomer units have also been described. This is highlighted in work on oligopyridine foldamers initiated by Lehn *et al.* and continued by Huc *et al.*[41,42]. As seen in oligomer **14** (Figure 1-12), the rotation about single bonds is restricted by two hydrogen bonding interactions. The primary interaction occurs between the amide hydrogen and the nitrogen of the pyridine ring as observed experimentally in the deshielded amide proton in the ^{1}H NMR spectrum (10-11 ppm)[41]. The second interaction is a weak C=O··H-C bonding between the amide oxygen and the *ortho* hydrogen on the adjacent pyridine ring. Though these interactions are weak, it must be stressed again that they are indeed additive, and the combined effect of these interactions restricts rotation about the bonds depicted in green (Figure 1-12).

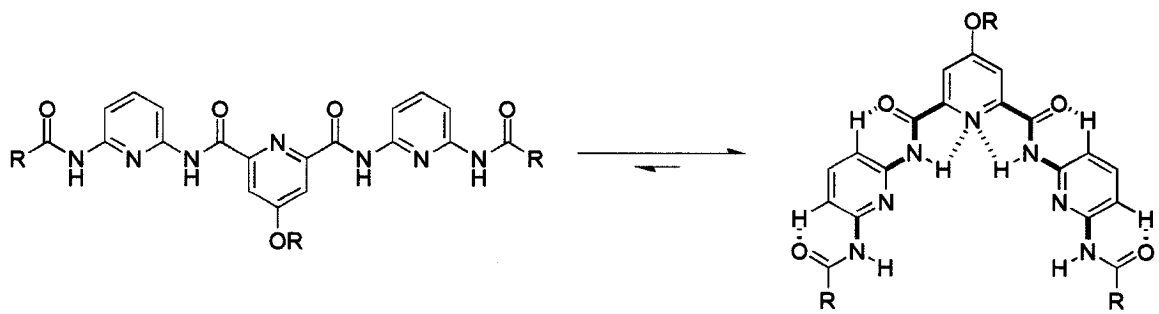

14a **14b**

Figure 1-12 Example of oligopyridine foldamers where restricted rotation about the amide bond occurs due to hydrogen bonding. The bonds with restricted rotation are highlighted in green.

1.2.3.4. Urea Linkage

Particularly of interest to the work presented in this thesis is the use of hydrogen bonding to restrict rotation and drive specific conformations in foldamers containing urea linkages. An example of these are ureidophthalimide urea-linked foldamers synthesized by Meijer and co-workers[43,44]. Oligomer **15** in Figure 1-13 is similar to Gong's amide

foldamers (Figure 1-10) as hydrogen bonding occurs on the periphery of the ring. As the urea linkage contains one more atom than the amide linkage, and due to the substitution pattern of the aromatic rings, the foldamer does not contain a three-point hydrogen bond center, but does form a *pseudo* six-membered ring between the urea hydrogen and the phthalimide carbonyl oxygen. Because of the peripheral location of the hydrogen bonding, the carbonyl oxygen atoms of the urea linkage point towards the center of the foldamer creating a polar cavity. Due to the relatively large size of the cavity, it has been proposed that the interior may be functionalized for use in materials science[44]. The exterior of the helix has also been functionalized at the nitrogen of the phthalimide moiety, and several dendrimer-like side chains have been incorporated[43].

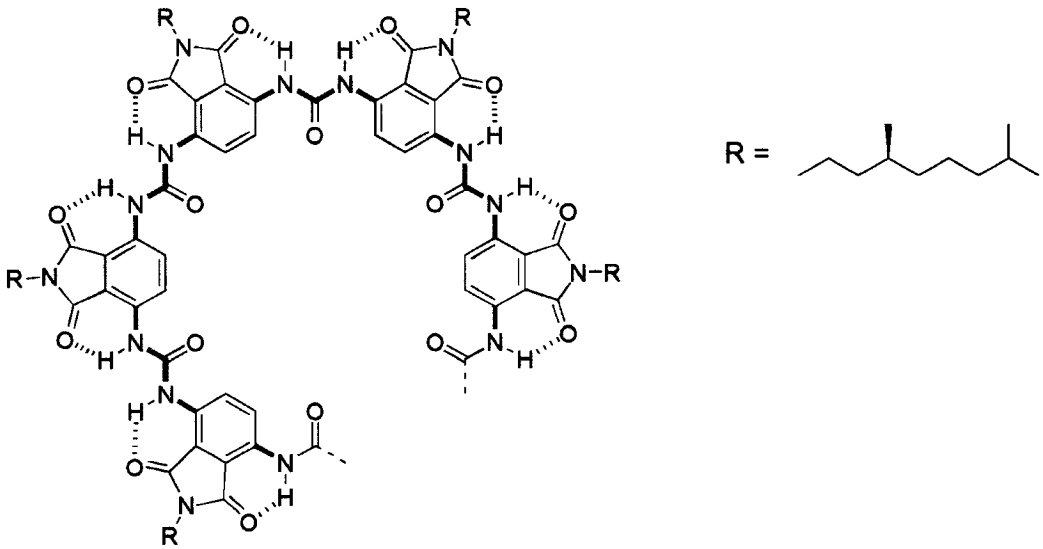

15

Figure 1-13 Ureidophthalimide based foldamers prepared by Meijer and co-workers. As in Gong's foldamers, rotation is restricted by exo-cyclic hydrogen bonding. The bonds with restricted rotation are highlighted in green.

Another example of oligoureas that use hydrogen bonding to restrict bond rotation has been reported by Tew and co-workers. Non-heterocyclic aromatic ureas were

synthesized where the rotation between monomeric units is restricted by hydrogen bonding between the urea hydrogen atoms and the side chain sulfur atoms. As shown by foldamer **16** in Figure 1-14, this creates a three-centered hydrogen bond giving two *pseudo* five-membered rings as was confirmed *via* ^{1}H NMR[45]. These oligomers were found to have anti-bacterial properties against both *E.coli* and *B.subtilis* with varying activity and selectivity based on chain length. Shorter oligomers (n = 0, 1, 2) were found to be more active and selective than longer oligomers (n = 5, 6) and it is believed that it should be possible to increase selectivity and activity by removing the *t*-butyl groups, increasing the water solubility of the oligomers[45].

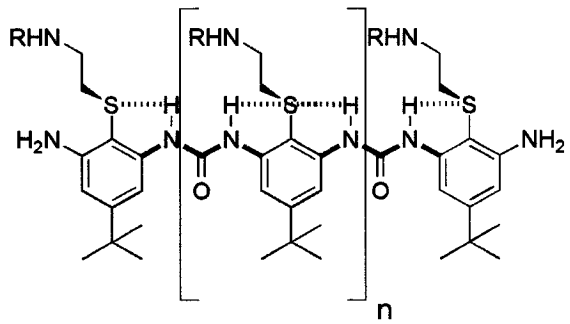

16

Figure 1-14 Tew's antimicrobial oligoureas. The bonds with restricted rotation are highlighted in green.

Gong and co-workers have also prepared foldamers containing urea linkages[16]. As shown in Figure 1-15, foldamer **17** is related to its amide-linked analogue **12** (Figure 1-10) where hydrogen bonding is observed on the periphery of the ring. The hydrogen bonding is indicated by the urea N-H chemical shift observed at approximately 11 ppm[16]. This hydrogen bonding restricts rotation along the bonds highlighted in green in Figure 1-15. This restriction has been used to self-template macrocyclization.

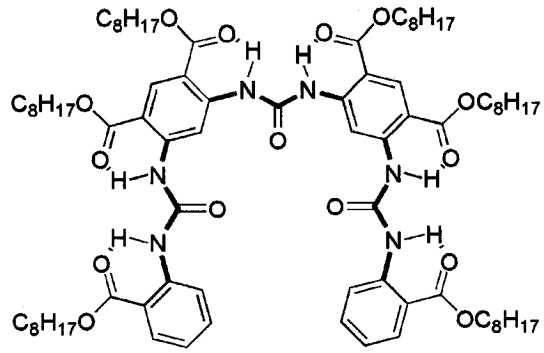

17

Figure 1-15 Example of Gong's oligourea foldamer. The bonds with restricted rotation are highlighted in green.

It is possible to also incorporate heterocycles to direct hydrogen bonding and restrict rotation in urea based foldamers. This has been highlighted by Zimmerman and co-workers in their urea linked naphthyridine foldamer **18** in Figure 1-16. Naphthyridinylurea oligomers have the potential to exist as an unfolded β-sheet **18b** (intermolecular H-bonding) or a folded helical structure **18c** (intramolecular H-bonding)[46,47]. Though there is evidence of the helical conformer at low concentrations, the predominant form is the β-sheet. This indicates hydrogen bonding is stronger in the dimer as the hydrogen bond dipoles are aligned in a head-to-tail fashion and there are more interactions per monomer unit. In the helical conformation the presence of both hydrogen bond donor and acceptor sites on the periphery of the ring, suggests the possibility to simultaneously undergo intermolecular interactions, permitting intermolecular interaction between helices[46,47].

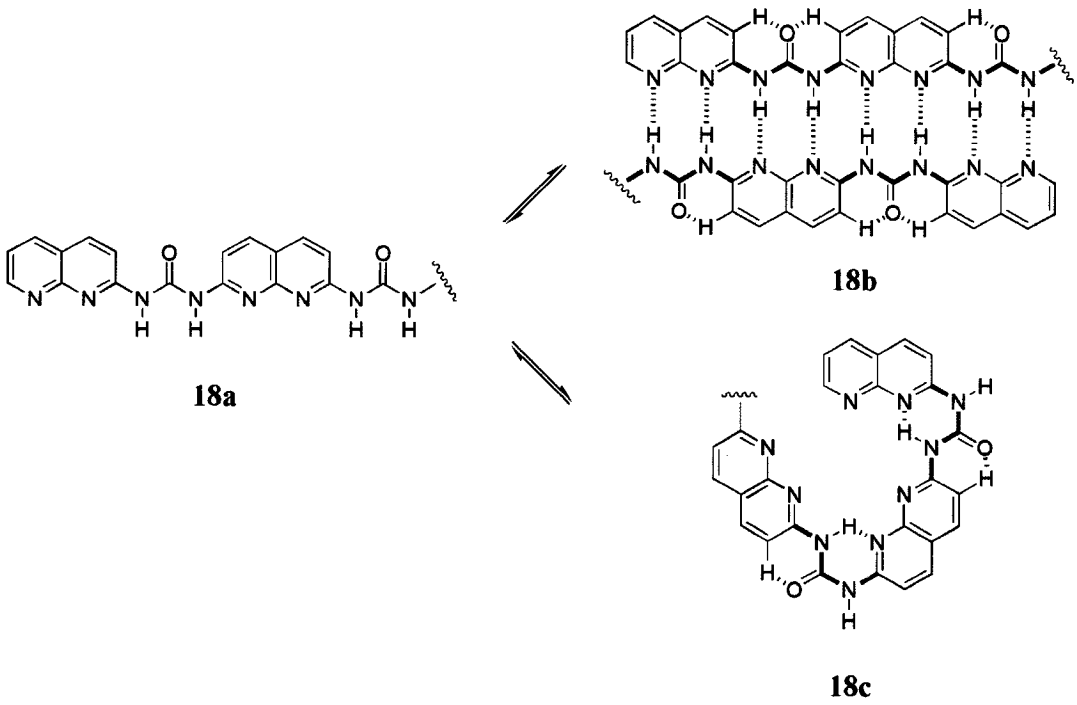

Figure 1-16 Zimmerman's urea linked naphthyridine foldamers. Hydrogen bonding occurs between the urea hydrogen and naphthyridine nitrogen atoms. The bonds with restricted rotation are highlighted in green.

1.3. Tunability in Foldamers

Our interest in foldamers is not only directed towards utilizing restricted rotation to drive folding, but also towards a design where the cavity size of the oligomer is tunable. Tunability is an important consideration in the design and synthesis of foldamers. Different sized foldamers will have different properties and characteristics[17,36]. Furthermore, if one wishes to bind target molecules, varying the cavity size is essential in order to selectively bind specific molecules. This is evident in crown ethers as different sized crown ethers have the ability to bind different cations (Figure 1-17). For example, 15-crown-5 (**19**) has been shown to be specific for sodium cations, where 18-crown-6 (**20**) is specific for potassium ions[48]. Though crown ethers are

macrocyclic compounds, it is possible to encode similar macrocyclic properties into rigid foldamers as they can be considered as open ended macrocycles.

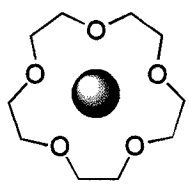

19

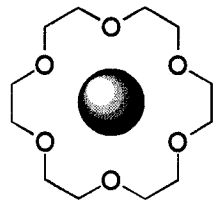

20

Figure 1-17 15-crown-5 (19) and 18-crown-6 (20) show selectivity in binding Na^+ and K^+ cations, respectively.

An example of a class of tunable heterocyclic foldamers was introduced in Figure 1-6. Folding in these alternating diazine pyridine foldamers is driven by the restricted rotation of the bonds linking successive heterocyclic units by co-operative non-covalent interactions. The cavity size of these foldamers can be varied by changing the diazine heterocycle between the pyridyl units[33,49]. This is highlighted in Figure 1-18 where the pyridine units in oligomer 21 are separated by pyrimidine monomers, yielding a cavity that is similar in size to 18-crown-6 with the interior of the cavity measuring about 2 Å in diameter[49]. By changing this diazine to pyridazine, the cavity of the foldamer changes in shape and dramatically increases in size to become akin to 42-crown-14. The cavity is larger and is estimated to have a diameter of 8 Å[33]. This change in cavity shape and size is caused by the position of the nitrogen atoms and linkages on the diazines. In the case of the pyrimidine foldamer (21), the linkage is *meta* with a 60° angle of curvature. In the pyridazine foldamer (22), the linkage is *para*, resulting a 0° angle, and thus curvature is caused only by the 60° angle of the pyridine ring.

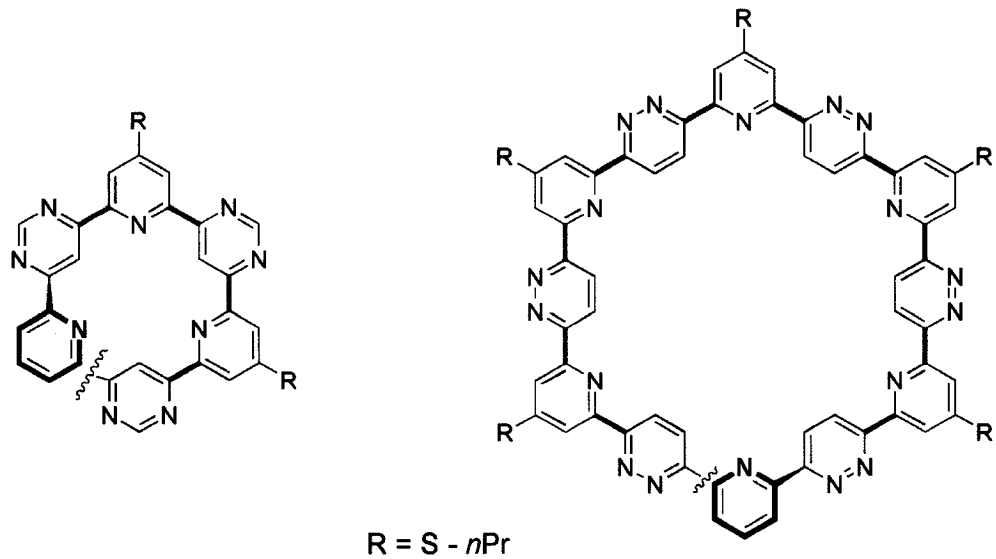

21 **22**

Figure 1-18 Lehn's oligopyridne systems comprised of alternating pyridine and diazine heterocycles. The bonds with restricted rotation are highlighted in green.

In Section 1.2.3.3 Gong's foldamer design was described. By varying the substitution pattern of the aromatic monomers the shape and size of the cavity can be tuned[37]. The judicious choice of monomer units and the variation of substitution pattern, leads to changes in the helical cavity size as seen in Figure 1-19. The substitution pattern in **23** (*meta meta meta*) gives a curvature angle of 180° and has been shown to form cavities measuring 10 Å. By altering the pattern to *para meta para* (**24**) the cavity size increases to 25 Å with a 60° angle of curvature. A very large cavity with a curvature of 90° is observed when the substitution is *meta para para* (**25**) where the cavity size doubles to 50 Å[37].

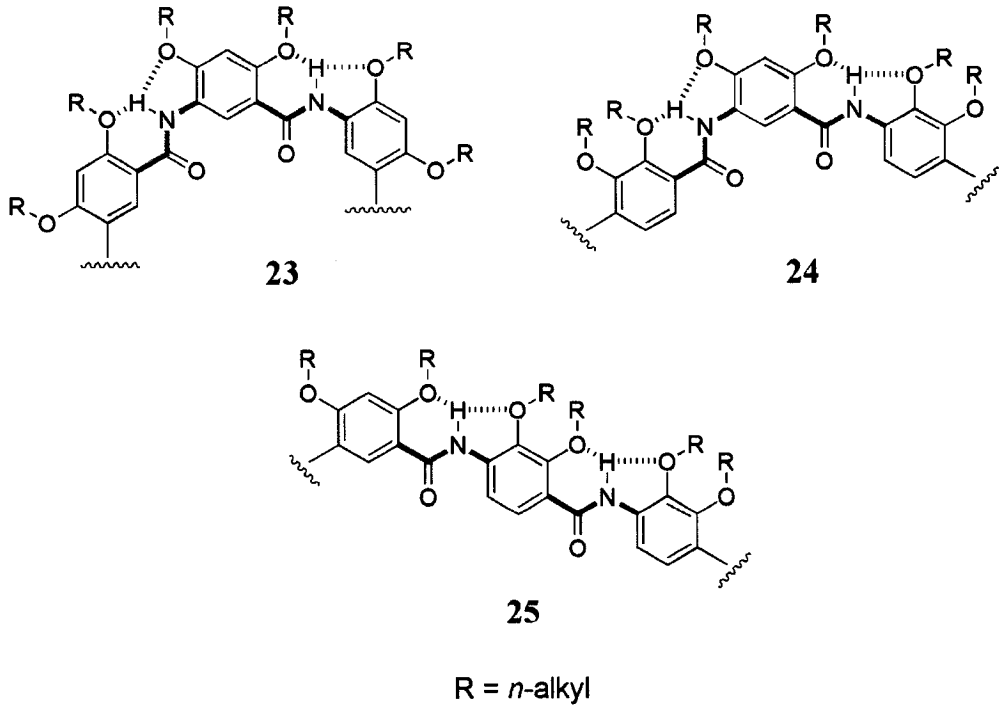

Figure 1-19 Tunability in Gong's foldamers. The bonds with restricted rotation are highlighted in green.

Huc's example of a molecular apple peel previously introduced in Section 1.1 is an excellent example of tunability in restricted rotation foldamers. Foldamer **26** is a heterocyclic aromatic oligoamide comprised of pyridyl and quinolyl segments. The concept behind this design is to have an oligomeric sequence comprised of monomers that code for a cavity, and monomers that encode for caps at both ends. As illustrated in Figure 1-20, the pyridine units code for the cavity while the quinolines act as the capping groups. This yields a helix with varying cavity size where the helix has a pitch of approximately 3 Å which is equivalent to the thickness of an aromatic ring[17]. Folding was observed using both 1D and 2D ^{1}H NMR where the overlapping aromatic units are deshielded due to anisotropy, and appropriate NOE contacts were noted. An interesting

feature of this system is the similar flexibility (*i.e.* unfold/refold) as Lehn's oligopyridine amide systems, and this foldamer has been shown to reversibly bind water molecules[17].

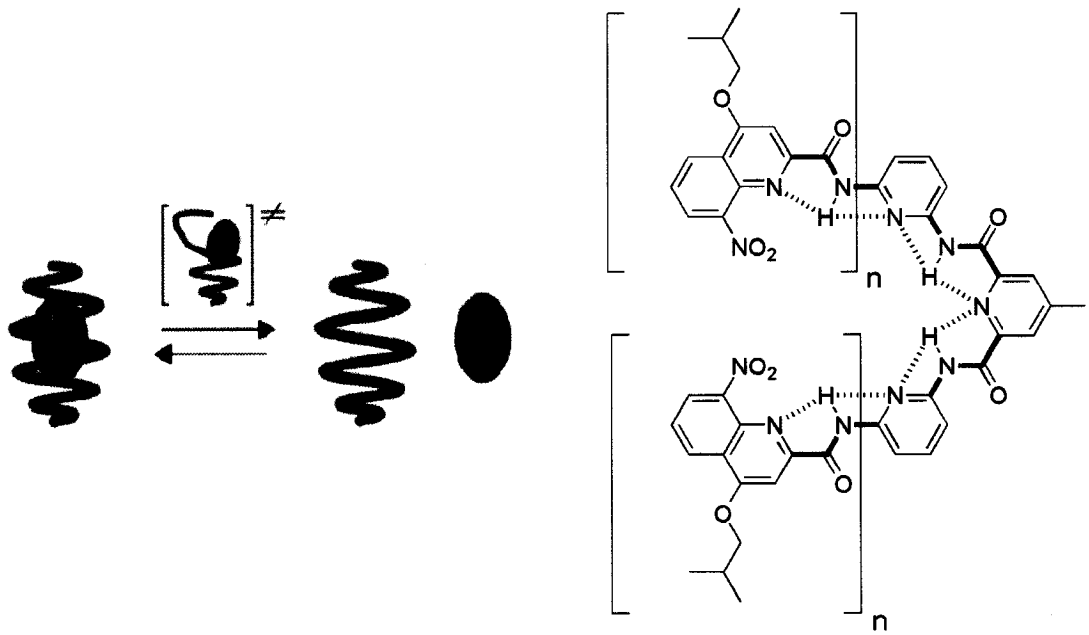

26

Figure 1-20 Huc's molecular apple peel. The bonds with restricted rotation are highlighted in green. Figure reproduced with permission.

To the best of our knowledge, there are no reports in the literature on tunable urea based foldamers based on restricted rotation. It has been demonstrated that tunability is possible in other systems, and should be applicable to urea-linked foldamers. These oligomers would yield sizes and geometries complementary to those seen in amide or other types of foldamers reported earlier in this Introduction. Therefore, the goal of this research project is to demonstrate that it is possible to use our heterocyclic diazine systems, coupled with non-heterocyclic aromatic groups, to create foldamers with unique size and geometry.

1.4. Goals and Outline of Research

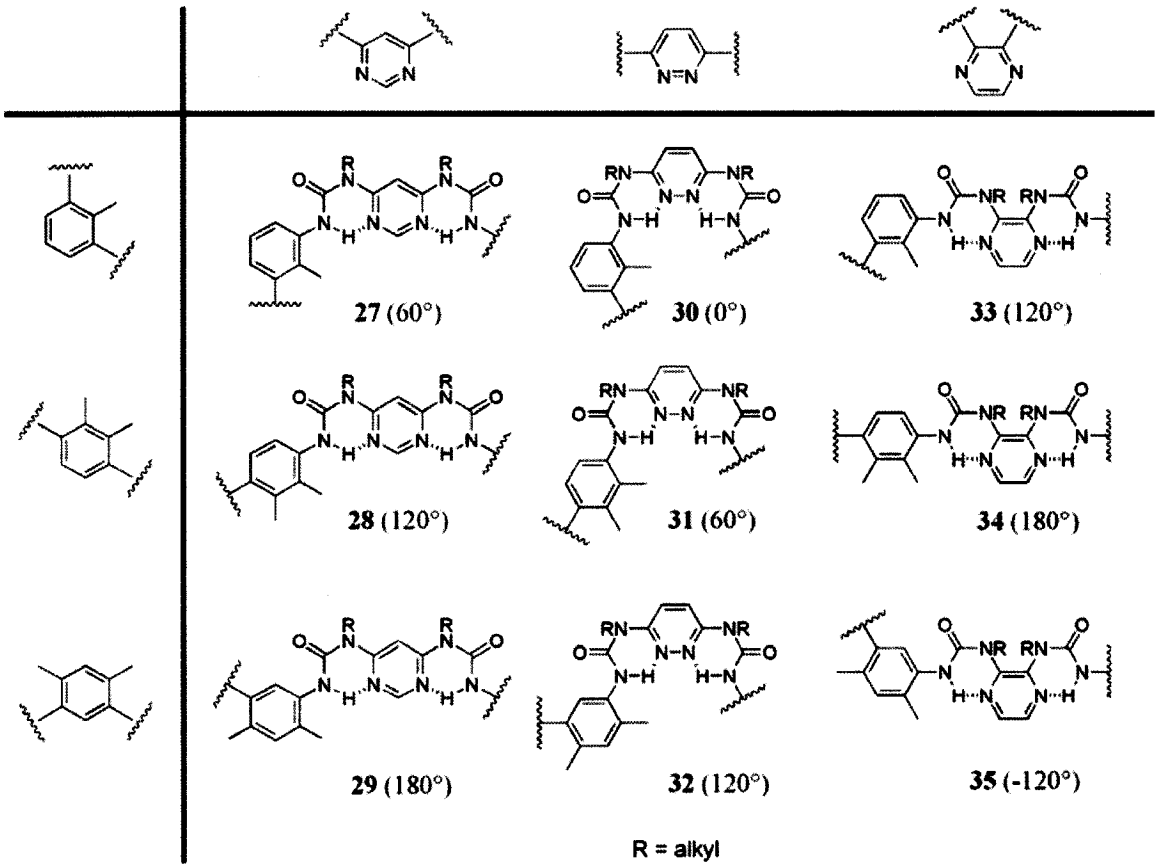

Figure 1-21 Tunability in pyrimidine, pyridazine, and pyrazine foldamers. By varying either or both the heterocycle and non-heterocycle the degree of curvature can be varied. The angles shown are the overall angles of the repeat units.

Our interest lies in preparing pyrimidine, pyridazine, and pyrazine based foldamers where the aromatic diazine heterocycle alternates with an aromatic non-heterocycle *via* a urea linkage. This design allows for tunability in foldamer curvature; as illustrated in Figure 1-21, by alternating either the aromatic or non aromatic moiety, different degrees of curvature can be obtained (the number in brackets indicates the overall angle of the repeat unit). Due to the position of the nitrogen atoms in the diazines (1-2, 1-3, 1-4 for pyridazine, pyrimidine, and pyrazine rings, respectively), the relative

positions of the branching or linking substituents on these rings will be *meta* in the pyrimidine system (**27-29**), *para* in the pyridazine system (**30-32**), and *ortho* in the pyrazine system (**33-35**). Likewise, as seen previously in Gong's foldamers, it is possible to vary the substitution in the non-heterocyclic monomers which also influences curvature. By varying the heterocyclic or non-heterocyclic groups individually, or simultaneously, a library of oligomers with unique geometries can be prepared. It should be noted that some of the systems shown in Figure 1-21 have the same expected degrees of curvature, though each system will have its own unique constitution.

Folding in our oligomers is driven by a combination of hydrogen bonding, steric, and aromatic stacking interactions. Consequentially, we are preparing tunable, well defined molecules where the conformation is driven by the additive effect of weak, non-covalent interactions. As shown in Figure 1-22, uncapped trimer **36** can adopt three planar conformations that allow for π-conjugation. These conformers, with coplanar π-systems allow for the π-orbitals of sp^2-hybridized atoms to overlap - *i.e.* limits or restricts the rotation about a single bond[6]. An uncapped oligomer is one that has reactive ends that can be used to undergo chain elongation whereas a capped molecule can no longer be extended. Conformer **36c** is least preferred due to steric interactions between the urea oxygen and the tolyl methyl group. Other interactions disfavouring this conformation are the dipole-dipole repulsion between the opposing carbonyl oxygen atoms as well as the unfavourable parallel arrangement of dipoles between the carbonyl groups and the pyridazine heterocycle. Both conformers **36a** and **36b** seem reasonable as there are neither steric interactions with the methyl group, nor dipolar repulsions between the carbonyl group and the heterocycle. Likewise there is possible hydrogen bonding

interactions in both cases. However, the conformation that is observed is conformer **36a** as the NH··N hydrogen bond is stronger than the CH··O hydrogen bond. This is because the N-H bond is more polarized than the C-H bond, resulting in a stronger hydrogen bond.

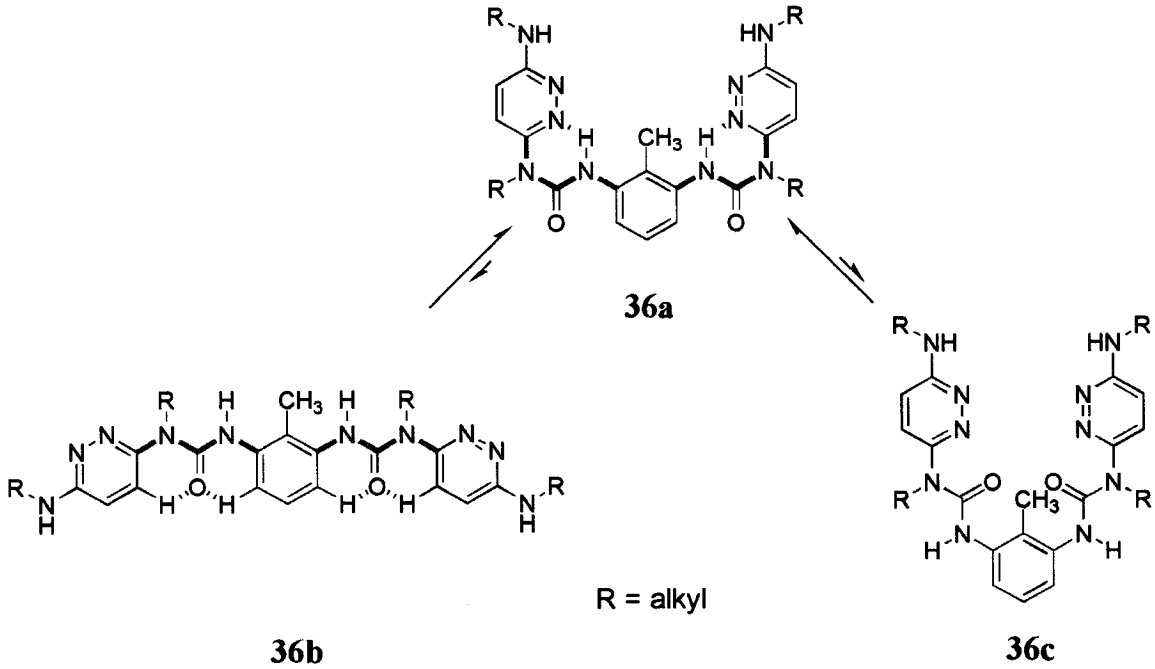

36a **36b** **36c**

Figure 1-22 Non-covalent interactions co-operating to form a well defined folded conformation. The bonds with restricted rotation are highlighted in green.

This thesis will explore the tuning of cavity size in heterocyclic urea-linked foldamers. Chapter 2 will discuss the synthesis of pyrazine based foldamers and subsequent characterization. Chapter 3 will describe pyrimidine based foldamers. Chapter 4 will focus on pyridazine foldamer as well as the preparation of two new xylyl building blocks.

2. Pyrazine Foldamers

2.1. Pyrazine Overview

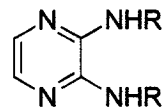

Figure 2-1 A substituted pyrazine ring.

In pyrazine the heterocyclic nitrogen atoms are situated at the 1,4-positions of the ring. As the heteroatoms are 180° from each other, the net dipole of the molecule caused by these atoms is zero[50] making pyrazine the most aromatic of the diazine heterocycles[51]. The pyrazine ring is observed throughout Nature; for example, in the fungal metabolite aspergillic acid as well as in various luciferins of beetles. Pyrazine derivatives have been determined to be relevant components of the flavouring and aromas of many fruits, vegetables, wines, and have been found to form during the preparation of maple syrup[52,53].

Pyrazine has also been incorporated into foldamers. Meijer and co-workers have described a polyaromatic foldamer **37** with alternating phenyl and pyrazyl groups (Figure 2-2)[54]. Hydrogen bonding between the peripheral amide hydrogen and the heterocyclic nitrogen of the pyrazine ring has been observed using ^{1}H NMR. The terminal amide protons not involved in hydrogen bonding exhibit chemical shifts of approximately 4 to 5 ppm. This is contrasted to the amide protons undergoing hydrogen bonding which are deshielded to 10-12 ppm. Furthermore, hydrogen bond distances were measured to be 1.8 to 2.7 Å by x-ray crystallography. These non-covalent intramolecular interactions keep

all the aromatic rings in the molecule coplanar through the restriction of rotation along the bonds connecting the aromatic groups. This co-planarity is essential in maintaining π-conjugation in the molecule as confirmed by cyclic voltammetry[54].

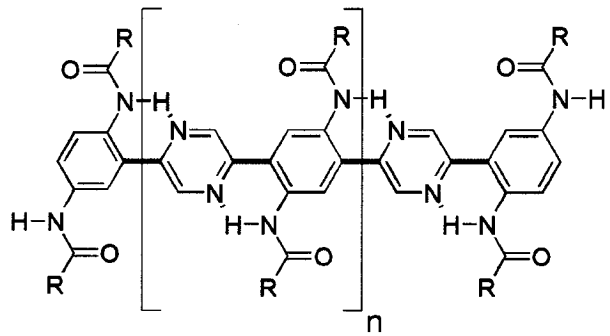

R = Boc, $C_{11}H_{23}$

37

Figure 2-2 Meijer's linear pyrazine foldamer stabilized by intramolecular hydrogen bonding. The bonds with restricted rotation are highlighted in green.

Kulike and co-workers prepared pentamer **38** containing alternating pyrazine and pyridine rings[55]. Studies have shown that this oligomer prefers a folded state as shown by conformation **38b** in Figure 2-3. This conformation is stabilized by favourable: (*i*) π-π stacking of overlapping pyridine rings (absent in conformer **38a**)[55]; (*ii*) transoid arrangement of the nitrogen dipoles of the adjacent monomeric units; and (*iii*) weak C-H··N hydrogen bonding interactions between the nitrogen atom of the pyrazine ring and the *ortho* hydrogen of the pyridine ring. X-ray analysis determined the length of this hydrogen bond to be 2.7 Å[55].

Oligomer **39** (Figure 2-3) is a similar pyrazine/pyridine system prepared by Endicott and co-workers to study complexation of different metal ions. This trimer is similar to Kulike's pentamer in that two pyridine units are attached at the 2- and 3-positions of the pyrazine ring. However the molecule has a different conformation when

ruthenium(II) ions are added. The conformation changes so that the heterocyclic nitrogen atoms act as bidentate ligands for these metal ions[56]. The difference in conformation between foldamers **38** and **39** demonstrates the dynamic nature of folding.

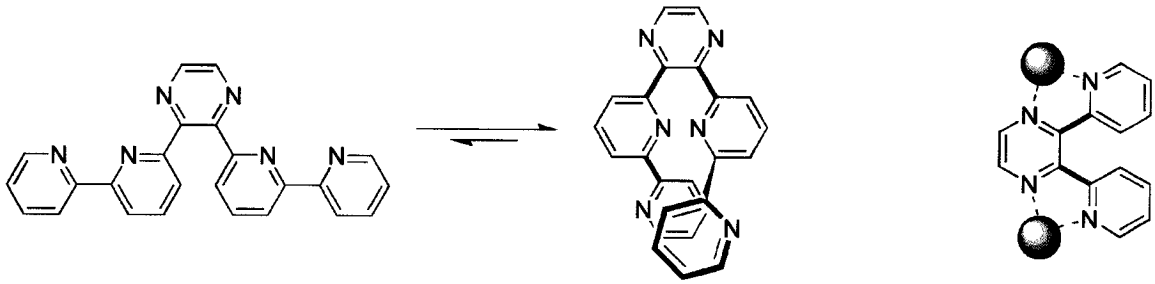

38a **38b** **39**

Figure 2-3 Oliogomer **38** is Kulike's oligopyrazine-pyridine foldamer. Oligomer **39** is Endicott's pyrazine-pyridine trimer complexing with Ru(II).

We are studying foldamers that fold based on restricted rotation and more specifically when hydrogen bonding restricts the rotation of particular bonds. Illustrated in Figure 1-4, the heteroatoms of pyrazine rings are intended to act as hydrogen bond acceptors for the hydrogen atoms of the urea linkages. The nitrogen heteroatoms in the 1,4-position require the urea linkage to be at the 2- and 3-positions. Though the curvature in foldamers **41** and **42** is the same, the properties of the proposed helical cavities are expected to be different. In oligomer **41** the interior of the cavity would be relatively non-polar due to the presence of the tolyl methyl groups and the fact that the pyrazine heterocyclic nitrogen atoms are not oriented towards the interior. The cavity in oligomer **42** would have both the carbonyl oxygen atoms and the urea side chains oriented towards the interior of the foldamer. Therefore, the properties of the cavity would be dependant on the characteristics of these groups. Due to the substitution pattern, the cavity size of these foldamers tends to be large, and in the extreme case of oligomer **40** a linear foldamer would result not unlike foldamer **37** (Figure 2-2).

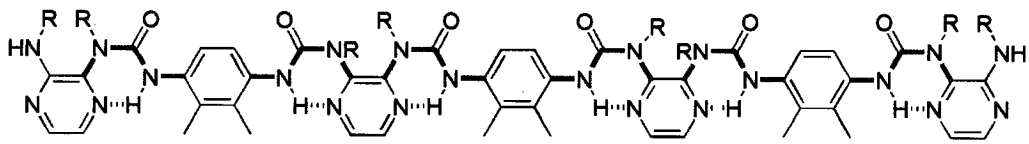

40

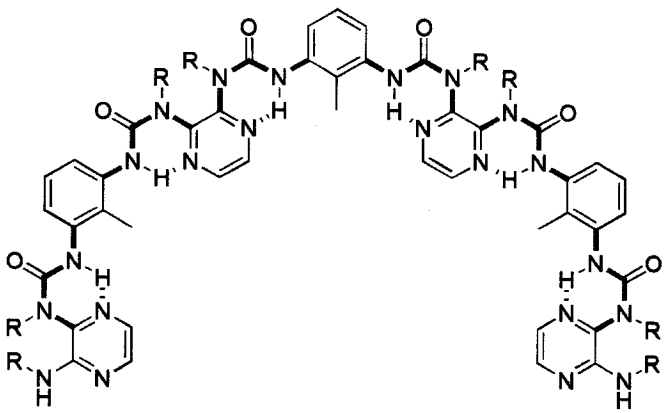

41

R = isobutyl, *n*-alkyl

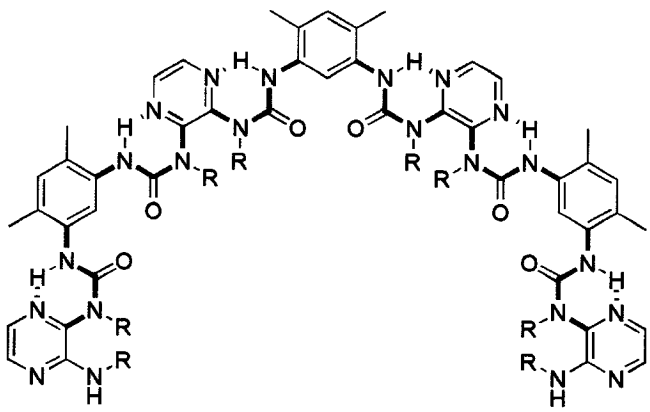

42

Figure 2-4 Examples of proposed pyrazine heptamers. The bonds with restricted rotation are highlighted in green.

2.2. Synthesis of N^2,N^3-diisobutylpyrazine-2,3-diamine Oligomers

2.2.1. Synthesis

The method used to prepare substituted diazines in our laboratory is illustrated in Scheme 2-1 and allows us to prepare various 3,6-diaminopyridazines and 4,6-diaminopyrimidines in multi-gram quantities[57,58]. N^2,N^3-Diisobutylpyrazine-2,3-diamine was prepared in 79 % yield from the reaction of 2,3-dichloropyrazine and isobutyl amine in a sealed tube at high temperature. A similar method was described by Kockerling and co-workers in the substitution of 2,3-dichloroquinoxaline with isopropyl amines[59]. The use of isobutyl side chains allows us to increase the solubility of our oligomers in common organic solvents by increasing hydrophobicity and preventing intermolecular hydrogen bonding. Furthermore, similar amide-linked foldamers with short-branched side chains have been shown to form single crystals suitable for crystallography[60].

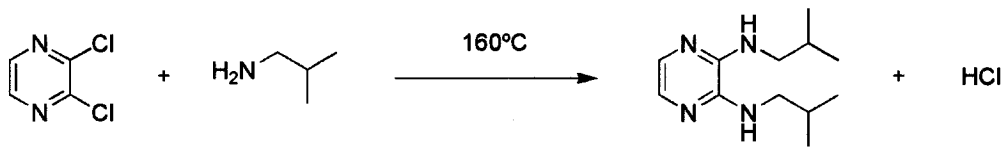

JM1

Scheme 2-1 Synthesis of N^2,N^3-diisobutylpyrazine-2,3-diamine.

Urea linkages can be formed from the reaction between an amine and an isocyanate. This method has been reported by several groups in order to prepare urea linkages in oligomeric compounds[44,61,62]. As shown in Scheme 2-2, the reaction involves a nucleophilic attack by the amine at the carbonyl of the isocyanate to form the urea bond.

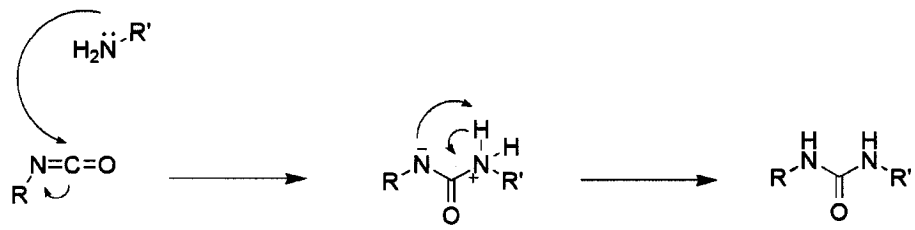

Scheme 2-2 Formation of urea linkages from isocyanates.

As will be discussed in Chapters 3 and 4, we have successfully prepared urea linkages by reacting pyrimidine and pyridazine diamines with tolyl isocyanates[57,58]. **JM1** was reacted with excess *o*-tolyl isocyanate at 50 °C in an attempt to synthesize trimer **43**, but only dimer **JM2** was isolated in 29 % yield. At 90 °C no trimer was obtained and the yield of the dimer increased to 59 % but did not increase further as the temperature was raised to 110 °C. As highlighted in Scheme 2-3, **JM2** was prepared in good yield but we were unable to synthesize trimer **43**. Reasons for this are not yet understood and consequently, different methods were explored in order to synthesize **43**.

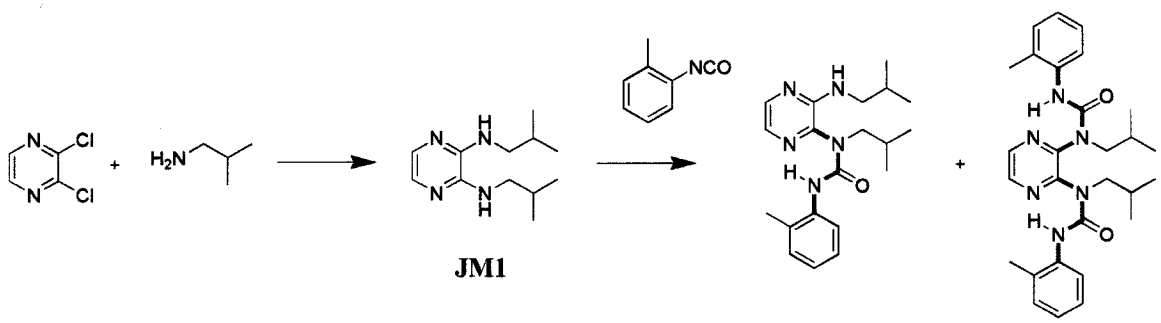

JM1 **JM2** **43**

59 % 0 %

Scheme 2-3 Synthesis of **JM2**. The bonds with restricted rotation are highlighted in green.

The pyrazine ring is an electron deficient ring due to the presence of two electron withdrawing heteroatoms[55,52]. Consequently, the ring has an electron withdrawing effect on its substituents, making the substituted amines less nucleophilic. It has been shown

that *N*-silylated aromatic amines are very reactive towards acid chlorides and can be used in amide polymerization reactions[63-65]. In these systems, the silyl group acts as an activator and a leaving group. As illustrated in Scheme 2-4, de la Campa *et al.* used this method where the silylated amine was prepared *in situ* and the silylating agent acted as a catalyst.[66,67].

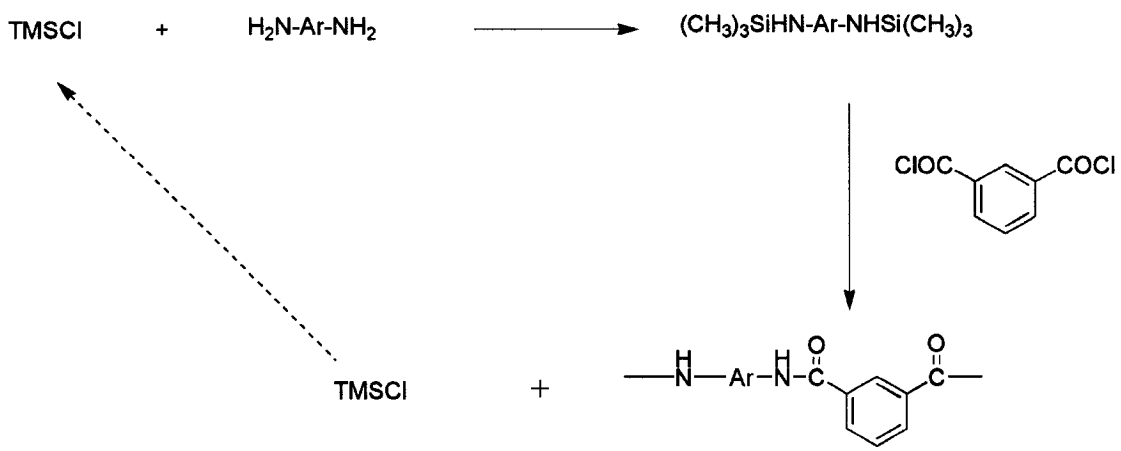

Scheme 2-4 de la Campa's method of using silyl groups to promote the reaction between aromatic amines and acid chlorides. The silyl group acts as a catalyst.

This same procedure was attempted with our pyrazine foldamers. Dimer **JM2** was prepared with 60 % yield, but trimer **43** was not obtained. *N*-Methyl-*N*-(trimethylsilyl)-trifluoroacetamide (MSTFA) is a more potent silating agent and one that has been used to activate secondary amines to react with aromatic isocyanates in order to synthesize urea linkages[68]. Unfortunately no reaction with MSTFA was observed and only starting material was recovered. This was thought to be due to the steric crowding in our pyrazine system, which may inhibit the reaction of the amine with the MSFTA, which is bulkier than TMSCl.

Another important consideration in our inability to form **43** is the substitution pattern of the N^2,N^3-diisobutylpyrazine-2,3-diamine. Since the two amines are *ortho* to

each other, a high degree of steric hinderance may limit the ability of the second amine to attack the isocyanate.

Since it was possible to obtain a reaction at one of the amino groups, the synthesis of trimer **JM3** was attempted as depicted in Scheme 2-5. The two terminal pyrazine groups have free amines that can, in principle, continue to undergo reaction with isocyanates to form other urea linkages. The reaction conditions employed were similar to what was described in the synthesis of dimer **JM2** with *o*-tolyl isocyanate being replaced with tolylene-2,6-diisocyanate (TDI). In this case, **JM3** was isolated in 44 % yield.

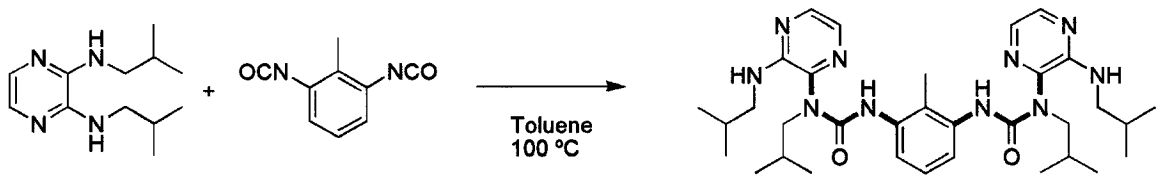

JM1 **JM3**

Scheme 2-5 Synthesis of pyrazine JM3. The bonds with restricted rotation are highlighted in green.

2.2.2. Characterization

The ^{1}H NMR spectrum of dimer **JM2** is given in Figure 2-5. The isobutyl amine peak is observed at 5.0 ppm, which is a triplet broadened due to quadrupolar relaxation by the nitrogen atom. The urea proton resonance was observed at 7.1 ppm, suggesting the absence of hydrogen bonding as similar chemical shifts are reported for pyridyl ureas where hydrogen bonding is not possible[69,70]. As seen in Meijer's foldamer (Figure 2-2),

the hydrogen bonded amide proton exhibited resonances at 10-12 ppm and a similar observation was expected for the urea protons of **JM2**.

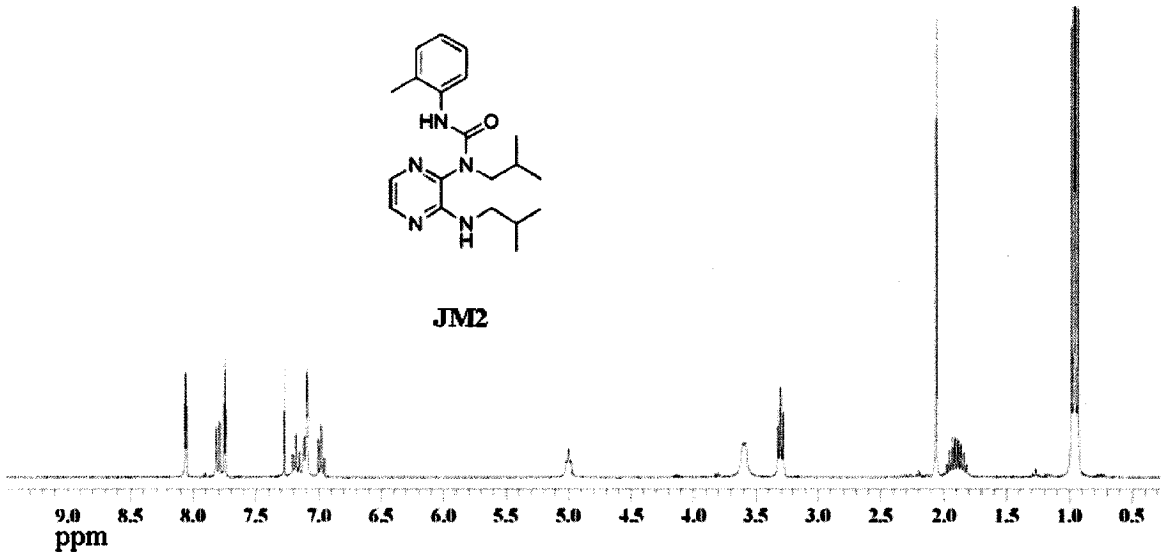

Figure 2-5 ^{1}H NMR spectrum of the tolyl pyrazine dimer.

The ^{1}H NMR spectrum of **JM3** is shown in Figure 2-6. The chemical shift of the urea proton was noted at approximately 7.0 ppm, similar to what was observed for **JM2**, indicating that there is likely little or no hydrogen bonding occurring between the urea hydrogen and the pyrazine heterocyclic nitrogen atoms. This is in contrast to what was observed in our pyrimidine and pyrazine foldamers reported in Chapters 3 and 4, respectively.

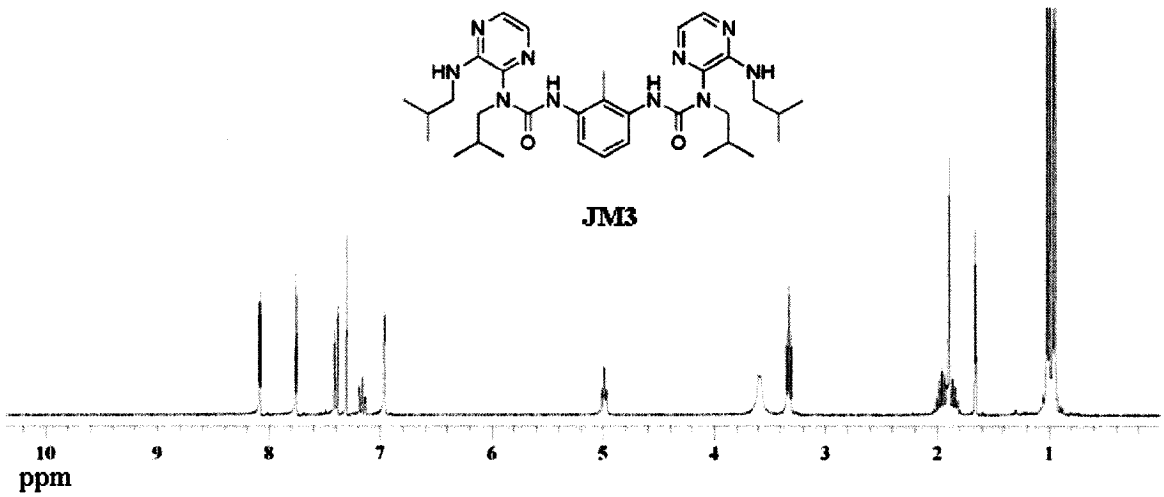

Figure 2-6 ^{1}H NMR spectrum of the uncapped pyrazine tolyl trimer

The conformation of **JM2** was probed by NOESY. If the molecule were to fold as designed, a cross-peak would be expected between the pyrazine proton **1** at 8.1 ppm (Figure 2-5) and the tolyl methyl group **11** at 2.1 ppm. With hydrogen bonding, the distance between these two groups would be approximately 2.4 Å, which is within the NOE detection limit of 5 to 6 Å[71]. However, an NOE cross peak between the two protons was not observed (Figure 2-7) indicating that they are not in close contact. This suggests that there is little or no hydrogen bonding taking place, in agreement with the absence of a downfield shift of the N-H signal expected if hydrogen bonding was present. The only significant cross-peak observed was between the tolyl methyl group and the urea hydrogen. This NOE is expected as the distance between the two protons is approximately 2.2 Å.

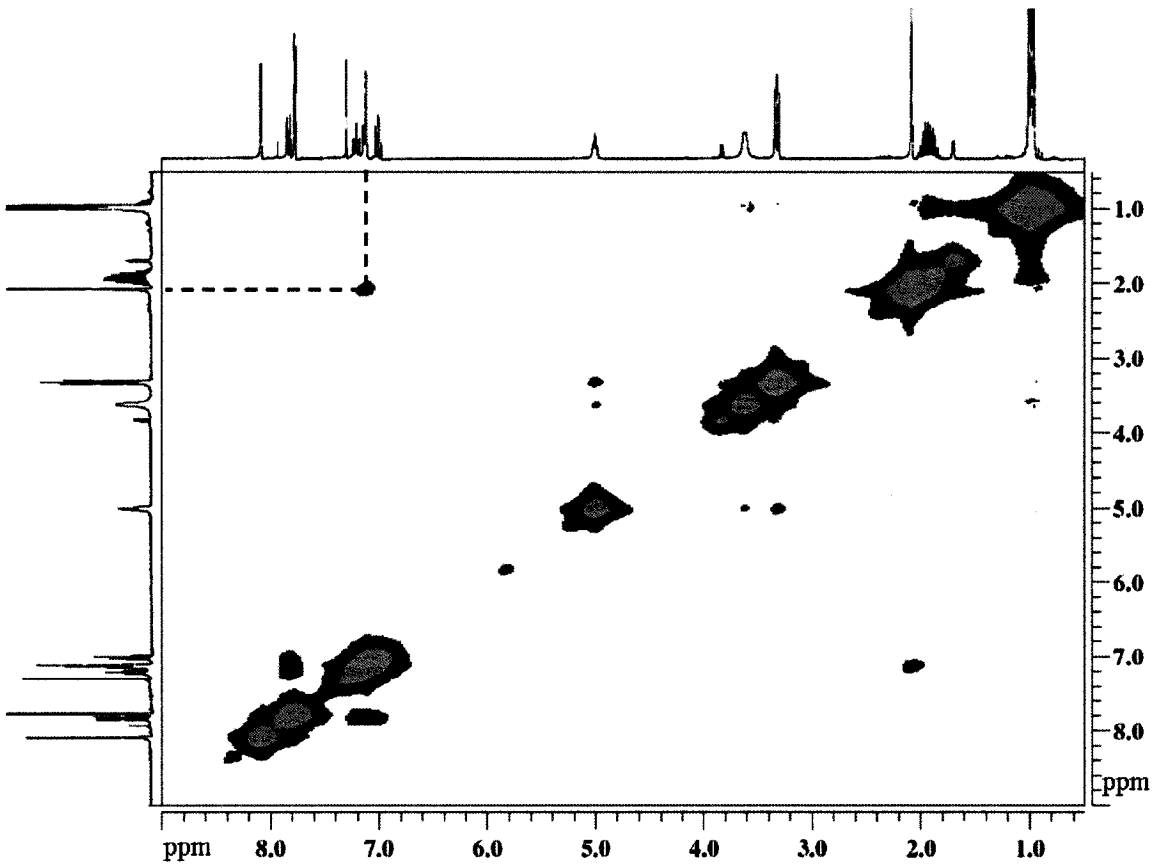

Figure 2-7 NOESY spectrum of **JM2**.

The absence of an NOE cross peak between the tolyl methyl group and the pyrazine hydrogen in the NOESY spectrum of **JM3** also suggests that no hydrogen bonding was taking place between the urea hydrogen and the pyrazine heterocycle (Figure 2-6).

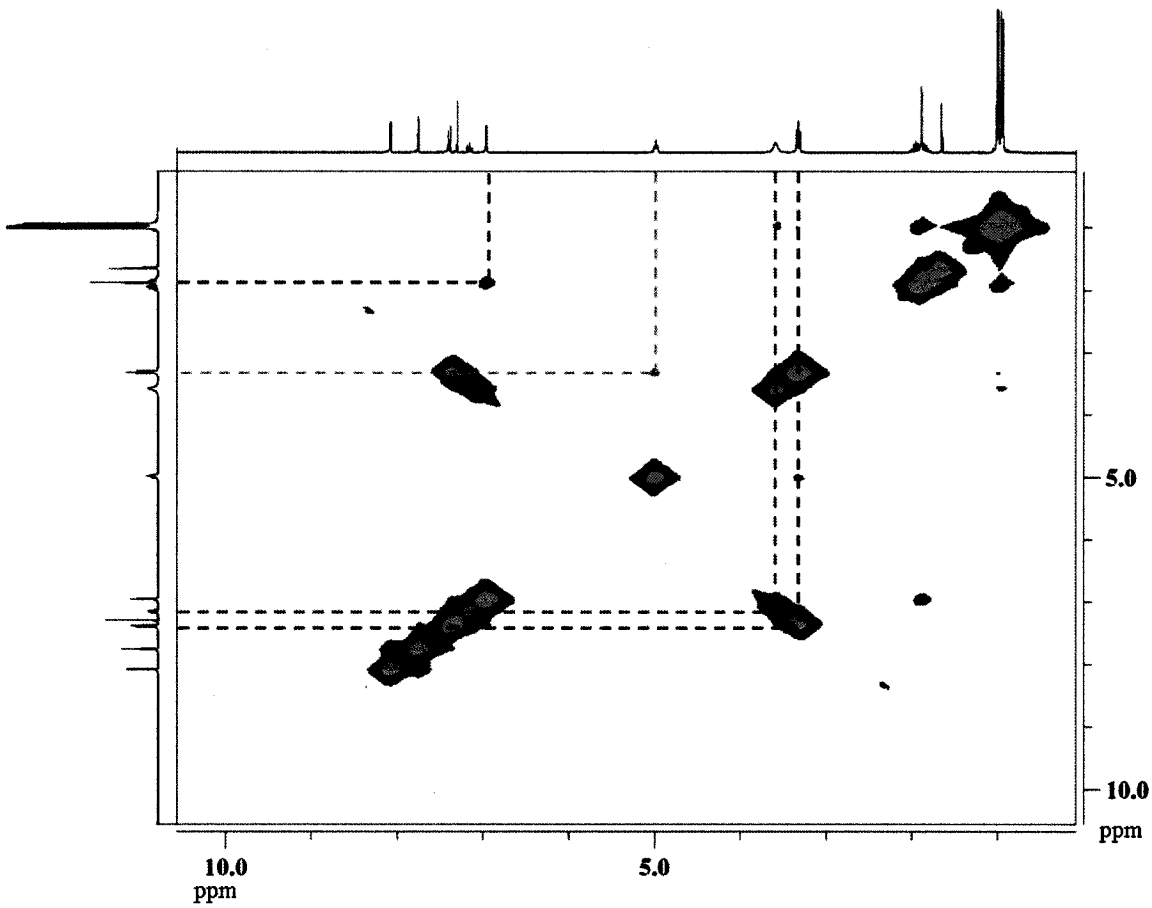

Figure 2-8 NOESY spectrum of **JM3**.

2.3. Future Work

It appears that steric effects of proximal isobutyl groups play an important role in both the reactivity and the conformation of these pyrazine molecules. A possible way to correct this is it remove the alkyl chains altogether, though this would inherently result in a decrease in solubility of these oligomers. A possible solution to this would be to use the phthalimide pyrazine derivatives described by Rebek and co-workers in our synthetic design[72-75]. As outlined in Figure 2-9, the procedure would require the oxidative cleavage of the phenyl component of 2,3-dichoroquinoxaline to form the bis-carboxylic acid. Using thionyl chloride, the carboxylic groups can be converted to an anhydride which can

readily be functionalized to the phthalimide. The chlorine atoms would be displaced by ammonia to prepare our desired diamine. The heterocyclic monomer would be similar to the ureidophthalimide foldamers (**15** Figure 1-13) prepared by Meijer and co-workers discussed in Section 1.2.3.4[43]. As mentioned, the value of such a design lies in the possibility of preparing diverse, highly functionalized foldamers (**44-46**, Figure 2-10). With the exception of **45**, steric strain in these systems is reduced, and reactivity of the amines should increase as they are now primary amines. Strain would be increased in **45** due to the orientation of the phthalimide units towards the interior of the cavity.

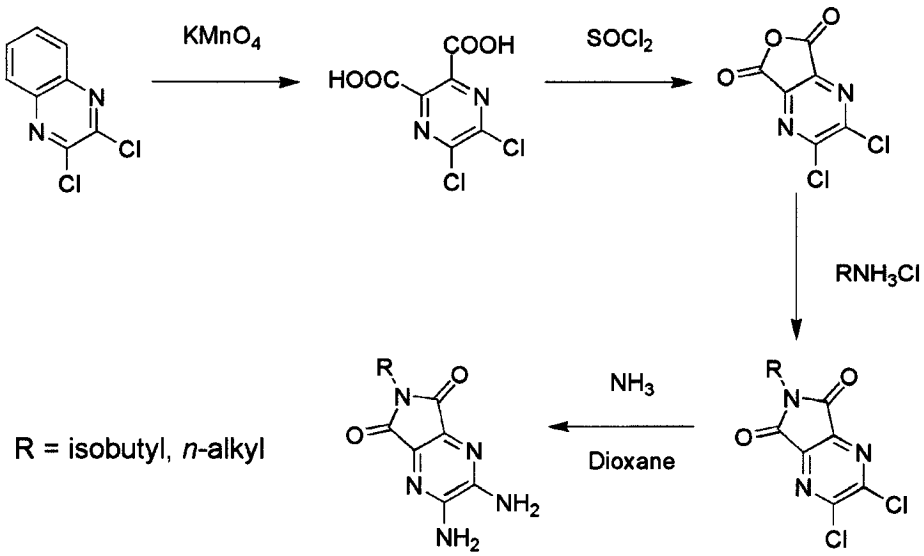

Figure 2-9 Synthesis of a pyrazine building block.

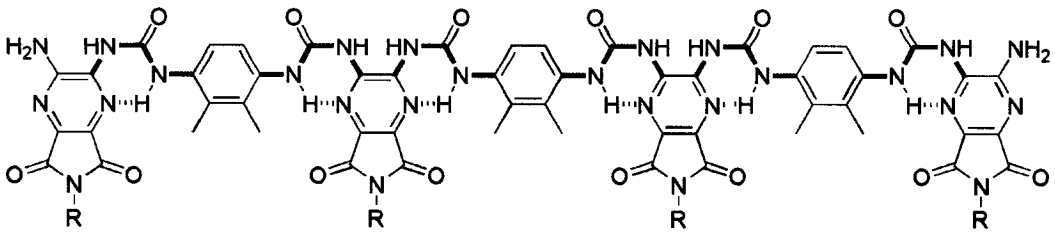

44

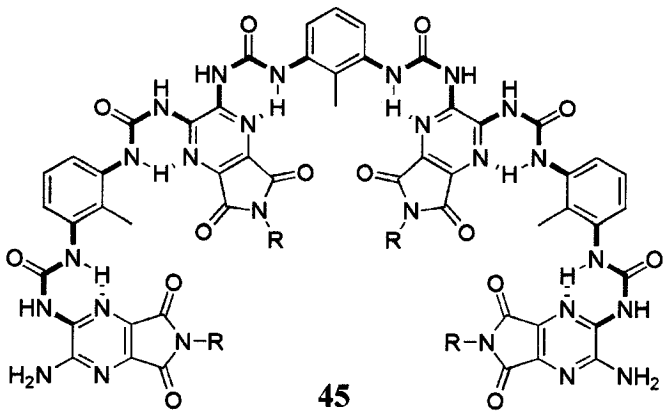

45

R = isobutyl, *n*-alkyl

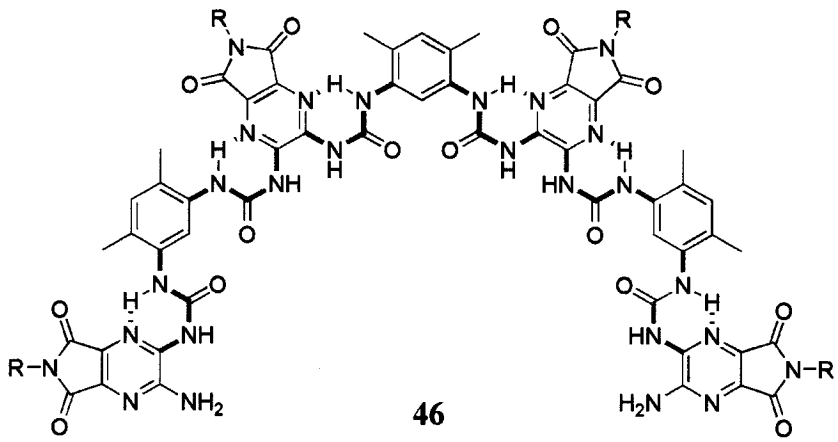

46

Figure 2-10 Proposed design for novel pyrazine foldamers. The bonds with restricted rotation are highlighted in green.

3. Pyrimidine Foldamers

3.1. Pyrimidine Overview

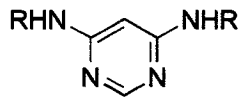

Figure 3-1 A substituted pyrimidine ring.

As the pyrimidine ring has a dipole of 2.4 D[76], it is slightly less aromatic than pyrazine, but more so than pyridazine[51]. Pyrimidine is an important heterocycle in Nature as it is the basis of two of the four bases of DNA and due to the 1-3 position of the heterocyclic nitrogen atoms it has often been included in supramolecular assemblies[77].

As described in Chapter 1, pyrimidine has been used in foldamers where restricted rotation is the result of the preferred *transoid* arrangement of adjacent monomer dipoles, as well as hydrogen bonding interactions[33,78,49]. It has also been used to prepare amide-linked foldamers as seen in Figure 3-2 where folding is caused by restricted rotation enforced by two, three-center hydrogen bonds per amide linkage[79] with hydrogen bonding occurring between the amide hydrogen and the heterocyclic nitrogen of the pyrimidine ring. Intramolecular hydrogen bonding was confirmed with x-ray crystallography yielding hydrogen bond distances between 2.1 Å and 2.5 Å. As illustrated, oligomers **47**, **48**, and **49** each have different curvatures (Figure 3-2). Based on the connectivity of the monomeric units, foldamer **47** would yield a straight chain, foldamer **48** a helical structure, and foldamer **49** a straight, undulating chain[79].

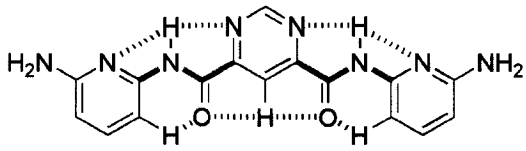

47

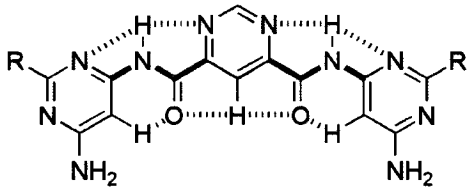

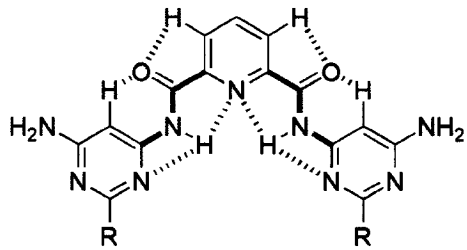

R = S-*n*-alkyl

48 49

Figure 3-2 Examples of pyrimidine based foldamers containing amide linkages. The bonds with restricted rotation are highlighted in green.

We would like to explore pyrimidine based foldamers containing urea linkages. Rotation along the bond linking the aromatic substituents to the urea group is restricted by the combination of hydrogen bonding and steric effects. As illustrated by the proposed heptamers **50**, **51**, and **52** in Figure 3-3 curvature for the various pyrimidine based foldamers can be similar as those described for the proposed pyrazine heptamers (Section 2.1). However, due to the unique substitution pattern of the pyrimidine ring, these foldamers are expected to have different properties.

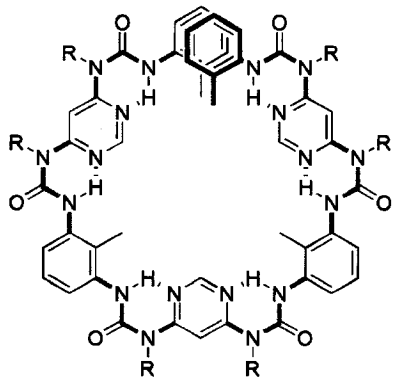

50

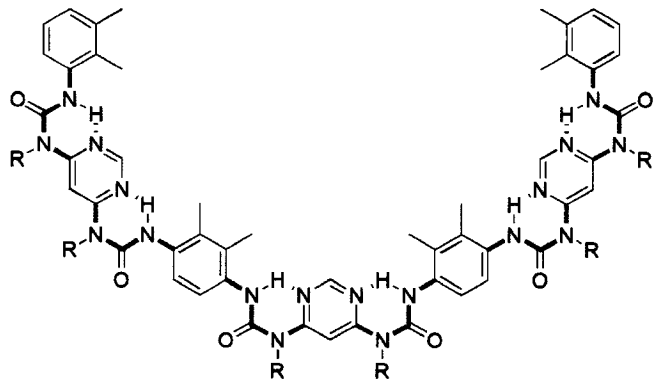

51

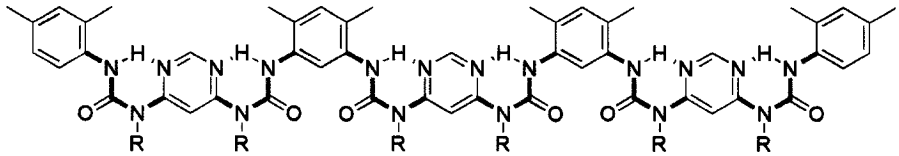

52

R = isobutyl, *n*-alkyl

Figure 3-3 Proposed pyrimidine heptamers. The bonds with restricted rotation are highlighted in green.

Target molecules **JM4**, **JM5**, and **53** are shown in Figure 3-4**.** Foldamers **JM4** and **JM5** have been previously prepared in our group[58], with reaction yields lower than reported for our pyridazine foldamers[57] (40 % *vs* 74 %). Herein we discuss efforts to improve the synthetic procedure and increase reaction yields in the synthesis of trimers **JM4** and **JM5**, as well as an attempt to synthesize pentamer **53.**

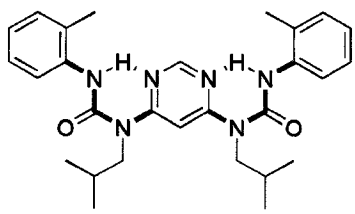

JM4

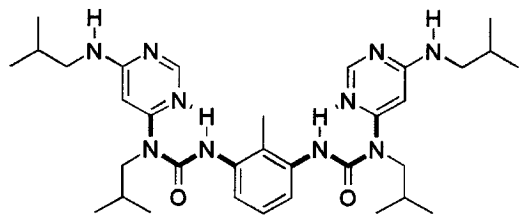

JM5

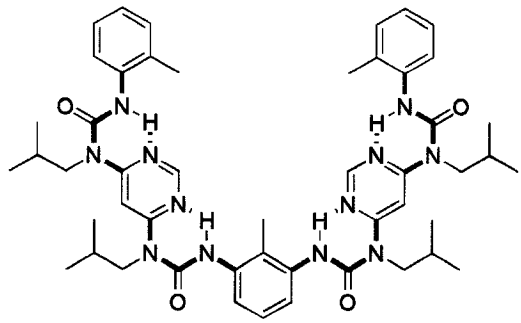

53

Figure 3-4 Target pyrimidine foldamers. Foldamers **JM4** and **JM5** are the capped and uncapped trimers, respectively. Foldamer **53** is the capped pentamer. The bonds with restricted rotation are highlighted in green.

3.2. Synthesis

Due to the lower reactivity of the pyrimidine heterocycle relative to pyridazine, an investigation was initiated in order to see if the reaction yield could be increased. As illustrated in Scheme 3-1, the synthetic route is similar to that used for the pyrazine foldamers.

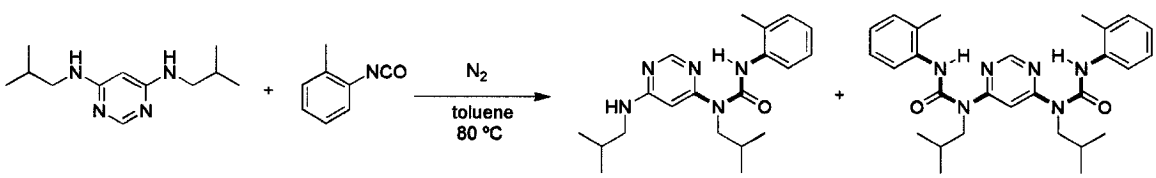

JM6 JM7 JM4

Scheme 3-1 Synthesis of **JM4**. The bonds with restricted rotation are highlighted in green.

N^4,N^6-Diisobutylpyrimidine-4,6-diamine (**JM6**) was prepared using previously developed methods[58]. When the reaction conditions described in Section 2.2.1 for the synthesis of the pyrazine trimer **JM3** were employed in the preparation of **JM4**, the product was isolated with a 75 % yield (*vs.* 40 % previously reported in our laboratory[58]) with **JM7** as the side product. It is thought that the increased yield is the result of the use of toluene rather than chloroform which allowed for a higher reaction temperature. Indeed, the reaction yield for the synthesis of trimer **JM5** (Scheme 3-2) increased from 18 % to 44 % when the reaction solvent was changed from chloroform to toluene.

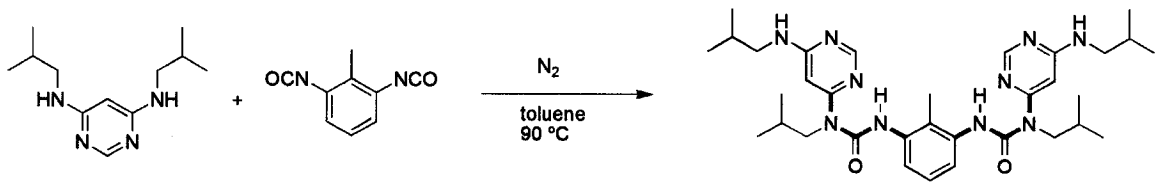

JM6 **JM5**

Scheme 3-2 Reaction scheme for the synthesis of **JM 5**. The bonds with restricted rotation are highlighted in green.

The same reaction conditions used for the synthesis of **JM4** and **JM5** were attempted in the unsuccessful synthesis of pentamer **53** as illustrated in Scheme 3-3.

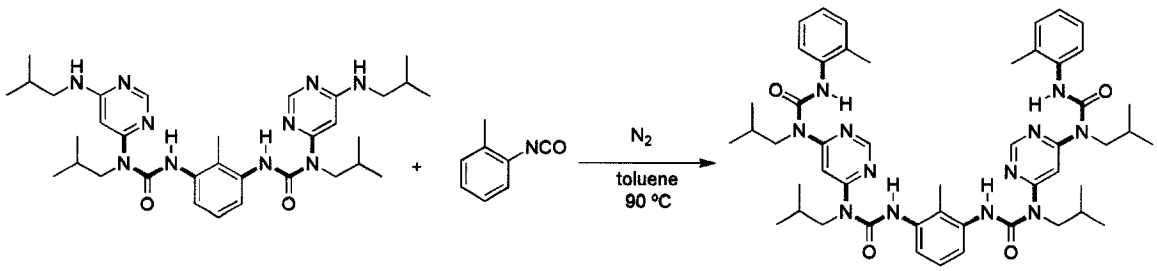

JM5 **53**

Scheme 3-3 Proposed scheme to synthesize 53. The bonds with restricted rotation are highlighted in green.

3.3. Characterization

The identity of **JM4** and **JM5** was confirmed using ^{1}H NMR. As illustrated in Figure 3-5, the chemical shift of the urea proton is observed at 12.6 ppm for trimer **JM4** and 12.8 ppm for trimer **JM5**. This indicates that hydrogen bonding is taking place between the urea hydrogen and the heterocyclic nitrogen of the pyrimidine ring in both foldamers, unlike what was described for the pyrazine oligomers. The fact that the urea proton resonances are similar suggests that the hydrogen bonding in both trimers is similar in strength.

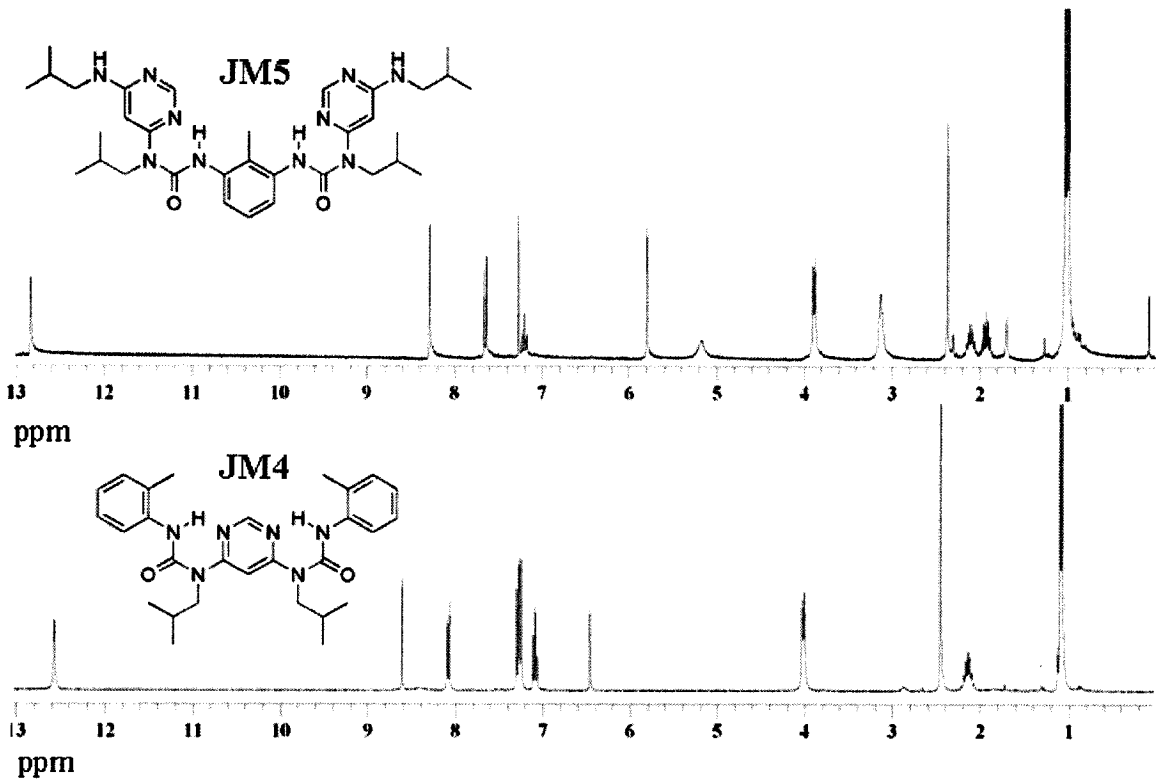

Figure 3-5 ^{1}H NMR spectra of **JM4** and **JM5**.

The spatial arrangement of **JM4** was probed using NOESY. The resulting spectrum (Figure 3-6) illustrates a NOE contact between the tolyl methyl group and the

proton on carbon 2 of the pyrimidine ring (highlighted by the black dotted line). This was expected as the distance between the two atoms is estimated to be 2.8 Å. NOE contacts were observed between the urea proton and both the protons on the tolyl methyl group and the proton on carbon two of the pyrimidine ring, demonstrating that steric interactions also aid in driving the folded conformation. Furthermore, an NOE contact is observed between the tolyl methyl protons and the *ortho* proton on the same tolyl ring.

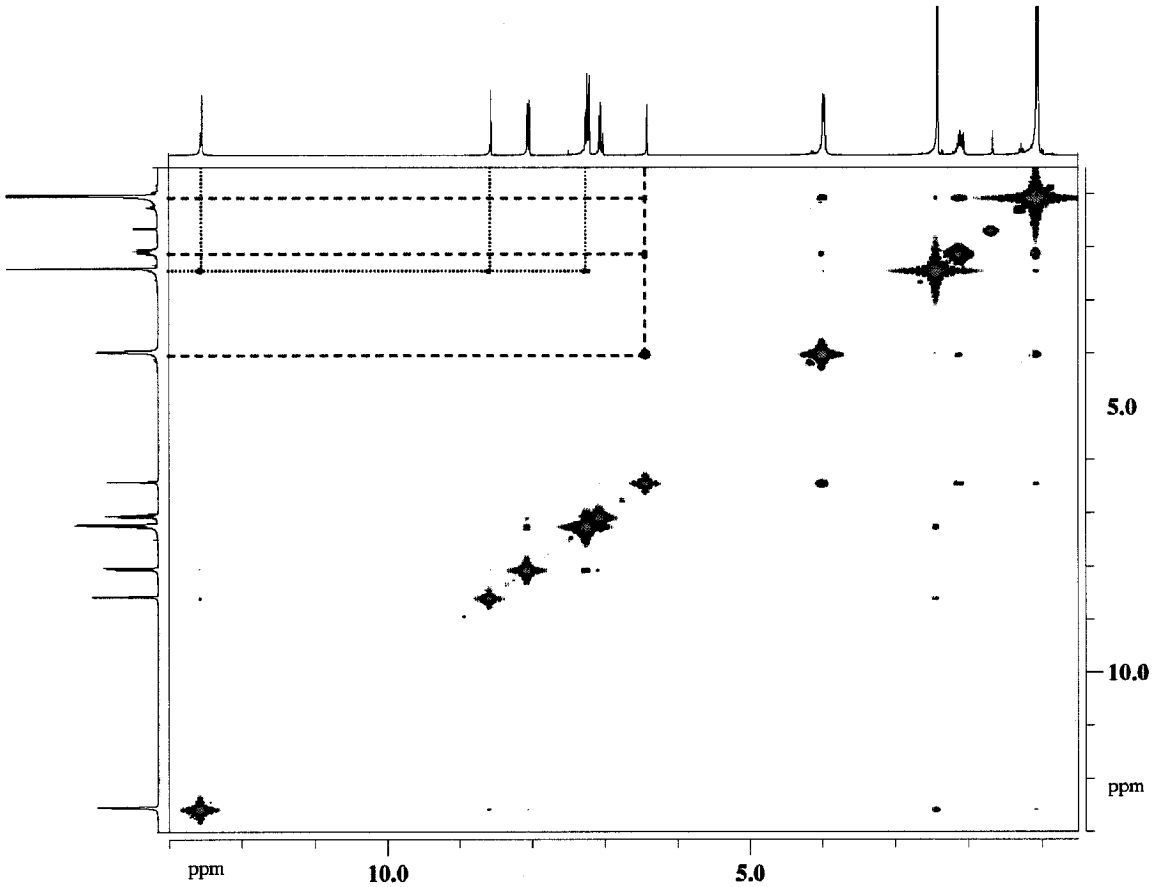

Figure 3-6 NOESY spectrum of **JM4**.

The conformational stability of **JM4** was probed by changing the solvent in which the trimer is dissolved. As indicated by the location of the urea peak in chloroform, folding is driven by restricted rotation caused by hydrogen bonding. If the hydrogen

bonding was masked by solvent effects, then the oligomer should 'denature' and adopt a non-folded conformation, illustrating the dynamics in the foldamer design. The intramolecular hydrogen bonding is expected to be masked by polar solvents such as methanol due to intermolecular hydrogen bonding with the solvent.

Spectra of **JM4** were obtained in both chloroform and methanol and are shown in Figure 3-7. Notable is the absence of the exchangeable urea proton chemical shift in methanol. The signals of the pyrimidine protons are shifted upfield by 0.2 to 0.4 ppm in methanol and this is likely due to interactions between the solvent and the pyrimidine heterocyclic nitrogen atoms.

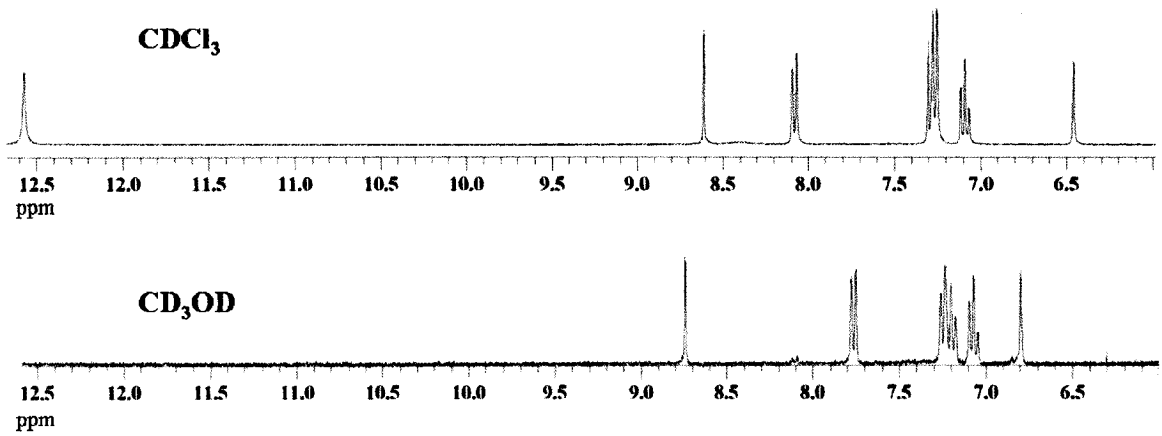

Figure 3-7 ^{1}H NMR spectra of **JM4** in chloroform and methanol.

A NOESY spectrum of **JM4** was recorded using deuterated methanol as solvent (Figure 3-8). The spectrum is similar to that obtained in chloroform (Figure 3-6), with the exception of the absence of the urea proton cross-peaks, as well as the cross-peak between the tolyl methyl group and the proton at carbon 2 of the pyrimidine ring. The former is explained by the aforementioned exchange with deuterium in the solvent. The latter may be due to unfolding, moving the groups beyond the NOESY detection range of 5 to 6 Å.

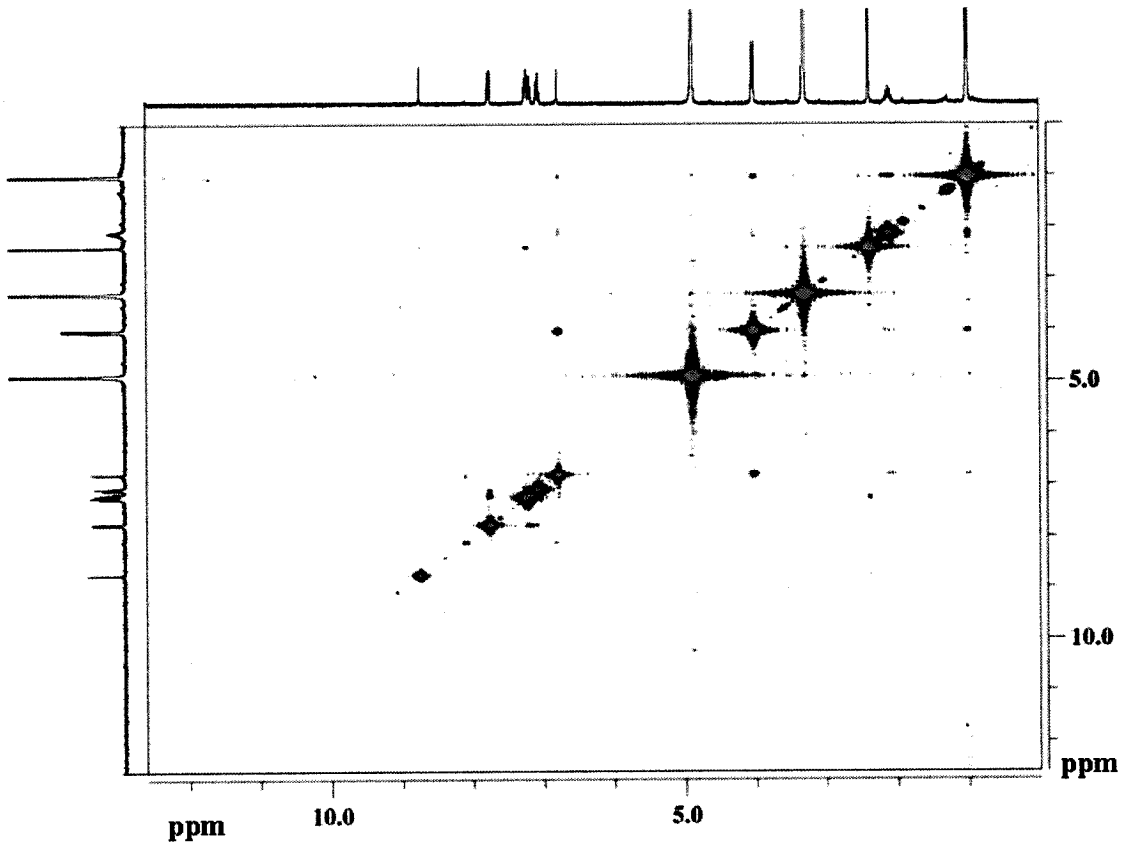

Figure 3-8 NOESY spectrum of **JM4** in CD_3OD.

A NOESY was obtained for **JM5** and a NOE contact was observed between the tolyl methyl group and the proton at carbon 2 of the pyrimidine ring. This confirms that the molecule is folding as expected. Furthermore, as was seen in **JM4**, NOE contacts were observed between the isobutyl chains and the proton at carbon 5 of the pyrimidine ring aiding with the assignment of proton peaks.

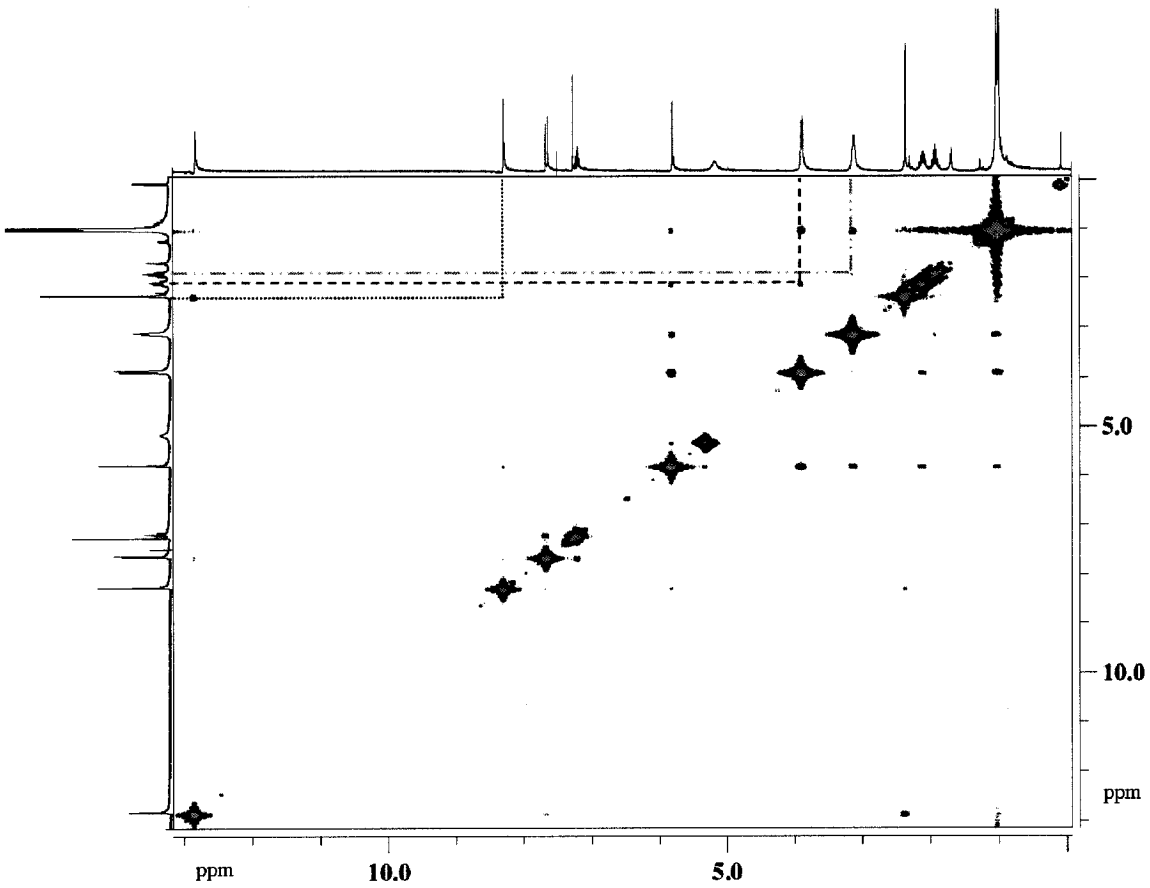

Figure 3-9 NOESY spectrum of **JM5**.

The product isolated in the synthesis of the pentamer **53** was **JM4**. Initially, this was not thought possible, however Chang and co-workers have recently described thermally reversible urea linkages in sol-gels and other polymers[80,81]. They have shown that it is possible for urea linkages to decompose to their corresponding amines and isocyanates under heat, and reform the urea linkages on cooling. These observations were used to explain our results. As illustrated in Scheme 3-4, **JM5** can dissociate to the corresponding TDI and **JM6** starting materials upon heating. With the addition of the *o*-tolyl isocyanate, newly formed **JM6** can preferentially react with *o*-tolyl isocyanate, forming **JM4**. **JM4** is expected to be more thermally stable than the uncapped derivative. The trimer is capped at its reactive ends and it can no longer undergo further reaction.

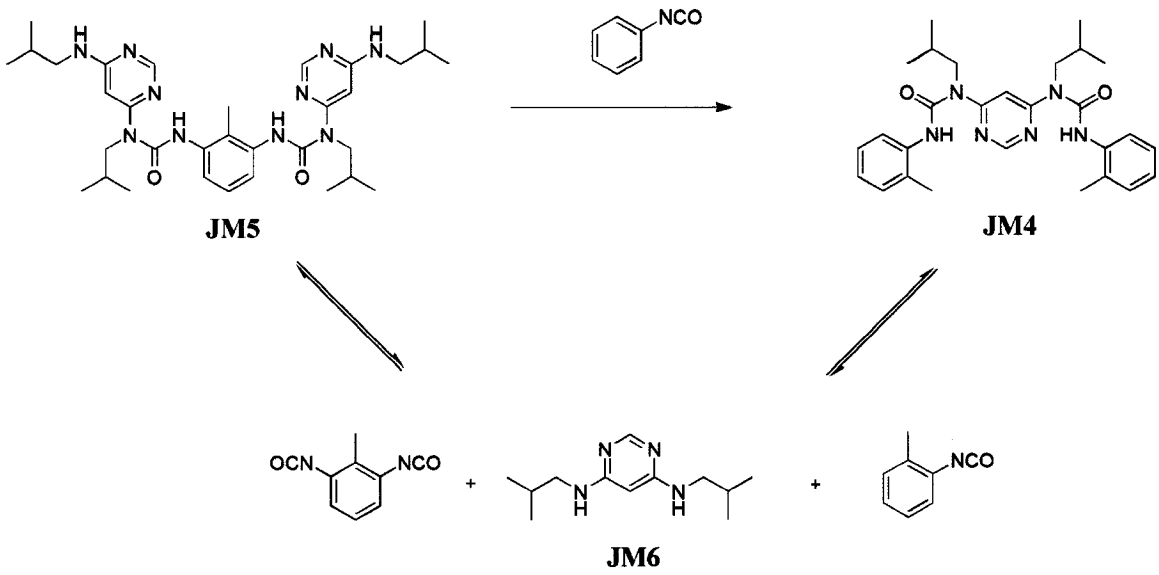

Scheme 3-4 Proposed reversible urea linkages as observed in the attempted synthesis of **53**.

As it appears that the reaction is thermally reversible, the reaction was attempted at a lower temperature in an effort to preserve the integrity of **JM5**. However, reactions conducted at 40 °C, 50 °C, and 60 °C did not yield product and only the starting material was recovered. At 70 °C, only the undesired **JM4** was obtained. The reactions were attempted at 10 °C intervals to 130 °C, all yielding the undesired product with no evidence of pentamer formation.

3.4. Future Work

Future work on the trimeric foldamer will include a detailed investigation of folding/unfolding dynamics. This can be carried out with exchange and titration NOE NMR studies. By knowing how to control folding of these molecules they could be used for host/guest interactions and in the transport of small molecules. Furthermore the dissociation constant of the urea linkage will be investigated using variable temperature NMR experiments. By understanding the nature of the urea linkage, future problems in

preparing longer oligomers may be avoided. Finally, a new procedure will likely have to be developed to synthesize the pentamer and possibly longer oligomers.

4. Pyridazine System

4.1. Pyridazine Overview

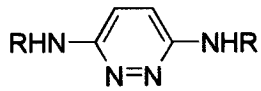

Figure 4-1 A substituted pyridazine ring.

The nitrogen atoms within the pyridazine ring are situated in the 1- and 2-positions. As shown in Figure 4-1, a consequence of this substitution pattern is that the dipoles of the heterocyclic nitrogen atoms are oriented in the same general direction (offset by 30°), giving this diazine the largest net dipole of 4.0 D[76]. Consequently pyridazine is the least aromatic of the three diazines[51]. Due to the relative positions of the heterocyclic nitrogen atoms, the pyridazine foldamers described herein require the urea linkages to be *para* with regards to one another (Figure 4-1).

Most of the previous work in our group has revolved around using pyridazine and toluene monomer units in urea linked foldamers[82]. As depicted in Figure 4-2, folding in pyridazine foldamers is the result of both hydrogen bonding and steric effects. For trimer **54**, conformer **54a** is favoured and hydrogen bonding between the urea hydrogen and the heterocyclic diazine nitrogen atoms is observed by ^{1}H NMR and the conformation was confirmed with x-ray crystallography (**54b**) where the hydrogen bond distance was determined to be 1.91 Å[82]. The ^{1}H NMR and x-ray studies both demonstrate that restricted rotation through hydrogen bonding is inducing the global folding of this molecule. Though this molecule does not contain a full helical turn, the out-of-plane twisting expected for a helix is observed due to steric repulsion between the two tolyl

methyl groups. These observations are important as they confirm the possibility to have some flexibility along the bonds linking the aromatic monomers and the urea bridge. In the extreme, this can give rise to less favourable conformers **54c** and **54d**. Conformer **54c** would be higher in energy relative to **54a** due to steric interactions and the absence of NH··N hydrogen bonding. Conformer **54d** is not optimal due to the lack of NH··N hydrogen bonding in addition to repulsive steric effects between the tolyl methyl groups and the carbonyl oxygen atoms of the urea linkages.

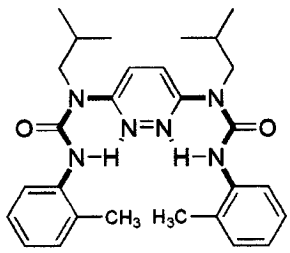

54a

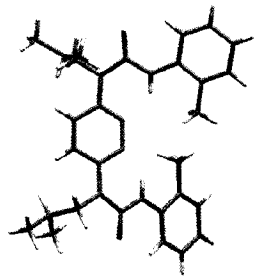

54b

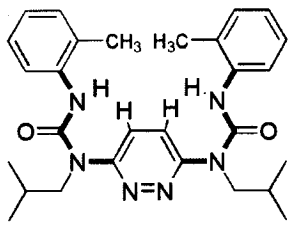

54c

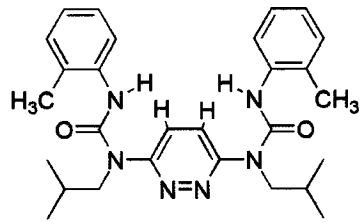

54d

Figure 4-2 Folding propensity in the pyridazine system. Conformer **54a** is preferred due to additive hydrogen bonding and steric effects as confirmed by x-ray crystallography (**54b**). The bonds with restricted rotation are highlighted in green.

A pyridazine pentamer containing tolyl units has also been synthesized (**55**). Folding in this oligomer is again induced by the restricted rotation about the bonds

linking the aromatic groups to the urea linkage. This was confirmed by ^{1}H NMR as the urea proton resonances were observed at 11.4 ppm and 11.6 ppm, indicative of hydrogen bonding between the urea hydrogen and the pyridazine heterocyclic nitrogen atoms[57]. In this case there are two observed resonances due to the fact that these urea protons are not chemically equivalent. There was also overlap of the terminal tolyl groups as the corresponding proton signals were shifted upfield relative to what was observed in the capped trimer **54**. This can be explained by the anisotropic effects that would occur when the tolyl rings overlap[57]. With these observations it can be said that conformer **55a** of Figure 4-3 is the most likely conformation for **55** as conformers **55b** and **55c** lack hydrogen bonding and exhibit some unfavourable steric interactions.

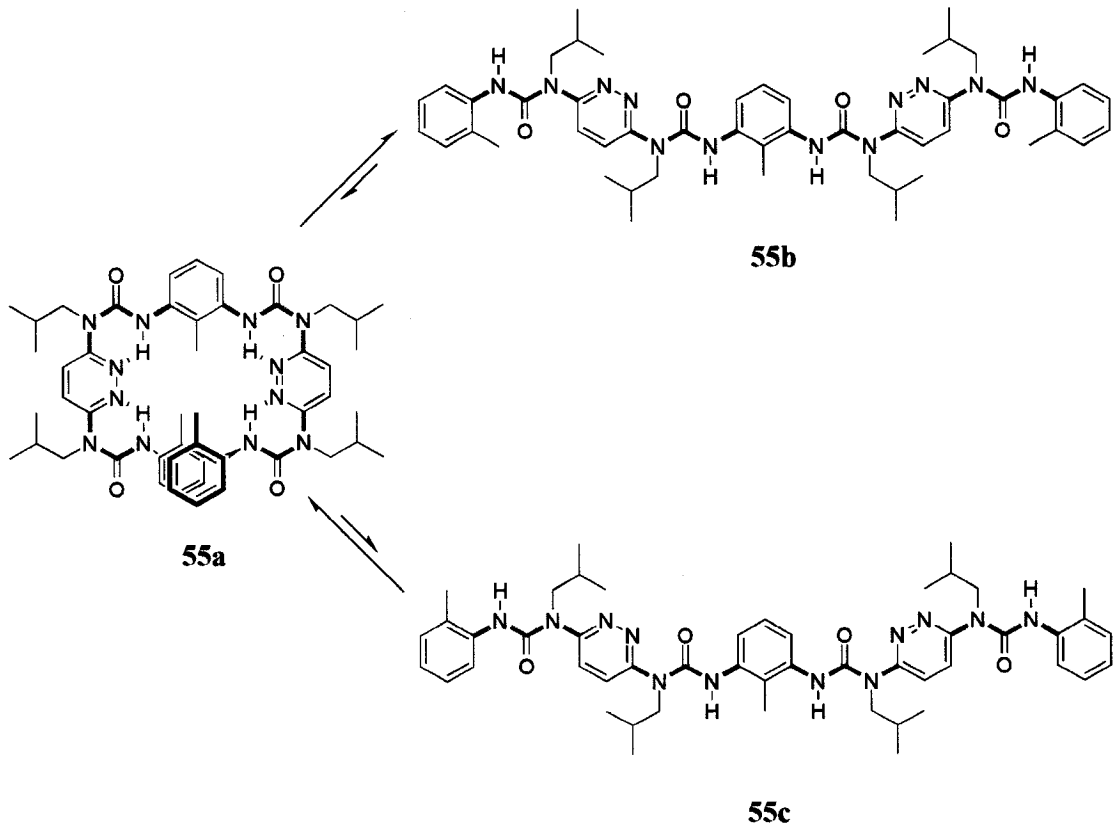

Figure 4-3 Folding propensity in the pyridazine tolyl pentamer. The bonds with restricted rotation are highlighted in green.

Due to the restricted rotation by non-covalent interactions in the tolyl trimer **54** and pentamer foldamer **55**, it is clear that these building blocks should be able to macrocyclize as the restricted rotation can also be thought of as a self-templating effect. As seen in Figure 4-3, the pentamer can be viewed as a macrocycle with unlinked, overlapping ends. Macrocycles **56** and **57** shown in Figure 4-4 were previously prepared in our laboratory. A crystal structure of both **56** and **57** were obtained and the hydrogen bond lengths were measured to be 2.6 Å[83]. Unlike what was reported for foldamers discussed in Chapters 2 and 3, formation of the macrocycle from the dimer (**JM8**) and TDI readily occurs[84]. An explanation for this is the relatively small size of the macrocycle (four aromatic units) which when combined with the self-templating effect by restricted rotation, creates a high effective molarity between the two reactive ends during the reaction. Therefore, the tetramer readily closes, yielding the macrocycle. An interesting property of these macrocycles is their ability to self-assemble at a graphite solution interface, which was observed using scanning tunneling microscopy[83].

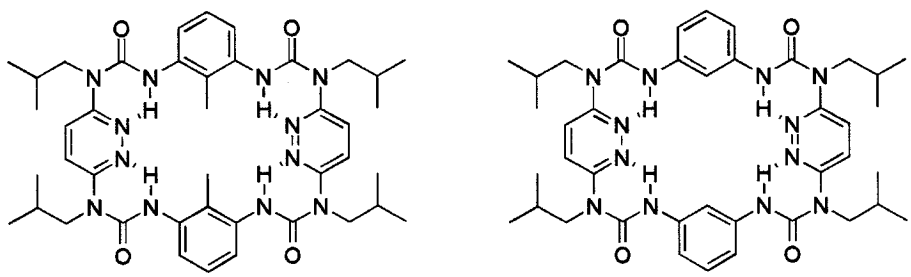

56 **57**

Figure 4-4 Pyridazine macrocycles. Macrocycle **56** contains a methyl group on the non-heterocyclic aromatic monomer that is absent in macrocycle **57**.

4.2. Synthesis of the *m*-Xylyl and *o*-Xylyl Monomers

4.2.1. Overview

As previously stated in this thesis, there are two ways to tune the curvature of our foldamers. The first is by altering the heterocyclic diazine, which has been described in this thesis. The second is to alter the non-heterocyclic aromatic unit. By altering the non-heterocyclic monomer while keeping the diazine constant as shown in Figure 4-5, we can access different curvatures that may lead to unique molecular geometries. Pentamer **55** was previously prepared by Liyan Xing and was discussed in the introduction of this thesis. Our goal is to now expand our system to incorporate *o*-xylyl and *m*-xylyl moieties as illustrated by heptamer **59** and tridecamer **60**.

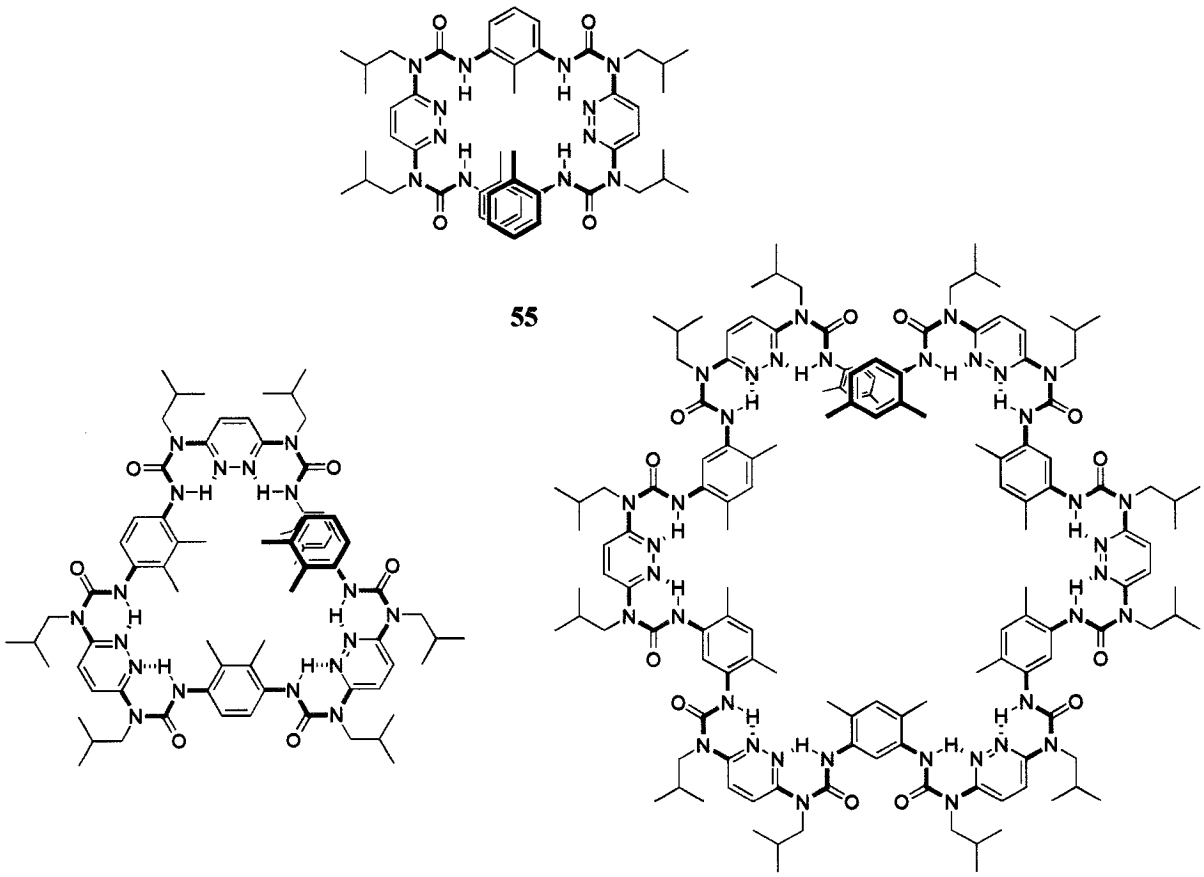

55

59

60

Figure 4-5 Pyridazine tolyl (**55**), *o*-xylyl (**59**), and *m*-xylyl (**60**) foldamers exhibiting one full helical turn. The bonds with restricted rotation are highlighted in green.

Synthetic methods used in the synthesis of the tolyl pentamer **55** are similar to those described for the pyrazine and pyrimidine foldamers in that isocyanates were used to prepare the urea linkages as depicted in Scheme 4-1. An advantage of this method is the commercial availability of the two tolyl isocyanates, which readily react with the pyridazine diamine. However, the isocyanates of the *o*-xylyl and *m*-xylyl monomers are not commercially available and must be prepared from their corresponding diamines. This in itself poses a challenge as neither of the two required diamines is commercially available and must be synthesized.

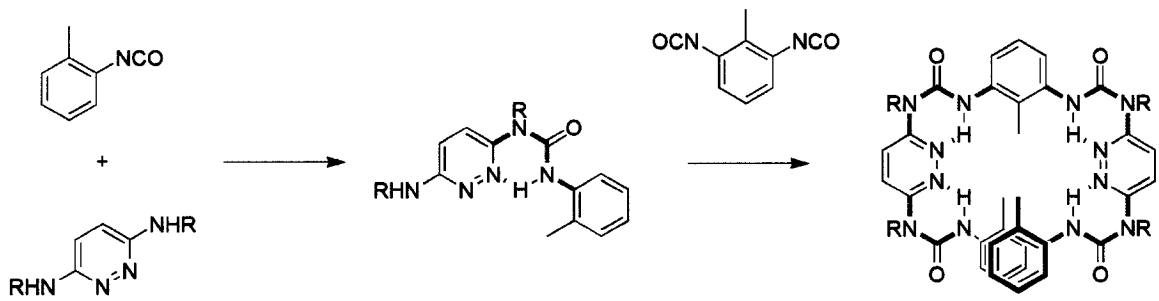

JM8 **55**

Scheme 4-1 Reaction scheme for the synthesis of **55**. The bonds with restricted rotation are highlighted in green.

The synthesis of the 4,6-diamino-*m*-xylene is reported throughout the literature as the reduction product of 4,6-dinitro-*m*-xylene[16]. The synthesis of the dinitro compound was reported by Thesmar and co-workers early in the last century by nitration of *m*-xylene[85]. As shown in Scheme 4-2, nitration occurs by aromatic substitution *ortho* and *para* to the methyl groups, which subsequently places the nitro groups *meta* relative to each other. Though three products were obtained, we are only interested in isolating the 4,6-dinitro-*m*-xylene **JM9**. Unfortunately, in the synthesis of the desired product from *m*-xylene a significant amount of the trinitro compound **62** is obtained due to the use of excess nitric and sulfuric acids[86].

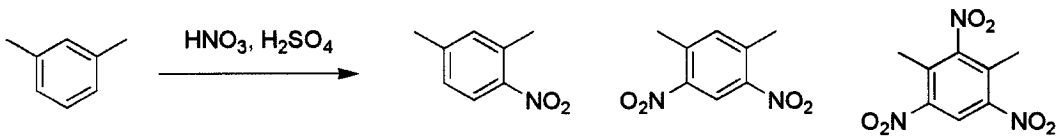

JM9 **62**

Scheme 4-2 Nitration of *m*-xylene as reported by Thesmar.

Suzuki and co-workers have more recently used zeolites to catalyze the Kyodai nitration of toluene[87] as shown in Scheme 4-3. The Kyodai nitration relies on the reaction

of nitrogen dioxide with ozone to prepare dinitrogen pentoxide *in situ*, which is used as a source for the nitronium ion. The process using zeolites is described as a two step process. The first nitration happens slowly *ortho* to the tolyl methyl group and the second nitration then occurs selectively in the *para* position due to the steric implications of the catalyst. The result of this is the predominant formation of 2,4-dinitro toluene. This method is attractive due to the preferential *ortho* and *para* positions of the two nitro substituents relative to the methyl group, which is the desired substitution in our xylene starting material.

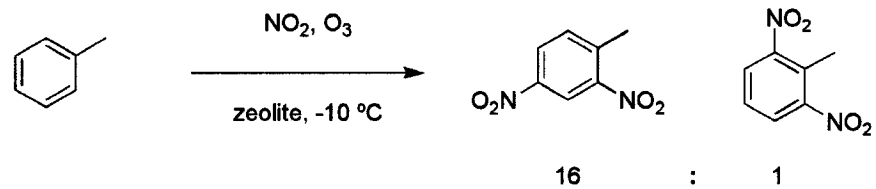

Scheme 4-3 Zeolites can be used to selectively nitrate toluene in the 2,4-positions.

Gong and co-workers have described the nitration of 4-nitro-*m*-xylene using the traditional nitric acid/sulfuric acid method[16]. The advantage of this method is the inexpensive commercial availability of 4-nitro-*m*-xylene. With careful control of the reaction conditions, it is possible to obtain the desired dinitro compound in high yield while minimizing nitration at the 2-position[16]. For this reason, and the reported high yield of the reaction, this method was used to prepare **JM9** followed by the reduction of the nitro groups to obtain **JM15**. There are two common methods to achieve the reduction: (*i*) reduction using iron filings and hydrochloric acid[86], and (*ii*) reductive hydrogenation with hydrogen gas over palladium on carbon[16]. The latter method was chosen due to the relative ease in the reaction work-up and the reported high yields[16].

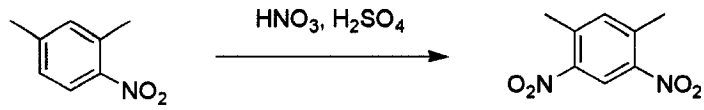

75 %

JM9

Scheme 4-4 Nitration of 4-nitro-*m*-xylene by Gong and co-workers.

The synthesis of 3,6-diamino-*o*-xylene cannot be carried out using the same methodology described in the synthesis of 4,6-diamino-*m*-xylene due to the *meta* directing nature of the nitro group. Therefore nitrating 3-nitro-*o*-xylene would yield 3,5-dinitro-*o*-xylene as shown in Scheme 4-5[85,88].

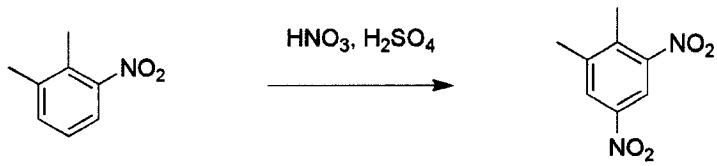

Scheme 4-5 Observed product from the nitration of 3-nitro-*o*-xylene.

Another route to prepare the desired *para* diamine was to nitrate 2,3-dimethyl aniline. The advantage of this route is that the amino group is strongly *ortho/para* directing, and therefore substitution would occur in both the 4- and 6-positions (Scheme 4-6), with the latter being the sterically preferred substitution. However, as the reaction is electrophilic in nature, the nucleophilicity of the amine group must be masked with the use of a protecting group[89,90]. The desired final product would be obtained by removal of the protecting group, followed by reduction of the nitro group. Nitration with dinitrogen pentoxide is not desirable due to selective nitration at the 4-position. As shown in Scheme 4-7, a complex is formed between the acetyl oxygen and one of the nitro groups of the dinitrogen pentoxide[91-93]. Nitration using nitric and sulfuric acids creates a mixture

of products as shown in Scheme 4-6 where the isomers can be separated and subsequent reduction yields the desired diamine product(**JM12**)[90].

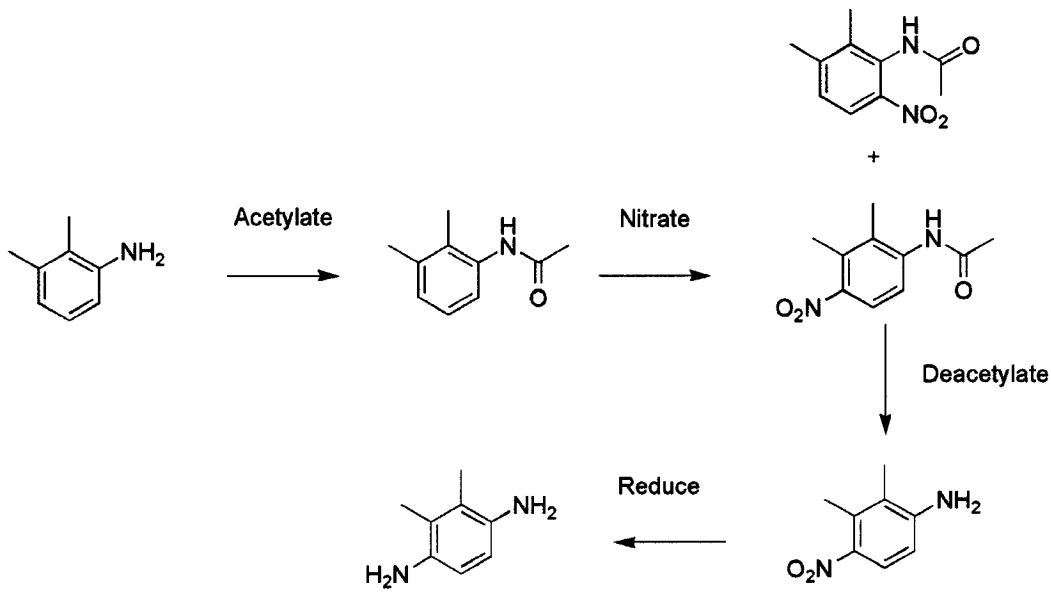

Scheme 4-6 Proposed scheme for the synthesis of 3,6-diamino-*o*-xylene.

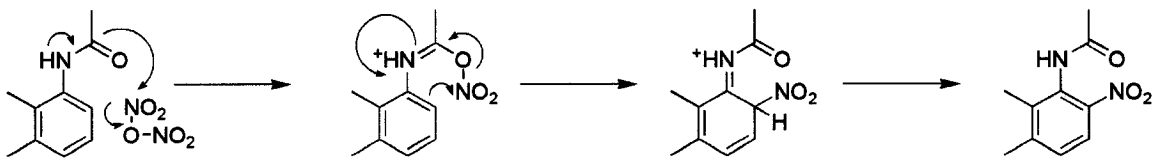

Scheme 4-7 Selective *ortho* nitration using nitrogen pentoxide.

In 1901 Thesmar and co-workers described an alternative means to prepare 3,6-diamino-*o*-xylene. The method involves an azo coupling between *m*-sulfanilic acid and 2,3-dimethyl aniline as depicted in Scheme 4-8. Subsequent reduction of the azo bond gives the desired diamine with good selectivity[85,89]. To the best of our knowledge, the use of this methodology to prepare 3,6-diamino-*o*-xylene has not since been reported in

the literature. However, the use of azo chemistry and the reduction of azo bonds has been reported in the efficient synthesis of various diamines for use as dyes[94,95].

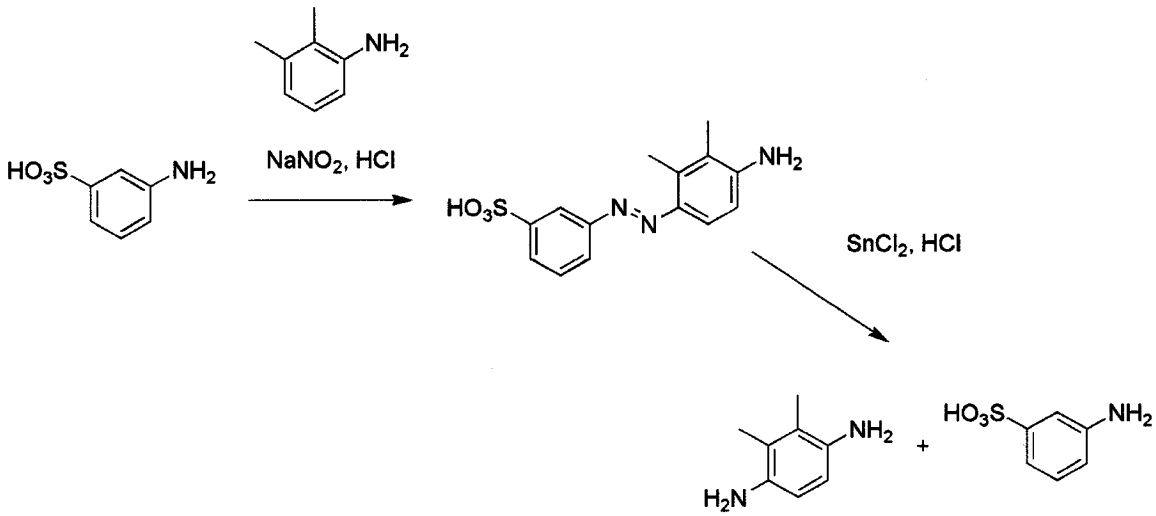

Scheme 4-8 Thesmar's method of preparing 3,6-diamino-*o*-xylene through azo coupling.

4.2.2. Synthesis

The 4,6-diamino-*m*-xylene was prepared from the 4-nitro-*m*-xylene according to the method described by Gong and co-workers[16]. The product was isolated in approximately 50% yield, with the remaining product being the trinitro compound. This reaction yield was not improved by decreasing the reaction time, as the decrease of the 2,4,6-trinitro-*m*-xylene formation was offset by the presence of unreacted starting material.

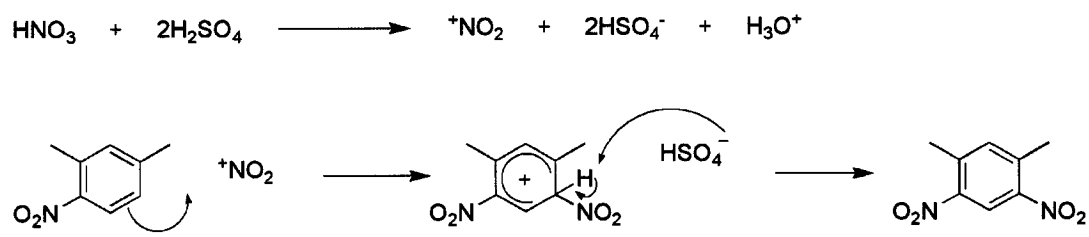

Scheme 4-9 Mechanism for the nitration of 4-nitro-*m*-xylene.

The first route for the synthesis of 3,6-diamino-*o*-xylene that was explored was the nitration of the acetylated 2,3-dimethyl aniline (**JM10**). As previously described, the amino group was protected with an acetyl group in order to minimize the reaction between the nucleophilic amine and the positively charged nitronium ion (Scheme 4-10).

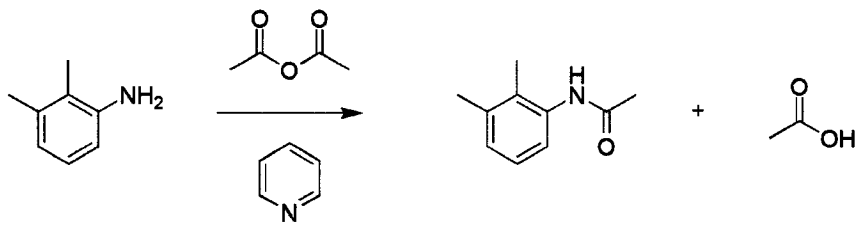

JM10

Scheme 4-10 Acetylation of 2,3-dimethyl aniline.

The nitration of **JM10** was more challenging than the nitration of **JM9**, due to the possible formation of several products as shown in Figure 4-6. Initial nitration conditions were the same as those used in the synthesis of 4,6-dinitro-*m*-xylene. The reaction yielded products **64** and **65** (Figure 4-6). **JM11** can be obtained if the nitration is quenched immediately following the addition of the nitric acid and removal of the acetyl group[90]. The products isolated where those with the nitro group *para* to the amine and with the nitro group *ortho* to the amine. The simultaneous nitration at the *ortho* and *para* positions was expected as it has been previously reported in the literature[91].

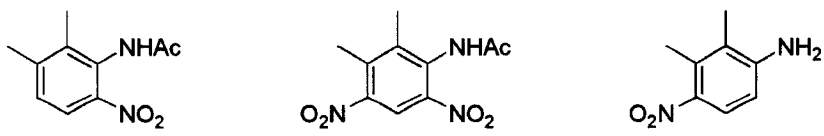

64 **65** **JM11**

Figure 4-6 Possible products from the nitration of acetylated 2,3-dimethyl aniline. **JM11** was isolated after the acetyl group was removed.

Though it was demonstrated that it is possible to prepare the 3,6-diamino-*o*-xylene (**JM12**) through the nitric/sulfuric acid nitration route, it was obtained in only 15 % yield. To increase the yield of the diamine, the azo coupling reaction was attempted. A more recent protocol was chosen in order to prepare this azo compound[96] and is highlighted in Scheme 4-11. The azo group was subsequently reduced using tin(II)chloride and hydrochloric acid and the 2,3-diamino-*o*-xylene was isolated[94]. This method has an advantage over the previous nitration method in that no chromatography is required. Most importantly, the overall reaction yield of the diamine is 61 % compared to 12 % by the nitration method.

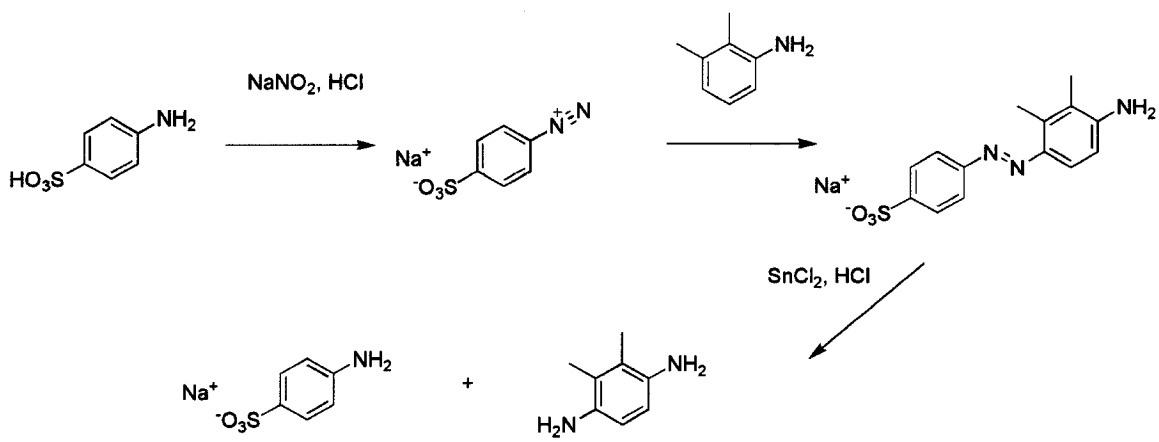

JM12

Scheme 4-11 Reaction pathway for the synthesis of **JM12** through an azo coupling mechanism.

4.3. Synthesis of Pyridazine Foldamers

4.3.1. Overview: Isocyanates

The purpose of synthesizing the above described diamines is to incorporate them into our foldamers. Some of the methods to prepare urea linkages from amines are highlighted in Figure 4-7. Phosgene or phosgene derivatives are often used to synthesize urea linkages[97,46,47]. In the case of phosgene, the carbon is a good electrophile as it is bound to an oxygen atom and two chlorine atoms, all of which are strongly electronegative. However, phosgene is known to have adverse health effects, and though diphosgene and triphosgene are relatively stable and safer to handle at room temperature, they are known to decompose to phosgene at higher temperatures[97]. A second method to prepare urea linkages is the use of *N,N'*-carbonyldiimidazole which contains an electrophilic carbon between two imidazole leaving groups[98,99]. Urea linkages can also be prepared from amines *via* carbamate intermediates.

Phosgene and Derivatives

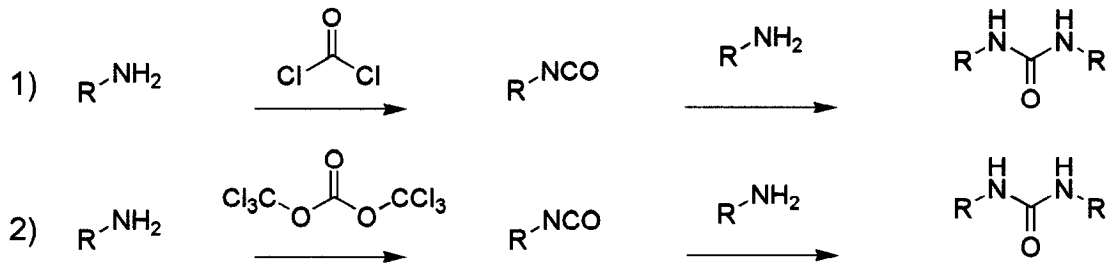

***N,N*-Carbonyldiimidazole**

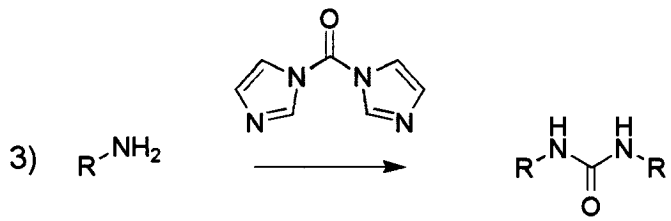

Carbamates

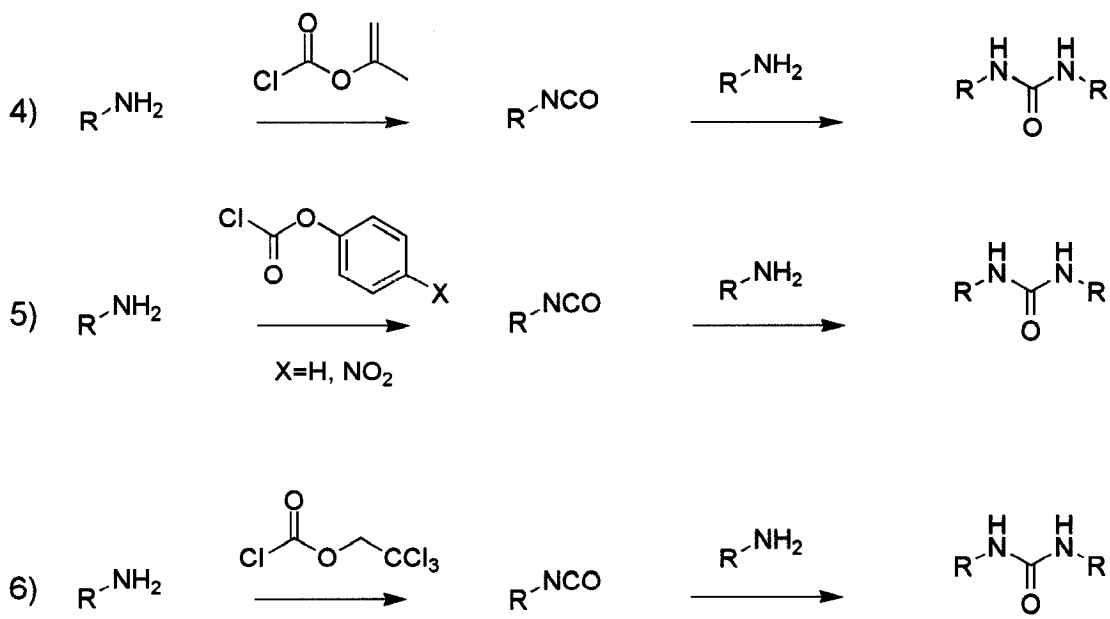

Figure 4-7 Methods used to prepare urea linkages.

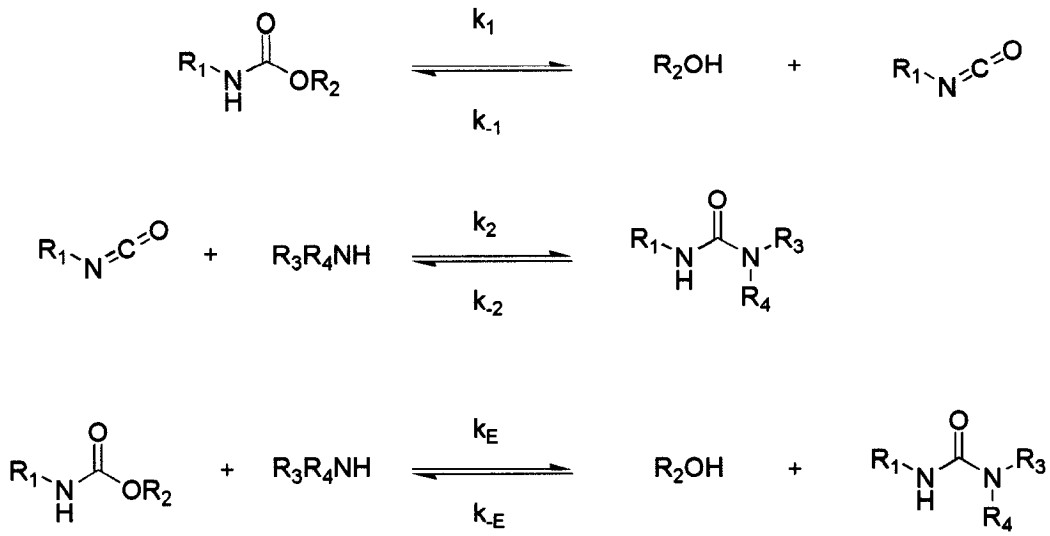

Scheme 4-12 Reaction mechanism for the formation of urea bonds with carbamates.

It is possible to use carbamates to prepare urea linkages due to the formation of an isocyanate intermediate in the reaction. As shown in Scheme 4-12, the carbamate reversibly dissociates into its corresponding alcohol and isocyanate, which can in turn react with an amine to form a urea linkage[57]. The acidity of the alcohol intermediate plays a key role in the progression of the reaction where more acidic alcohols favour urea dissociation[57]. 2,2,2-Trichloroethyl carbamates, or Troc-carbamates, (reaction **6** of Figure 4-7) are commonly used to prepare ureas[57,100,101]. Phenyl carbamates are also good candidates for the synthesis of urea linkages due to the known acidity of phenol[57]. Nitrophenyl carbamates are even better reagents for the synthesis of urea linkages due to the electron withdrawing effects of the nitro group. Nitrophenyl carbamates have been used to prepare oligourea peptidomimetics using both solution phase[102-104] and solid phase synthesis[105]. Indeed, it has been demonstrated that nitrophenyl carbamates can give urea linkages with higher yields than *N,N'*-carbonyldiimidazole or phosgene[103]. Vittorio and co-workers have recently described the use of isopropenyl carbamates in the

preparation of urea linkages[57]. Isopropenyl carbamates have the advantage that the enol formed during the carbamate dissociation quickly tautomerizes to form acetone, which is easily removed from the reaction mixture (Scheme 4-13). As the alcohol is removed from the equilibrium the reaction is driven to form the isocyanate[57]. Due to the reported use of *p*-nitrophenyl carbamates in the preparation of oligoureas, and the facile work up reported with the use of isopropenyl carbamates, these two methods were tested in the synthesis of our urea linkages.

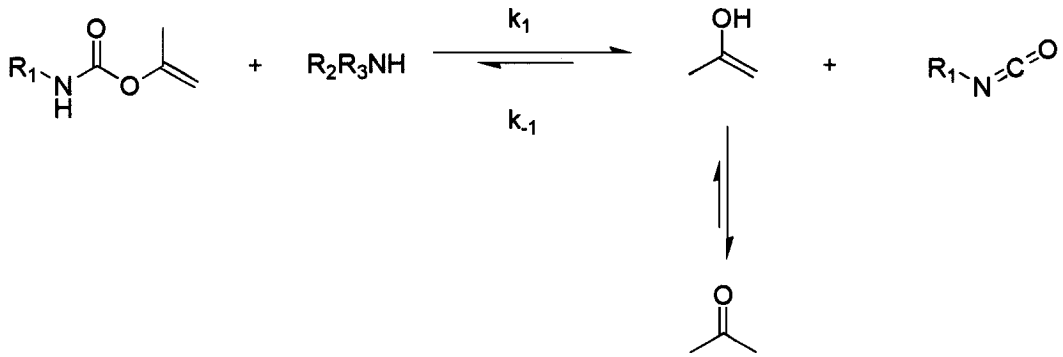

Scheme 4-13 Reaction mechanism for the *in situ* synthesis of isocyanates from isopropenyl carbamates.

4.3.2. Synthesis

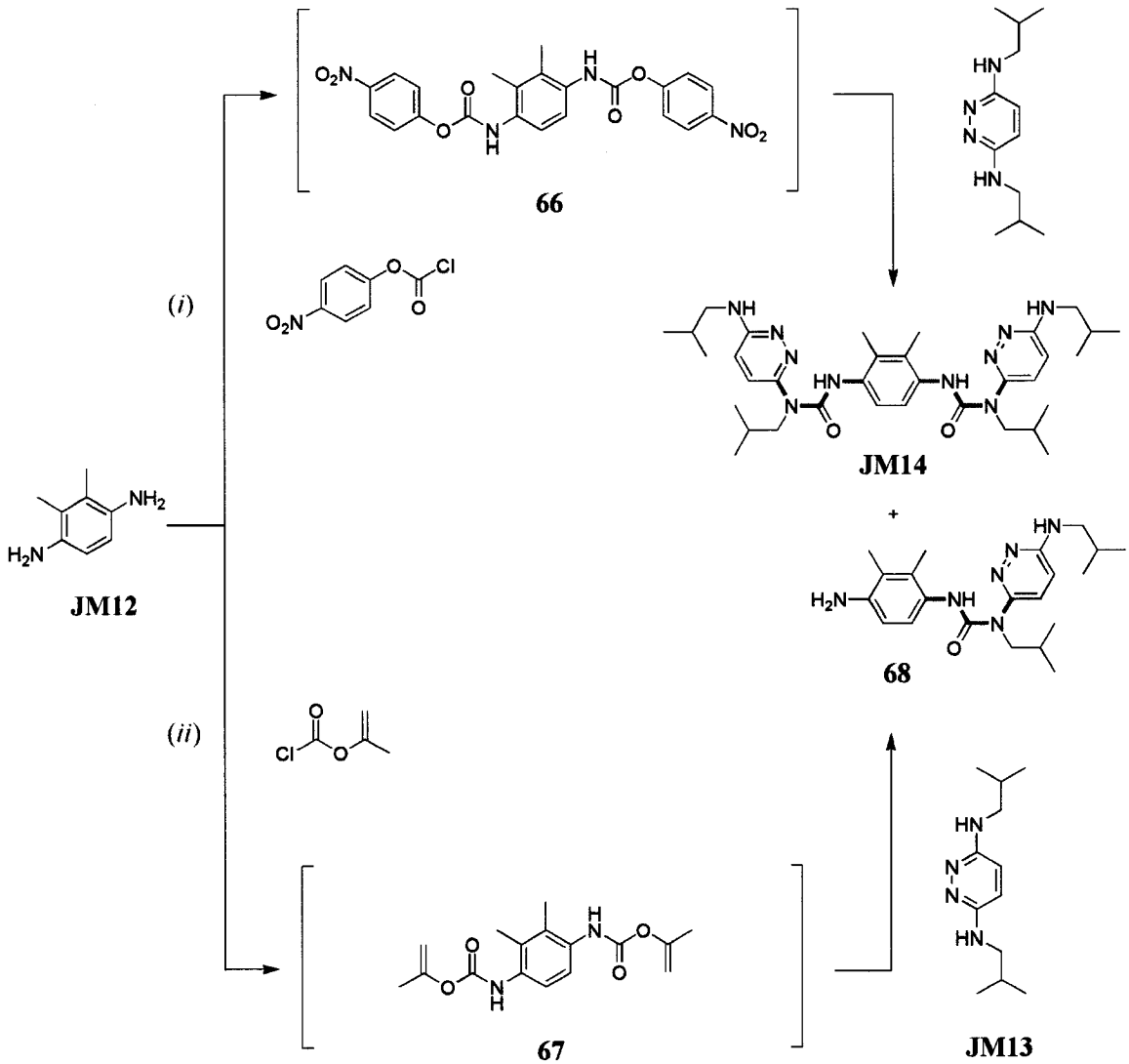

Scheme 4-14 Two routes used to prepare **JM14**. Both methods generate the bis-isocyanate *in situ*. The bonds with restricted rotation are highlighted in green.

The first method described in the synthesis of the *o*-xylyl pyridazine trimer (**JM14**) uses *p*-nitrophenyl carbamates in forming the urea linkages (Route (*i*) in Scheme 4-14). Efforts to characterize the bis-carbamate (**66**) were unsuccessful and it was decided to generate it *in situ* as previously described in the literature[103-105].

N^3,N^6-diisobutylpyridazine-3,6-diamine (**JM13**) was prepared as previously reported[57] and was reacted with freshly made **66**. One of the products generated in the

reaction was determined to be *p*-nitrophenol, which is expected (Section 4.3.1), demonstrating that the isocyanate was generated *in situ*. Both dimer **68** and the trimer **JM14** were prepared, though they were difficult to separate from one another by chromatography.

The second method described in the synthesis of **JM14** used isopropenyl carbamates (Route (*ii*) in Scheme 4-14). The bis-isopropenyl carbamate (**67**) of the *o*-xylyl diamine was prepared under Schotten Baumann conditions[57]. In order to avoid possible degradation, **67** was used immediately to prepare **JM14**. Carbamate **67** was reacted with excess **JM13** to yield two products, corresponding to the **68** and **JM14**. **JM14** was isolated in 16 % yield after chromatography on silica and alumina.

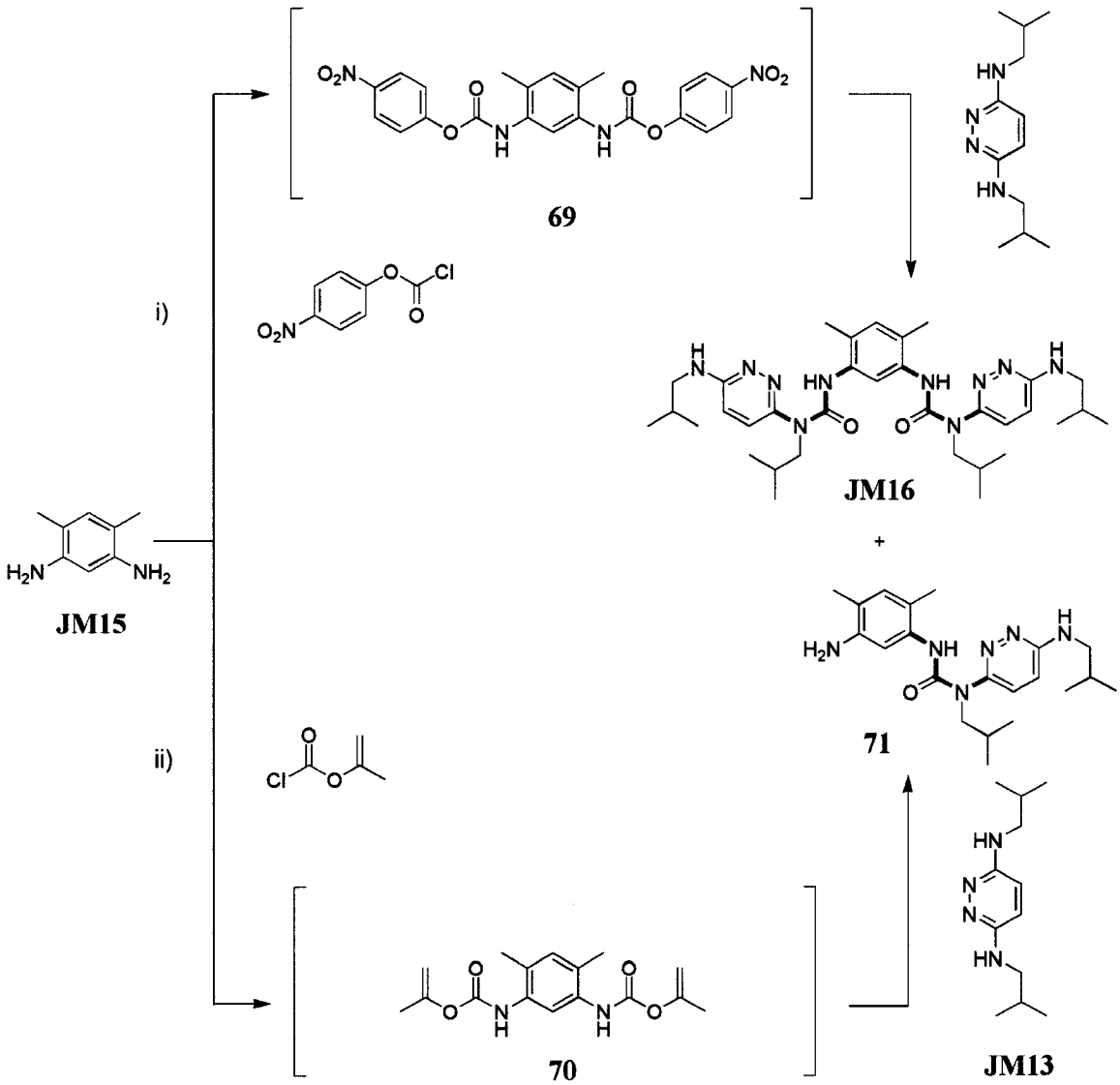

Scheme 4-15 Synthetic routes for the synthesis of **JM16**. As in the o-xylyl system, both *p*-nitrophenyl and isopropenyl carbamates were used. The bonds with restricted rotation are highlighted in green.

As illustrated in Scheme 4-15, the same synthetic route for the synthesis of **JM14** was used for **JM16**. The first route involves the use of *p*-nitrophenyl carbamates (**69**). Similar reaction conditions were followed to prepare the *m*-xylyl trimer **JM16** as described in the preparation of the *o*-xylyl trimer. Both the dimer **71** and trimer **JM16** were synthesized and **JM16** was isolated in 13 % yield. This lower than expected yield

prompted the synthesis of trimer **JM16** using the isopropenyl carbamate (**70**, Scheme 4-2). The same reaction conditions for the synthesis of **JM14** by this route were applied, but the overall reaction yield was only 8 %.

The *o*-xylyl trimer was capped using *o*-tolylene isocyanate (Scheme 4-16). This was chosen as N^3,N^6-diisobutylpyridazine-3,6-diamine has good reactivity towards tolyl isocyanates, facilitating the synthesis of longer foldamers. Moreover, a successful reaction would demonstrate that the monomer units can not only be varied from oligomer to oligomer, but also within the oligomer itself, greatly increasing the tunability of curvature in our system design.

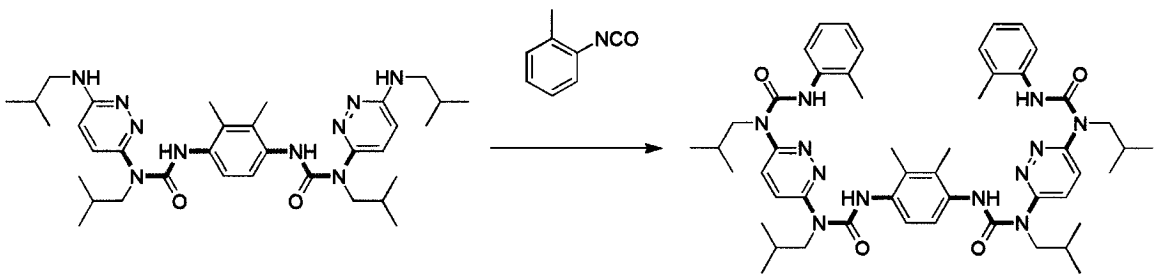

JM14 **JM17**

Scheme 4-16 Synthesis of **JM17** from **JM14**. The bonds with restricted rotation are highlighted in green.

It is preferable to complete a reaction from pure starting materials. However, due to the limited amount of pure **JM14**, a mixture of the *o*-xylyl trimer and dimer was used to prepare pentamer **JM17**. The amount of **JM14** used in the reaction was calculated based on the integration ratios between the urea and tolyl protons of the dimer and trimer. This value was then used to estimate the reported yield.

Pentamer **JM17** was synthesized from the dimer/trimer mixture and was isolated in approximately 50 % yield with respect to the amount of trimer estimated in the starting mixture. Though this route differs slightly from that described for the synthesis of **55**

(Scheme 4-1), the same reaction conditions were used for the synthesis of both the tolyl pentamer and the *o*-xylyl pentamer. Furthermore, lower reaction temperatures and reaction times were required for the preparation of pyrazine (**JM3**) and pyrimidine (**JM5**) trimers (Section 2.2 and Section 3.2).

The same methodology and reaction conditions reported for the synthesis of the *o*-xylyl pentamer were used in the synthesis of **JM18** (Scheme 4-17). As with the *o*-xylyl oligomer, a mixture of dimer and trimer was used to prepare the pentamer. The product was synthesized in approximately 50 % yield with respect to the amount of trimer estimated in the starting mixture.

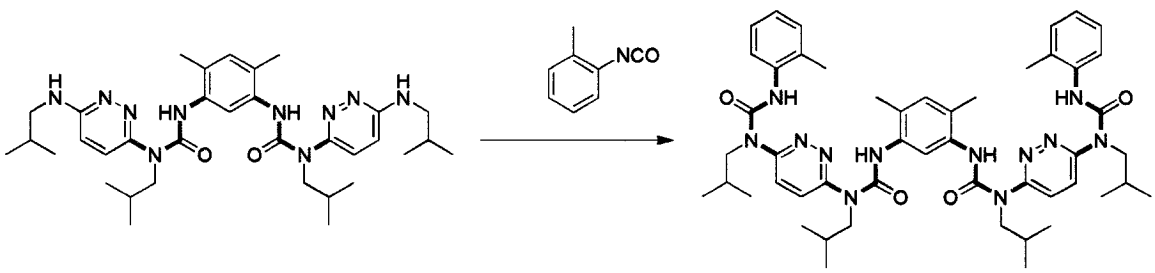

JM16 **JM18**

Scheme 4-17 Synthetic route for the synthesis the *m*-xylyl capped pentamer. The bonds with restricted rotation are highlighted in green.

4.3.3. Characterization

Figure 4-8 illustrates the ^{1}H NMR spectra of trimers **JM14** and **JM16**. The urea protons are observed at 10.1 and 10.3 ppm for **JM14** and **JM16,** respectively. This is in the same chemical shift range as has been observed by both Zimmerman and our group and is indicative of hydrogen bonding. As the urea chemical shifts are similar, this suggests that the hydrogen bonding in both foldamers is similar in strength.

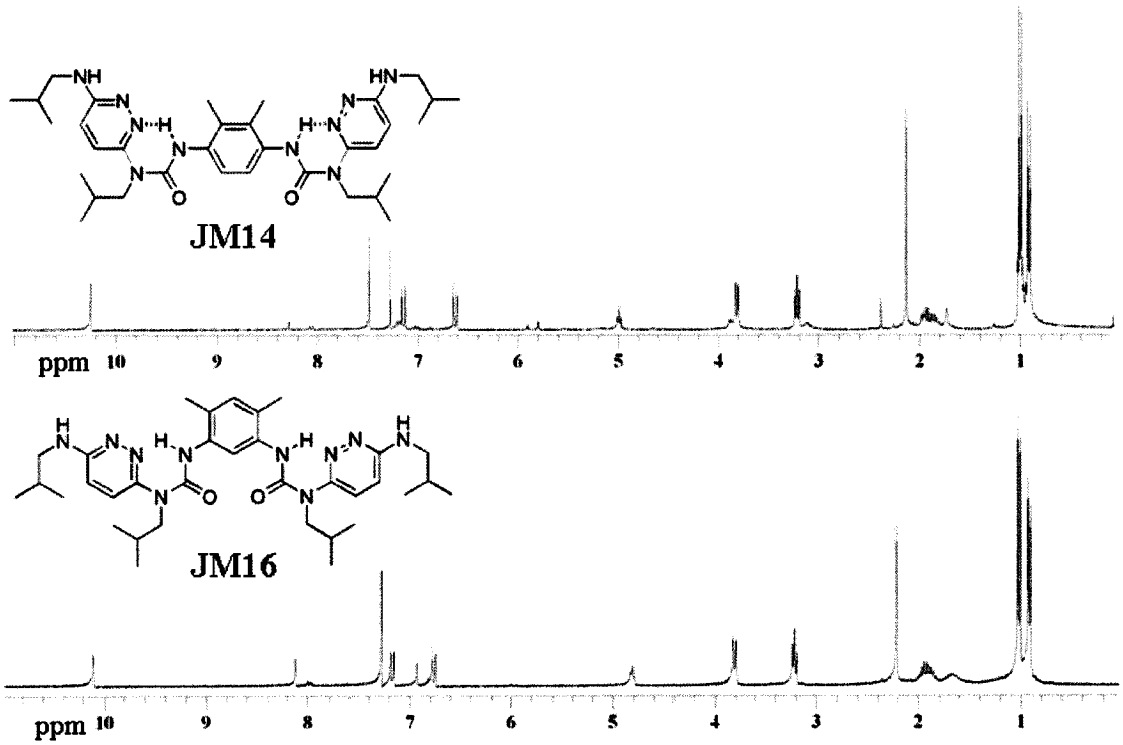

Figure 4-8 ^{1}H NMR spectra of the *o*-xylyl uncapped pyridazine trimer.

The conformation of **JM14** was investigated using NOESY. An important cross-peak between the protons of the urea linkages and the protons of the xylyl methyl groups were expected. The distance between the two groups in the expected conformation is approximately 2 Å (see Section 2.2.2). Indeed there is a cross-peak between the two groups, as indicated by the black dashed line in Figure 4-9.

Similar results were observed in the NOESY spectrum of the *m*-xylyl trimer **JM16** (Figure 4-10). There was a NOE contact between the xylyl methyl group and the urea hydrogen and a cross-peak between the methyl group and the aromatic proton *ortho* to the methyl group.

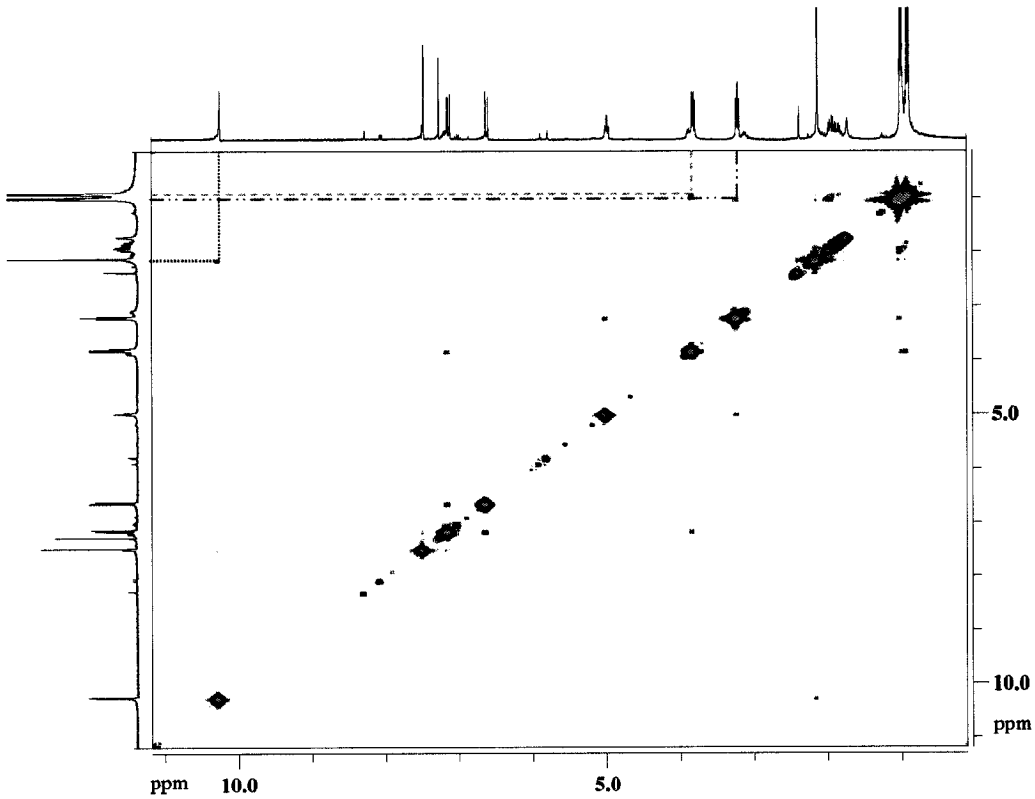

Figure 4-9 NOESY spectrum of the uncapped *o*-xylyl trimer.

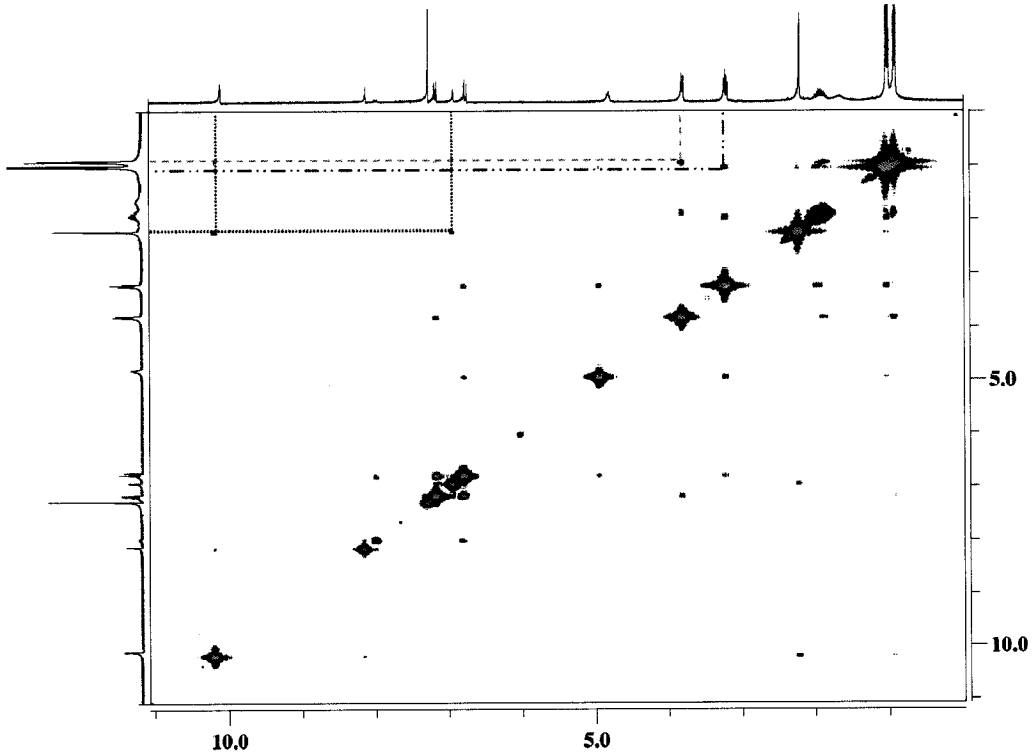

Figure 4-10 NOESY spectrum of the *m*-xylyl uncapped trimer.

A comparison was made between the ^{1}H NMR spectra of the **55**, **JM17**, and **JM18**. As seen in Figure 4-11 the three spectra are very similar with only slight differences observed in the urea, aromatic, and non-heterocyclic methyl resonances. The urea resonances for the three foldamers are observed between 11 and 12 ppm, however the difference between the peaks is 0.4 ppm in both the *o*-xylyl and *m*-xylyl oligomers, where it is less than 0.2 ppm in the tolyl system.

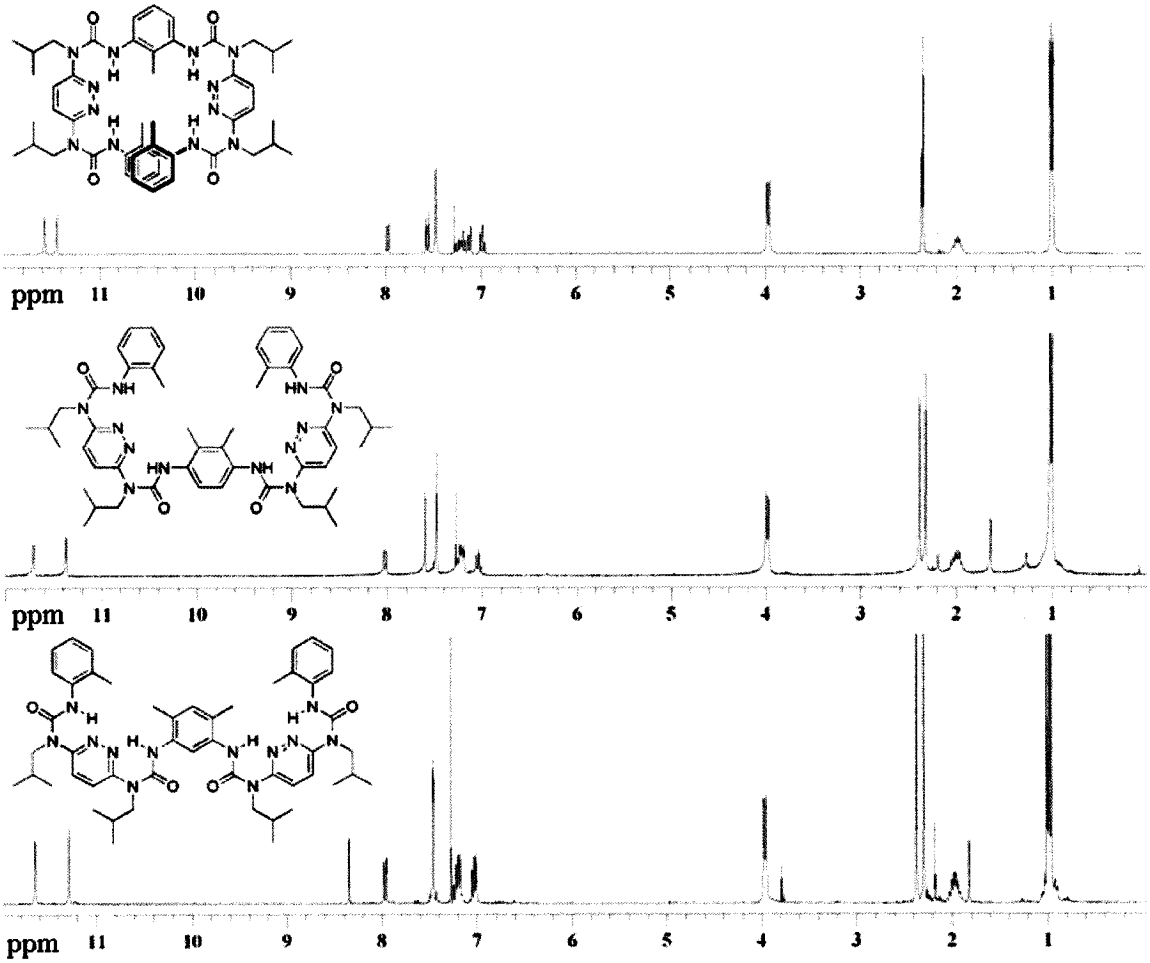

Figure 4-11 ^{1}H NMR of the three pyridazine pentamers.

A NOESY spectrum for **JM17** was obtained and is shown in Figure 4-12. As previously discussed for trimer **JM14**, there were observed NOE contacts between the

urea N-H and methyl protons of the xylyl substituents, indicating that the oligomer is folding as designed thus the system lies in the same plane to maximize π- π conjugation. The NOE contacts were used to assign the urea and methyl resonances, and the methyl peaks were distinguished since only one has a cross-peak (black hashed line) with the aromatic region.

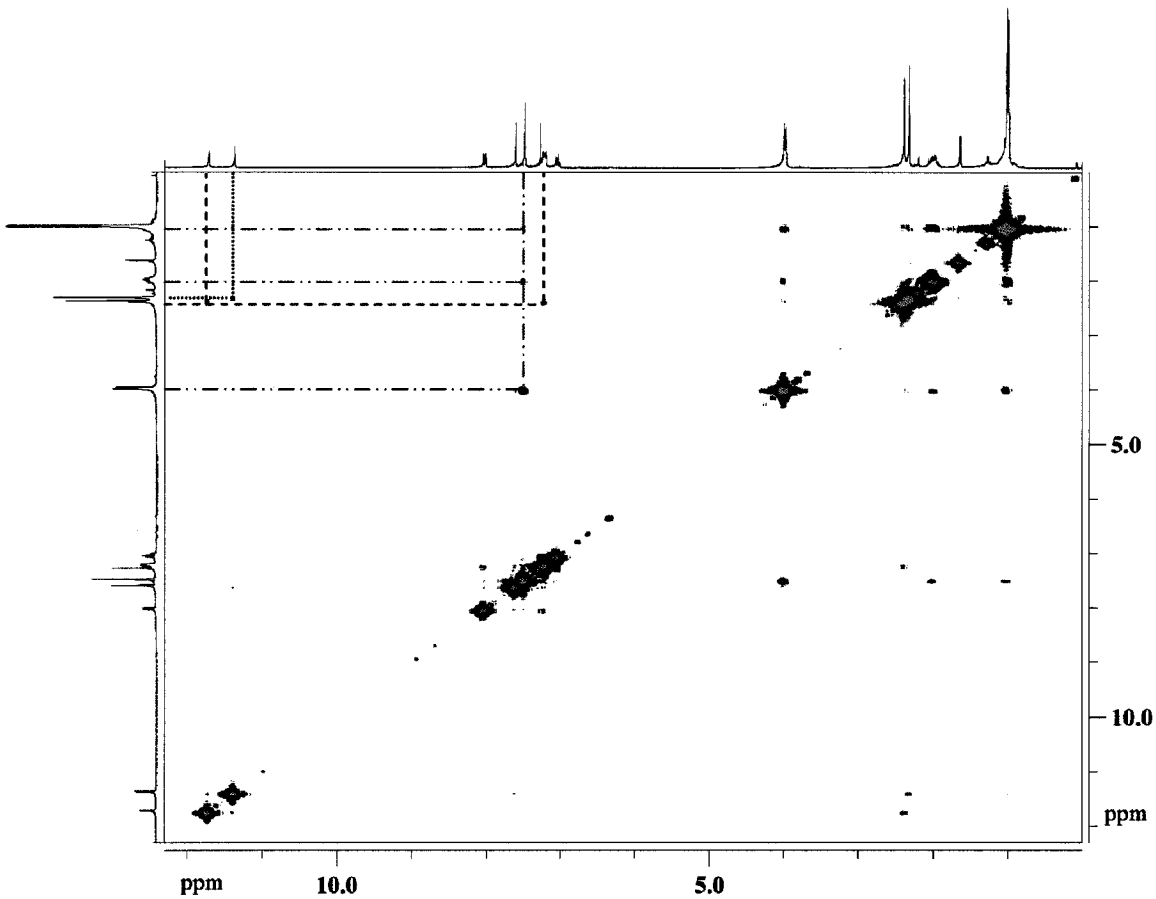

Figure 4-12 NOESY spectrum of the *o*-xylyl capped pentamer.

NOESY experiments were conducted in order to study the conformation of **JM18** (Figure 4-13). The tolyl and xylyl methyl protons yielded cross peaks with their corresponding urea protons, which is expected with the design hydrogen bonding of our system.

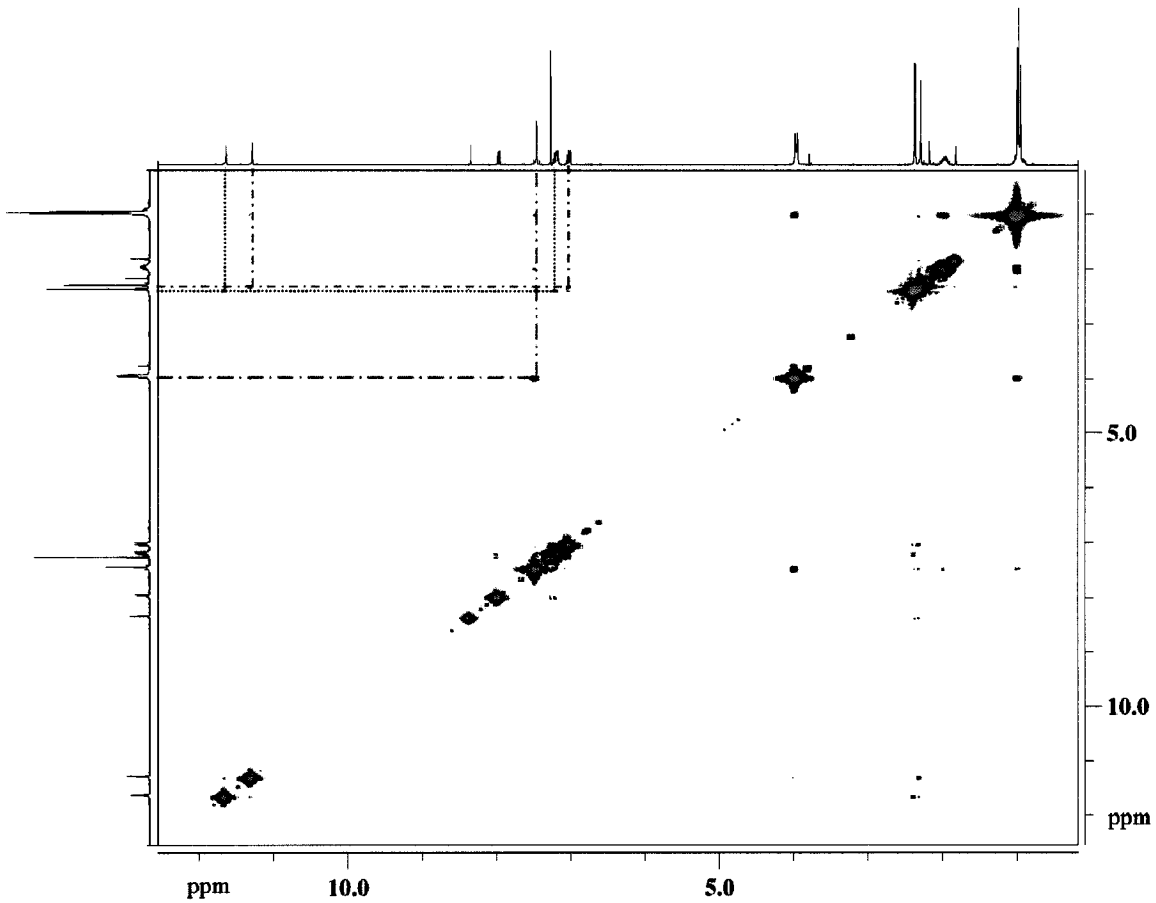

Figure 4-13 NOESY spectrum of the *m*-xylyl capped pentamer.

4.4. Future Work

At the moment, the overall yield of pentamer (and eventually longer oligomers) is limited by the ease of formation of the urea linkage. Future work will focus on the optimization of reaction conditions to increase reaction yields. Also, as nitrophenyl carbamates have been used to prepare urea linkages by solid phase synthesis, this method may be investigated for foldamers as shown in Scheme 4-18.

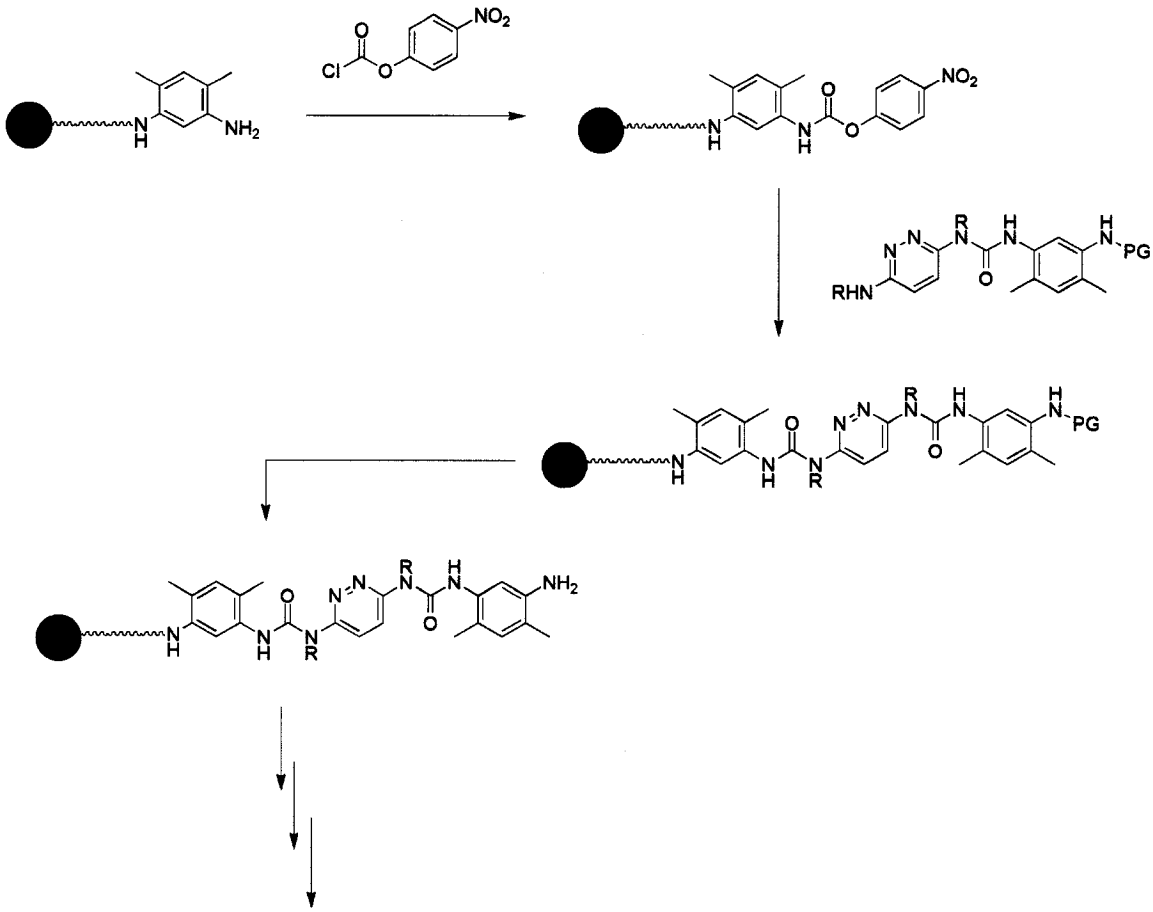

Scheme 4-18 Proposed scheme to prepare long oligomers using solid phase synthesis.

5. Summary and Conclusion

The N^2,N^3-diisobutylpyrazine-2,3-diamine, dimer **JM2**, and uncapped trimer **JM3** were prepared. The expected hydrogen bonding between the urea hydrogen atoms and the pyrazine heterocyclic nitrogen was not observed. Steric crowding of the isobutyl groups may influence the ability to form the desired hydrogen bonds and may play a role in inhibiting the synthesis of the capped trimer. This is in contrast to what was observed for pyrimidine trimers **JM4** and **JM5**. The conformations of these foldamers were studied using 1D and 2D ^{1}H NMR. The NOE contact between the tolylene methyl protons and the proton on carbon 2 of the pyrimidine ring indicates that the molecule is folding as designed. This indicates the folding is caused by restricted rotation in the molecule primarily due to hydrogen bonding interactions between the urea proton and the nitrogen atoms of the pyrimidine heterocycle. In addition, it was shown that by masking the hydrogen bonding interactions with polar solvents, the molecule can unfold. The capped pentamer **53** was not prepared and the ^{1}H NMR of the reaction product indicated that the urea linkages in our oligomers are thermally reversible due to the formation of the capped trimer.

Novel xylyl pyridazine foldamers (**JM14**, **JM16**, **JM17**, and **JM18**) were prepared where folding is driven by restricted rotation due to hydrogen bonding between the urea hydrogen atom and the nitrogen atoms of the heterocyclic substituents. This is similar to what was observed in the pyrimidine foldamers (**JM4** and **JM5**). Xylyl diamines (**JM12** and **JM15**) were prepared using nitration and reduction. However, in the case of the *o*-xylyl diamine an azo coupling method was found to be more efficient. It was shown that

both *p*-nitrophenyl and isopropenyl carbamates can be used to synthesize urea linkages. We are currently investigating means to improve reaction yields for these reactions. The uncapped xylyl trimers (**JM14** and **JM16**) readily reacted with *o*-tolyl isocyanate to yield pentamers **JM17** and **JM18** which demonstrates that the non-heterocylic monomers within the oligomeric system can be varied. This has implications in that a plethora of foldamer cavities could theoretically be prepared, fully demonstrating the tunability of our design.

A general strategy involving the use of carbamates and isocyanates was described to prepare pyrazine, pyrimidine, and pyridazine oligomers. This has increased the number of monomer units in our 'tool box', unlocking a wide variety of possible foldamers with different shapes. Furthermore, this is believed to be the first instance in urea-based foldamers where both heterocyclic and non-heterocyclic segments can be altered to tune the cavity size of these oligomers. These foldamers clearly complement those that have already been reported in the literature. By having a wide variety of different foldamers to chose and study from, foldamer chemists will undoubtedly gain further insight into natural design, and provide advancements in many disciplines of science.

6. Experimental

6.1. General methods

All the chemicals were obtained from Sigma-Aldrich Canada Ltd. (Oakville) and were used without further purification. All the solvents used were HPLC grade. Toluene and tetrahydrofuran (THF) where obtained anhydrous from a Braun solvent purification system (using packed copper and alumina columns) whereas chloroform was obtained anhydrous in SureSeal bottles and used under nitrogen flow. Choroform-d ($CDCl_3$, 99.8%), DMSO-d_6 (99.8%), and methanol-d_4 were purchased from Cambridge Isotopes Ltd. (Andover). 2,6–tolylene diisocyanate (TDI) and *o*-tolylene isocyanate, sodium nitrite, *p*-nitrophenyl chloroformate, and isopropenyl chloroformate were stored at 4 °C and were warmed to room temperature before use.

Melting points (m.p.) were recorded with a capillary melting point apparatus (Thomas Hoover). The recorded R_f values were determined by a standard thin-layer chromatography (TLC) procedure: 0.25 mm silica gel plates (Aldrich, Z122785-25EA) eluting with the specified solvents. FTIR spectra were recorded with a Thermo Electron Corporation Nicolet 6700 FT-IR in KBr liquid cell. 300 MHz ^1H NMR spectra and 75 MHz ^{13}C NMR spectra were recorded on a Inova Varian 300 spectrometer at room temperature. NOESY spectra were obtained in an absolute value mode with a mixing time of 0.3 s and a d1 of 1 s. The residual proton signals of the deuterated solvents were used as internal standards (DMSO-d_6: δ (^1H) = 2.50 ppm, δ (^{13}C) = 39.51 ppm; $CDCl_3$: δ (^1H) = 7.27 ppm, δ(^{13}C) = 77.23 ppm); CD_3OD: δ (^1H) = 4.87 ppm, 3.31 ppm, δ (^{13}C) = 49.15. The following notation is used for the ^1H NMR splitting patterns: singlet (s), doublet (d), triplet (t), mutiplet (m) and broad signal (bs). ^1H coupling constants are given

in Hz and the values are for three-bond coupling protons. MALDI-TOF mass spectra were obtained using a Micromass BAA037 time-of-flight mass spectrometer. A nitrogen laser (337 nm wavelength) was used to desorb the sample ions. The matrix used was dithranol (DIT), and the spectra were recorded in the positive reflectron mode.

6.2. Experimental procedures

N^2,N^3-diisobutylpyrazine-2,3-diamine (JM1)

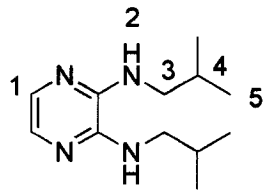

To a pressure reactor was added 2,3-dichloropyrazine (2.5 g, 16.8 mmol) and isobutyl amine (7 mL, 70.4 mmol). The solution was stirred at 170 °C overnight after which a precipitate formed. The crude product was dissolved in chloroform and washed with saturated $NaHCO_3$ (2 x 50 mL) and water (2 x 50 mL). The solvent was concentrated to 5 mL and the mixture was then purified by column chromatography (chloroform/acetone, 9/1) to yield a brown solid in 79 % yield (2.95 g). R_f = 0.56 (chloroform/acetone, 9/1); m.p.: 88-90 °C; ^{1}H NMR (300 MHz, $CDCl_3$): δ = 7.46 (s, 2H, H-1), 3.96 (bs, 2H, H-2), 3.23 (m, 4H, H-3), 1.95 (m, 2H, H-4), 1.01 (d, ^3J = 6.7 Hz, 12H, H-5); ^{13}C NMR (75 MHz, $CDCl_3$): δ = 144.87, 129.68, 49.21, 27.98, 20.47; IR (cm^{-1}): 3426, 3020, 2962, 2872, 1600, 1550, 1504, 1223; MALDI-TOF: m/z: 222.79 $[M]^+$ Calc $[M]^+$: 222.18; Elemental Analysis: Calculated: %C 64.83, %H 9.97, %N 25.20; Found: %C 64.55, %H 9.72, %N 24.93.

N^2,N^3-diisobutylpyrazine-2,3-diamine dimer (JM2)

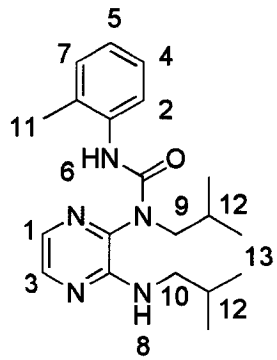

To a flame dried flask with stir bar was added N^2,N^3-diisobutylpyrazine-2,3-diamine (0.11 g, 0.5 mmol). The flask was purged with nitrogen and fitted with a nitrogen filled balloon, after which anhydrous toluene (2 mL) was added. *o*-Tolyl isocyanate (0.2 g, 1.5 mmol) was added dropwise and the solution was heated at 90 °C for 48 h. The solution was allowed to cool and methanol (5 mL) was added to quench any remaining isocyanate. The solvent was evaporated and chloroform (10 mL) was added to the resulting white solid. The mixture was filtered to remove insoluble materials, and the filtrate concentrated to half its volume and was purified by column chromatography (methylene chloride/ethyl acetate, 9.5/0.5) to yield a cream coloured solid in 57 % yield (0.105 g). R_f = 0.43 (methylene chloride/ethyl acetate, 9.5/0.5); mp: 134-136 °C; ^{1}H NMR (300 MHz, $CDCl_3$): δ = 8.06 (d, ^{3}J = 2.4 Hz, 1H, H-1), 7.80 (d, ^{3}J = 7.9 Hz, 1H, H-2), 7.15 (d, ^{3}J = 2.4 Hz, 1H, H-3), 7.18 (t, ^{3}J = 7.1 Hz, 1H, H-4), 7.10 (m, 2H, H-5,6), 6.98 (m, 1H, H-7), 5.00 (m, 1H, H-8), 3.59 (m, 2H, H-9), 3.30 (dd, ^{3}J = 6.7 Hz, 2H, H-10), 2.05 (s, 3H, H-11), 1.91 (m, 2H, H-12), 0.96 (m, 12H, H-13); ^{13}C NMR (75 MHz, $CDCl_3$): δ = 154.23, 150.96, 141.66, 137.24, 136.57, 130.22, 129.80, 127.75, 126.22, 123.77, 121.53, 52.96, 48.61, 28.44, 28.52, 20.26, 20.17. 17.51; IR (cm^{-1}): 3444, 3019, 2963, 1683, 1528, 1456, 1208; MALDI-TOF: m/z: 356.26 $[M+H]^+$ Calc $[M+H]^+$: 356.23.

N^2,N^3-diisobutylpyrazine-2,3-diamine uncapped trimer (JM3)

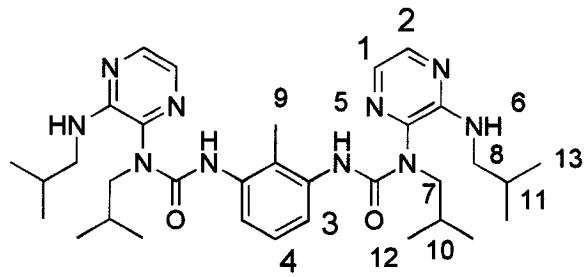

To a flame dried flask with stir bar was added N^2,N^3-diisobutylpyrazine-2,3-diamine (0.5 g, 2.25 mmol). The flask was purged with nitrogen and fitted with a nitrogen filled balloon, after which anhydrous toluene (10 mL) was added. Tolylene-2,6-diisocyanate (0.160 mL, 1.12 mmol) was added dropwise and the solution was heated at 90 °C for 24 h, after which additional tolylene-2,6-diisocyanate was added (0.050 mL, 0.35 mmol) and the solution was allowed to stir for an additional 24 h at 90 °C. The solvent was evaporated to give a brown gum, which was purified by column chromatography (chloroform/acetone, 8.5/1.5) to give a cream coloured solid in 21 % yield (0.130 g). R_f = 0.49 (chloroform/acetone, 8.5/1.5); mp: 198-200 °C; ^{1}H NMR (300 MHz, $CDCl_3$): δ = 8.042 (d, ^{3}J = 2.4 Hz, 2H, H-1), 7.72 (d, ^{3}J = 2.4 Hz, 2H, H-2), 7.35 (d, ^{3}J = 7.8 Hz, 2H, H-3), 7.11 (t, ^{3}J = 7.8 Hz, 1H, H-4), 6.93 (s, 2H, H-5), 4.99 (t, ^{3}J = 5.9 Hz, 2H, H-6), 3.55 (b, 4H, H-7), 3.29 (dd, ^{3}J = 5.9 Hz, 4H, H-8), 1.85 (m, 7H, H-9,10,11), 0.96 (d, ^{3}J = 6.8 Hz, 12H, H-12), 0.91 (d, ^{3}J = 6.8 Hz, 12H, H-13); ^{13}C NMR (75 MHz, $CDCl_3$): δ = 154.51, 151.05, 141.86, 137.05, 136.76, 129.91, 126.35, 122.76, 119.91, 52.98, 48.58, 28.39, 28.15, 20.28, 20.15, 12.08; IR (cm^{-1}): 3443, 3020, 2962, 1682, 1505, 1472, 1213; MALDI-TOF: m/z: 619.50 $[M+H]^+$ Calc $[M+H]^+$: 619.41.

N^4,N^6-diisobutylpyrimidine-4,6-diamine (JM6)

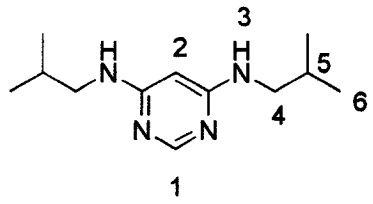

To a sealed tube was added 4,6-dichloropyrimidine (6.48 g, 43.4 mmol) and isobutyl amine (25.9 mL, 260 mmol). The solution was heated at 160 °C for three days after which a precipitate formed. The crude reaction mixture was recrystallized from 99 % ethanol to obtain a white crystalline solid in 64 % yield (5.67 g). R_f = 0.95 (chloroform/acetone, 8/2); m.p. = 188-189 °C; ^{1}H NMR (300 MHz, $CDCl_3$): δ = 8.05 (s, 1H, H-1), 5.21 (s, 1H, H-2), 4.83 (bs, 2H, H-3), 3.02 (t, ^{3}J = 6.7 Hz, 4H, H-4), 1.86 (m, 2H, H-5), 0.99 (d, ^{3}J = 6.7 Hz, 12H, H6); ^{13}C NMR (75 MHz, $CDCl_3$): δ = 163.22, 157.94, 79.25, 49.54, 28.42, 20.54; IR (cm^{-1}): 3431, 2962, 2875, 1603, 1528, 1471, 1248; MALDI-TOF: m/z: 223.09 $[M+H]^+$ Calc $[M+H]^+$: 223.18; Elemental Analysis: Calculated: %C 64.83, %H 9.97, %N 25.20; Found: %C 64.84, %H 9.65, %N 25.08.

N^4,N^6-diisobutylpyrimidine-4,6-diamine tolyl dimer (JM7)

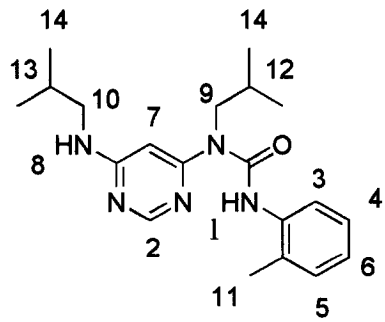

To a flame dried flask with stir bar was added N^4,N^6-diisobutylpyrimidine-4,6-diamine (0.50 g, 2.25 mmol). The flask was purged with nitrogen and fitted with a nitrogen filled

balloon, after which anhydrous toluene (10 mL) was added. *o*-Tolyl isocyanate (0.28 mL, 2.25 mmol) was added dropwise and the solution was heated at 90 °C for 24 h. The solution was allowed to cool and methanol (5 mL) was added to quench any remaining isocyanate. The solvent was evaporated and chloroform (10 mL) was added to the resulting white solid. The mixture was filtered to remove insoluble material, and the filtrate was purified by column chromatography (methylene chloride/ethyl acetate, 9.5/0.5) to yield a white solid in 73 % yield (0.583 g). R_f = 0.33 (methylene chloride/ethyl acetate, 9.5/0.5); m.p.: 110-111 °C; ^{1}H NMR (300 MHz, $CDCl_3$): δ = 12.93 (s, 1H, H-1), 8.23 (s, 1H, H-2), 8.06 (d, ^3J = 7.7 Hz, 1H, H-3), 7.15 -7.25 (m, 2H, H-4, H-5), 7.00 (t, ^3J = 8.4 Hz, 1H, H-6), 5.82 (s, 1H, H-7), 5.40 (bs, 1H, H-8), 3.88 (d, ^3J = 7.1 Hz, 2H, H-9), 3.12 (bm, 2H, H-10), 2.38 (s, 3H, H-11), 2.10 (m, 1H, H-12), 1.92 (m, 1H, H-13), 1.00 (m, 12H, H-14); ^{13}C NMR (75 MHz, $CDCl_3$): δ = 163.61, 160.07, 155.47, 153.76, 137.77, 130.11, 128.17, 126.45, 123.31, 121.54, 86.81, 50.10, 49.16, 28.20, 26.66, 20.21, 20.11, 18.80; IR (cm^{-1}): 3430, 3034, 2964, 2872, 1687, 1599, 1550, 1460, 1152; MALDI-TOF: m/z: 356.25 $[M+H]^+$ Calc $[M+H]^+$: 356.23.

Capped N^4,N^6-diisobutylpyrimidine-4,6-diamine tolyl trimer (JM4)

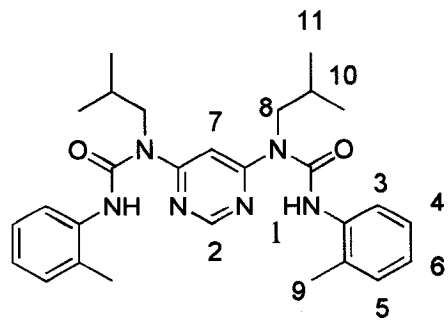

To a flame dried flask with stir bar was added N^4,N^6-diisobutylpyrimidine-4,6-diamine (0.11 g, 0.5 mmol). The flask was purged with nitrogen and fitted with a nitrogen filled

balloon, after which anhydrous toluene (2 mL) was added. *o*-Tolyl isocyanate (0.2 g, 1.5 mmol) was added dropwise and the solution was heated at 90 °C for 48 h. The mixture was allowed to cool to room temperature and methanol (5 mL) was added to quench any remaining isocyanate. The solvent was evaporated and chloroform (10 mL) was added to the resulting white solid. The mixture was filtered to remove insoluble material, and the filtrate was purified by column chromatography (methylene chloride/ethyl acetate, 9.5/0.5) to yield a cream coloured solid in 75 % yield (0.183 g). R_f = 0.67 (methylene chloride/ethyl acetate, 9.5/0.5); m.p.: 143-145 °C; ^{1}H NMR (300 MHz, $CDCl_3$): δ = 12.55 (s, 2H, H-1), 8.58 (s, 1H, H-2), 8.05 (d, ^{3}J = 8.2 Hz, 2H, H-3), 7.20-7.260(m, 4H, H-4, 5), 7.06 (t, ^{3}J = 8.2 Hz, 2H, H-6), 6.43 (s, 1H, H-7), 3.99 (bd, ^{3}J = 7.3 Hz, 4H, H-8), 2.42 (s, 6H, H-9), 2.11 (m, 2H, H-10), 1.05 (d, ^{3}J = 6.7 Hz, 12H, H-11); ^{13}C NMR (75 MHz, $CDCl_3$): δ = 161.40, 153.67, 153.38, 137.56, 130.57, 128.68, 126.96, 124.25, 122.18, 92.82, 50.84, 27.14, 20.42, 19.11; IR (cm^{-1}): 3028, 2965, 1694 1582, 1539, 1458, 1201, 1148; MALDI-TOF: m/z: 489.34 $[M+H]^+$ Calc $[M+H]^+$: 489.29.

Uncapped N^4,N^6-diisobutylpyrimidine-4,6-diamine tolyl trimer (JM5)

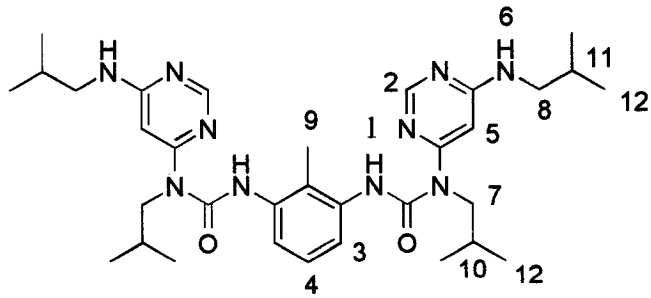

To a flame dried flask with stir bar was added N^4,N^6-diisobutylpyrimidine-4,6-diamine (1 g, 4.5 mmol). The flask was purged with nitrogen and fitted with a nitrogen filled balloon, after which anhydrous toluene (16 mL) was added. Tolylene-2,6-diisocyanate

(0.3 mL, 2.1 mmol) was added dropwise and the solution was heated at 90 °C for 24 h. The solvent was evaporated to give a white solid, which was then redissolved in 10 mL of chloroform. Insoluble material was removed *via* vacuum filtration. The filtrate was concentrated to half its volume and purified by column chromatography (chloroform/acetone, 8/2) to give a white solid in 44 % yield (0.560 g). R_f = 0.68 (chloroform/acetone, 8/2); mp : 174-175 °C; ^{1}H NMR (300 MHz, $CDCl_3$): δ = 12.80 (s, 2H, H-1), 8.28 (s, 2H, H-2), 7.65 (d, ^{3}J = 7.9 Hz, 2H, H-3), 7.20(t, ^{3}J = 8.2 Hz, 1H, H-4), 5.80 (s, 2H, H-5), 5.35 (bs, 1H, H-6), 3.88 (bd, ^{3}J = 7.3 Hz, 4H, H-7), 3.12 (bm, 4H, H-8), 2.35 (s, 3H, H-9), 2.10 (m, 2H, H-10), 1.92 (m, 2H, H-11), 1.00 (m, 24H, H-12); ^{13}C NMR (75 MHz, $CDCl_3$): δ = 163.50, 160.17, 155.48, 154.07, 137.71, 126.15, 122.40, 119.51, 50.24, 49.20, 28.23, 26.70, 20.24, 20.14, 13.46; IR (cm^{-1}): 3431, 3027, 2964, 2973, 1686, 1596, 1551, 1470, 1216, 1153; MALDI-TOF: m/z: 619.64 $[M+H]^+$ Calc $[M+H]^+$: 619.41.

_N_-(2,3-dimethylphenyl)-acetamide (JM10)

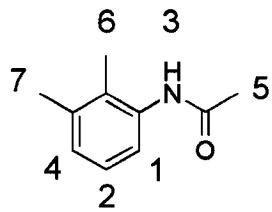

To a 100 mL round bottom flask with stir bar was added pyridine (20 mL, 247 mmol) and 2,3-dimethyl aniline (5 g, 41 mmol). The solution was cooled to 0 °C on ice while stirring after which acetic anhydride (6 mL, 63 mmol) was added dropwise. Within five minutes after the addition of acetic anhydride a yellow/pink mass had formed. The mixture was

stirred for 2 h at room temperature and the reaction was quenched by mixing with ice water (100 mL) and the white precipitate was filtered and washed (50 mL 0.5 M HCl and 150 mL cold H_2O). The precipitate was then dried under vacuum to give a white powder in 80 % yield (5.342 g). R_f = 0.19 (chloroform/ethyl acetate, 9/1); mp: 134-135 °C; ^1H NMR (300 MHz, $CDCl_3$): δ = 7.37 (d, ^3J = 7.8 Hz, 1H, H-1), 7.05-7.18 (m, 2H, H-2, H-3), 7.02 (d, ^3J = 7.3 Hz, 1H, H-4), 2.29 (s, 3H, H-5), 2.18 (s, 3H, H-6), 2.13 (s, 3H, H-7); ^{13}C NMR (75 MHz, $CDCl_3$): δ = 168.73, 137.42, 135.15, 129.43, 127.63, 125.79, 122.63, 23.90, 20.52, 13.81.

2,3-dimethyl-4-nitro-aniline (JM11)

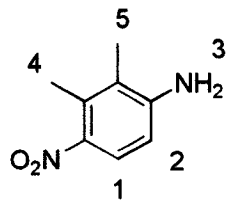

In a round bottom flask *N*-(2,3-dimethylphenyl)-acetamide (8 g, 49 mmol) was dissolved in cold sulfuric acid (35 mL). This solution was stirred for 10 min at 0 °C after which chilled nitric acid (3.3 mL) was added dropwise over 30 min at 0 °C. The reaction was quenched on ice water immediately following the addition of the last drop of nitric acid using an ice water bath and a yellow precipitate formed. The precipitate was then refluxed for 1h in 60 % H_2SO_4 (25 mL) in order to hydrolyze the acetyl group. The mixture extracted with ethyl acetate (2 x 25 ml). The ethyl acetate extract was washed with saturated $NaHCO_3$ (2 x 25 mL), followed by water (2 x 25 mL). The solvent was concentrated to 5 mL and the mixture was purified by column chromatography (chloroform/acetone, 9/1) to give a yellow solid in 14 % yield (1.1 g). R_f = 0.12

(methylene chloride/hexane, 6/4); mp : 110-111 °C; ^{1}H NMR (300 MHz, DMSO): δ = 7.66 (d, ^{3}J = 9.0 Hz, 1H, H-1), 6.54 (d, ^{3}J = 9 Hz, 1H, H-2), 6.15 (s, 2H, H-3) 2.37 (s, 3H, H-4), 2.02 (s, 3H, H-5); ^{13}C NMR (75 MHz, DMSO): δ = 151.95, 138.72, 133.48, 124.80, 119.41, 110.73, 19.83, 17.26.

2,3-dimethylbenzene-1,4-diamine (JM12)

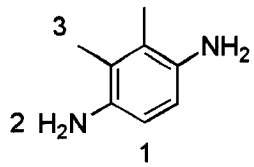

Sulfanilic acid (5.25 g, 30.3 mmol) and sodium carbonate (1.59g 15.2 mmol) were dissolved in water (50 mL) and the mixture was heated gently until all the acid and salt was dissolved. The solution was then cooled to 15 °C. To the cooled solution was added sodium nitrite (2.28 g, 36.4 mmol) in 5 mL of water with vigorous stirring. The reaction mixture was then poured on 30 g of ice with 6 mL of concentrated HCl and the slurry was mixed until a positive test was obtained on KI paper. 2,3-dimethyl aniline (3.15 mL, 25 mmol) in acetic acid (1.5 mL) was then added to the solution with vigorous stirring for 1 h to yield a red mixture. A 20 % NaOH solution (20 mL) was added slowly and the reaction mixture was heated until everything dissolved, after which NaCl (5 g) was added with continued heating until complete dissolution. The reaction solution was then cooled on ice for 15 min and the red claylike solid was collected *via* vacuum filtration (6.5 g, 80 %). A portion of the azo compound (0.5 g, 1.53 mmol) was dissolved in methanol (5 mL). The solution was brought to a boil and $SnCl_2$ (0.579 g, 3 mmol) in HCl (1 mL) was subsequently added. The mixture was boiled until decolourization (red to beige). Sodium carbonate was then added until the solution had a pH of 7-8. The

methanol was evaporated and the diamine was extracted from the salt solution using ethyl acetate (50 mL). The EtOAc extract was dried over $MgSO_4$ and concentrated to give a brown solid in 61 % yield (0.131 g) relative to the azo compound. R_f = 0.22 (chloroform/methanol /acetone, 8.5/1.0/0.5); mp: 102-104 °C; ^1H NMR (300 MHz, DMSO): δ = 6.30 (s, 2H, H-1), 3.95 (s, 4H, H-2), 1.94 (s, 6H, H-3); ^{13}C NMR (75 MHz, $CDCl_3$): δ = 137.21, 120.89, 113.14, 13.36.

1,5-dimethyl-2,4-dinitrobenzene (JM9)

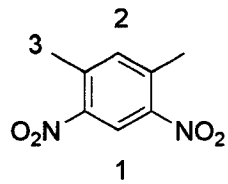

Sulfuric acid (25 mL) and 2-nitro-*m*-xylene (10 mL, 73.89 mmol) were added to a round bottom flask and cooled to 0 °C in an ice bath. Once cooled, 70% nitric acid (5.2 mL, 81 mmol) was added dropwise. After 30 min the reaction was quenched by pouring the reaction mixture on ice-water slurry. The resulting precipitate was subsequently filtered and recrystallized from methanol to give a white solid with a 52 % yield (7.5 g). R_f = 0.41 (hexane/ethyl acetate, 8.5/1.5); mp: 88-90 °C; ^1H NMR (300 MHz, $CDCl_3$): δ = 8.71 (s, 1H, H-1), 7.39 (s, 1H, H-2), 2.70 (s, 6H, H-3); ^{13}C NMR (75 MHz, $CDCl_3$): δ = 146.69, 139.04, 137.32, 121.84, 20.65.

1,5-dimethyl-2,4-phenylenediamine (JM15)

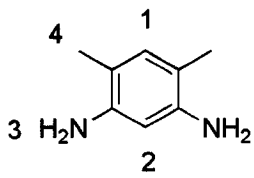

In a Parr reactor was dissolved 1,5-dimethyl-2,4-dinitrobenzene (0.284 g, 1.45 mmol) in ethanol (20 mL). 10 % Pd/C (0.15 g) was added to the solution and the reaction vessel was purged with argon, followed by hydrogen. Hydrogen was added to a pressure of 50 psi. The reactor was immersed in an oil bath at 100 °C and the solution was stirred for 2 h. The reactor was purged with argon gas and the crude mixture was filtered through Celite to remove the catalyst. The reaction mixture was concentrated under vacuum and purified by column chromatography (chloroform/methanol/acetone, 8.5/1.0/0.5) to give an orange solid in 96 % yield (0.190 g). R_f = 0.20 (chloroform/methanol/acetone, 8.5/1.0/0.5); m.p.: 85-86 °C; ^{1}H NMR (300 MHz, DMSO): δ = 6.45 (s, 1H, H-1), 5.93 (s, 1H, H-2), 4.26 (s, 4H, H-3), 1.87 (s, 6H, H-4); ^{13}C NMR (75 MHz, DMSO): δ = 144.48, 131.29, 109.52, 100.95, 16.45.

N^3,N^6-diisobutylpyridazine-4,6-diamine (JM13)

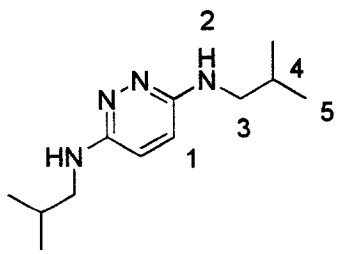

To a Parr reactor was added 3,6-dichloropyrazine (10 g, 67.1 mmol) and isobutyl amine (30 mL, 302 mmol). The solution was stirred at 155 °C for five days. The dark brown solid obtained was dissolved in chloroform and washed with $NaHCO_3$ (2 x 25 mL) and

distilled water (2 x 25 mL). The mixture was then concentrated and purified by column chromatography (chloroform/methanol/acetone, 8.5/1.0/0.5) to give the desired product in 76 % yield (10.78 g). R_f = 0.48 (chloroform/methanol/acetone, 8.5/1.0/0.5); m.p.: 141.4 – 142.5 °C; ^{1}H NMR (300 MHz, $CDCl_3$): δ = 6.66 (s, 2H, H-1), 4.50 (b, 2H, H-2), 3.14 (m, 4H, H-3), 1.91 (m, 2H, H-4), 0.96 (d, ^{3}J = 6.3 Hz, 12H, H-5); ^{13}C NMR (75 MHz, $CDCl_3$): δ = 134.49, 118.03, 50.40, 28.32, 20.40; IR (cm^{-1}): 3437, 3021, 2916, 1566, 1501, 1485, 1215; MALDI-TOF: m/z: 223.25 $[M+H]^+$ Calc $[M+H]^+$: 223.18.

N^3,N^6-diisobutylpyridazine-4,6-diamine *o*-tolyl dimer (JM8)

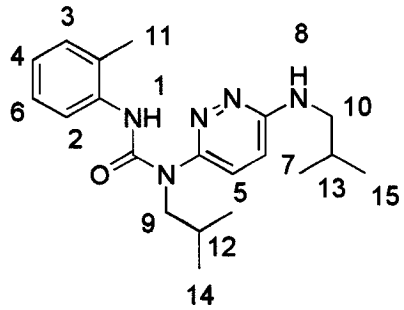

N^3,N^6-diisobutylpyridazine-4,6-diamine (0.50 g, 2.25 mmol) was added to a round bottom flask and dissolved in anhydrous chloroform (10 mL). The flask was fitted with a nitrogen filled balloon and heated to 50 °C. *O*-tolyl isocyanate (0.28 mL, 2.25 mmol) was added dropwise through a syringe and the solution was left to stir overnight. Methanol (5 mL) was added to quench any unreacted isocyanate and the chloroform was evaporated under vacuum. The solid was redissolved in chloroform and insoluble material was filtered. The filtrate was concentrated to half its volume and the product was purified by column chromatography to give a pale yellow solid with 56 % yield (0.465 g). R_f = 0.6 (chloroform, acetone 9/1); m.p. : 89-90 °C; ^{1}H NMR (300 MHz, $CDCl_3$): δ = 10.60 (s, 1H, H-1), 7.82 (d, ^{3}J = 7.5 Hz, 1H, H-2), 7.10-7.13 (m, 2H, H-3, 4), 7.07 (d, ^{3}J = 9.3 Hz,

1H, H-5), 6.95 (t, ^3J = 7.5 Hz, 1H, H-6), 6.73 (d, ^3J = 9.3 Hz, 1H, H-7), 5.23 (m, 1H, H-8), 3.79 (d, ^3J = 6.9 Hz, 2H, H-9), 3.17 (m, 2H, H-10), 2.27 (s, 3H, H-11), 1.87 (m, 2H, H-12, 13), 0.95 (d, ^3J = 6.3 Hz, 6H, H-14), 0.91 (d, ^3J = 6.3 Hz, 6H, H-15); ^{13}C NMR (75 MHz, $CDCl_3$): δ = 156.81, 154.27, 151.70, 137.42, 130.19, 129.31, 126.35, 123.67, 122.53, 122.40, 117.44, 52.12, 49.58, 28.15, 27.68, 20.31, 19.93, 18.37.

N^3,N^6-diisobutylpyridazine-4,6-diamine *o*-xylyl trimer (JM14)

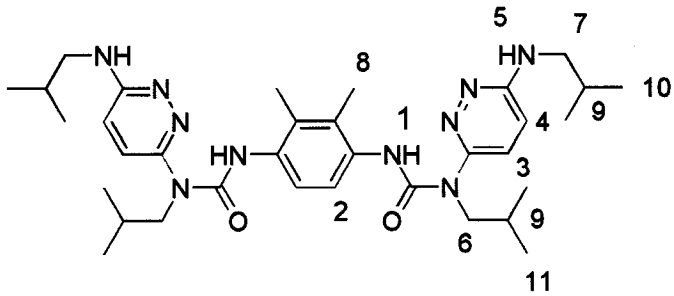

NaOH (0.120g, 3.00 mmol) was dissolved in water (1 mL) in a round bottom flask and cooled on ice. 2,3-dimethylbenzene-1,4-diamine (0.118 g, 0.87 mmol) was dissolved in ethyl acetate (2 mL) and added to the NaOH solution. The mixture was stirred for 10 min on ice after which isopropenyl chloroformate (0.270 mL, 2.40 mmol) was added dropwise. After 45 min at 0 °C, the flask was removed from the ice and stirred at room temperature for 3 h. The mixture was then diluted in ethyl acetate (20 mL) and washed with saturated NaCl solution (2 x 50 mL) and distilled water (2 x 50 mL). The ethyl acetate was evaporated and the beige bis-carbamate was triturated with cold heptane. The *o*-xylyl bis-isopropenyl carbamate was then added to a round bottom flask with N^3,N^6-diisobutylpyridazine-4,6-diamine (0.222 g, 1.00 mmol) and the flask was purged with nitrogen and fitted with a nitrogen filled balloon. Anhydrous THF (1 mL) was added, the resulting solution was heated to 55 °C and *N*-methyl pyrolidine (0.020 mL, 0.2 mmol)

was added dropwise. The mixture was stirred at 55 °C for 48 h. The product was then purified by column chromatography, first with silica (chloroform/acetone, 8/2), then with alumina (methylene chloride/ethyl acetate, 9/1) to yield a cream coloured solid in 16% yield (0.088 g). R_f = 0.3 (chloroform/acetone, 8/2); m.p. : 140-142 °C; ^{1}H NMR (300 MHz, $CDCl_3$): δ = 10.25 (s, 2H, H-1), 7.48 (s, 2H, H-2), 7.14 (d, ^{3}J = 9.6 Hz, 2H, H-3), 6.62 (d, ^{3}J = 9.6 Hz, 2H, H-4), 4.99 (bt, ^{3}J = 4.2 Hx, 2H, H-5), 3.81 (d, ^{3}J = 7.49 Hz, 4H, H-6), 3.21 (t, ^{3}J = 6.7, 4H, H-7), 2.13 (s, 6H, H-8), 1.83-1.99 (m, 4H, H-9), 1.00 (d, ^{3}J = 6.7 Hz, 12H, H-10), 0.92 (d, ^{3}J = 6.6 Hz, 12H, H-11); ^{13}C NMR (75 MHz, $CDCl_3$): δ = 156.56, 154.57, 152.01, 133.64, 130.19, 122.82, 121.88, 116.82, 52.17, 49.72, 28.21, 27.67, 20.31, 19.91, 14.92; IR (cm^{-1}): 3443, 3020, 2963, 1666, 1494, 1464, 1260; MALDI-TOF: m/z: 633.50 $[M+H]^+$ Calc $[M+H]^+$: 633.43.

N^3,N^6-diisobutylpyridazine-4,6-diamine *m*-xylyl trimer (JM16)

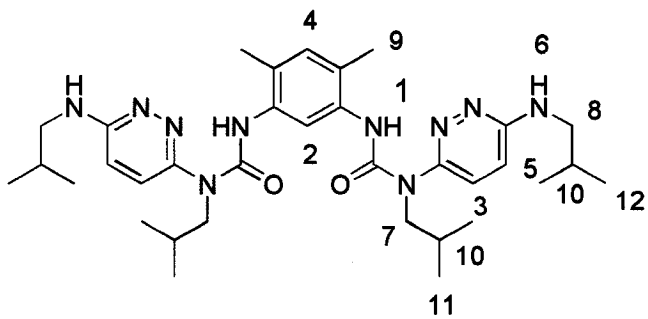

4-Nitrophenyl chloroformate (0.566 g, 2.8 mmol) was added to a round bottom flask and purged with nitrogen. The flask was fitted with a nitrogen filled balloon and anhydrous methylene chloride (4 mL) was added to give a suspension. 1,5-Dimethyl-2,4-phenylenediamine (0.153 g, 1.1 mmol) and DIEA (0.4 mL, 2.2 mmol) in anhydrous methylene chloride (4 mL) was added dropwise yielding an orange solution. The solution was left to stir at room temperature for 1 h. N^3,N^6-diisobutylpyridazine-4,6-diamine

(0.428 g, 1.9 mmol) with triethyl amine (0.3 mL) dissolved in methylene chloride (1 mL) was added dropwise. The solution was left to stir for 20 h and the reaction was monitored using TLC. The solution was left to stir for an additional 4 days with no apparent change shown on TLC. The solvent was evaporated and the yellow solid was dissolved in chloroform and filtered to remove insoluble material. The filtrate was washed with distilled water concentrated and purified by column chromatography (chloroform/acetone, 0.77/0.23) to give a white solid in 13 % yield (0.080 g). R_f = 0.5 (chloroform/acetone, 0.77/0.20); mp: 187-190 °C; ^{1}H NMR (300 MHz, $CDCl_3$): δ = 10.146 (s, 2H, H-1), 8.148 (s, 1H, H-2), 7.113 (d, ^{3}J = 9.8 Hz, 2H, H-3), 6.912 (s, 1H, H-4), 6.761 (d, ^{3}J = 9.8 Hz, 2H, H-5), 5.033 (bt, ^{3}J = 5.5 Hz, 2H, H-6), 3.775 (d, ^{3}J = 7.3 Hz, 4H, H-7), 3.184 (t, ^{3}J = 6.4 Hz, 4H, H-8), 2.191 (s, 6H, H-9), 1.894 (m, 4H, H-10), 0.987 (d, ^{3}J = 6.7 Hz, 12H, H-11), 0,893 (d, ^{3}J = 6.7 Hz, 12H, H-12); ^{13}C NMR (75 MHz, $CDCl_3$): δ = 156.66, 154.10, 152.10, 135.06, 131.60, 125.63, 123.02, 117.74, 116.28, 52.31, 49.82, 28.24, 27.69, 20.29, 19.95, 17.72; IR (cm^{-1}): 3444, 3019, 2970, 1675, 1593, 1523, 1426, 1210; MALDI-TOF: m/z: 633.52 $[M+H]^+$ Calc $[M+H]^+$: 633.43; Elemental Analysis: Calculated: %C 64.53, %H 8.28, %N 22.13; Found: %C 63.40, %H 7.04, %N, 20.94.

N^3,N^6-diisobutylpyridazine-4,6-diamine *o*-xylyl Pentamer (JM17)

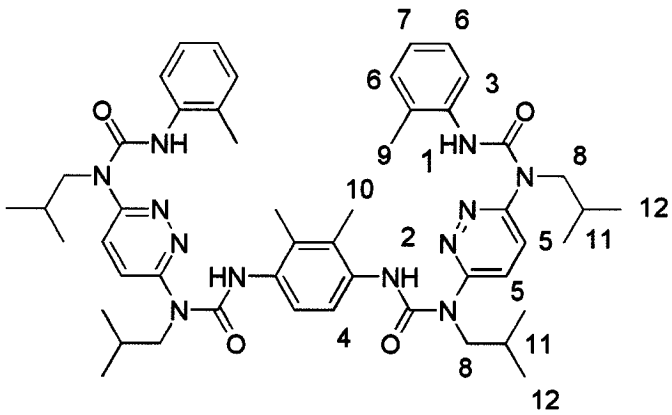

0.130 g of the crude N^3,N^6-diisobutylpyridazine-4,6-diamine *o*-xylyl trimer (0.068 g, 0.11 mmol calculated from ^{1}H NMR) was dissolved in anhydrous chloroform (3 mL) under a nitrogen atmosphere. *o*-Tolyl isocyanate (0.080 mL, 0.7 mmol) was added dropwise and the reaction mixture was heated at 55 °C for 24 h. After cooling to room temperature, methanol (5 mL)) was added and the mixture was stirred for 4 h. The solvent was concentrated to 2 mL and purified by column chromatography (chloroform/acetone, 9/1) to give a cream coloured solid in 54 % yield (0.053 g). R_f = 0.7 (chloroform/acetone, 9/1); m.p. : 117-118 °C; ^{1}H NMR (300 MHz, $CDCl_3$): δ = 11.71 (s, 2H, H-1), 11.37 (s, 2H, H-2), 8.02 (d, ^{3}J = 8.1 Hz, 2H, H-3), 7.59 (s, 1H, H-4), 7.47 (s, 4H, H-5), 7.17 - 7.26 (m, 4H, H-6), 7.03 (t, 2H, H-7), 3.98 (d, ^{3}J = 7.5 Hz, 8H, H-8), 2.38 (s, 6H, H-9), 2.31 (s, 6H, H-10), 1.92-2.09 (m, 4H, H-11), 1.00 (d, ^{3}J = 6.6 Hz, 24H, H-12); ^{13}C NMR (75 MHz, $CDCl_3$): δ = 154.58, 154.46, 154.10, 153.54, 137.49, 133.78, 130.53, 130.03, 128.56, 126.89, 124.07, 122.29, 122.07, 121.91, 121.79, 51.65, 51.50, 27.81, 20.23, 18.95, 15.47; IR (cm^{-1}): 3027, 2964, 1679, 1541, 1449, 1210; MALDI-TOF: m/z: 899.62 $[M+H]^+$ Calc $[M+H]^+$: 899.53.

N^3,N^6-diisobutylpyridazine-4,6-diamine *o*-xylyl Pentamer (JM18)

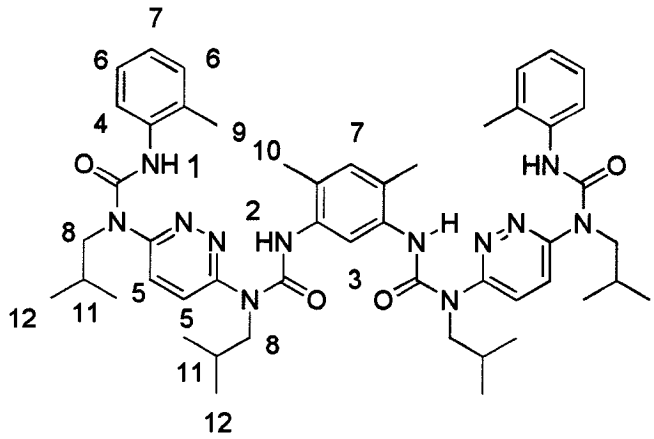

0.130 g of the crude N^3,N^6-diisobutylpyridazine-4,6-diamine *m*-xylyl trimer (0.074 g, 0.12 mmol calculated from ^{1}H NMR) was dissolved in anhydrous chloroform (3 mL) under a nitrogen atmosphere. *o*-Tolyl isocyanate (0.080 mL, 0.7 mmol) was added dropwise and the reaction mixture was heated at 55 °C for 24 h. After cooling, methanol (5 mL) was added and the mixture was stirred for 4 h. The solvent was concentrated to 2 mL and purified by column chromatography (chloroform/acetone, 9/1) to give a white solid in 51 % yield (0.055 g). R_f = 0.7 (chloroform/acetone, 9/1); m.p.: 122-123 °C; ^{1}H NMR (300 MHz, $CDCl_3$): δ = 11.64 (s, 2H. H-1), 11.28 (s, 2H, H-2), 8.35 (s, 1H, H-3), 7.97 (d, 2H, H-4), 7.44 – 7.46 (m, 4H, H-5), 7.16 - 7.26 (m, 4H, H-6), 6.99 – 7.06 (m, 3H, H-7), 3.96 (d, ^{3}J = 7.4 Hz, 8H, H-8), 2.37 (s, 6H, H-9), 2.29 (s, 6H, H-10), 1.89 – 2.05 (m, 4H, H – 11), 0.96 – 1.00 (m, 24H, H-12); ^{13}C NMR (75 MHz, $CDCl_3$): δ = 154.58, 154.53, 153.66, 153.64, 137.42, 135.25, 132.01, 130.51, 128.87, 126.82, 125.75, 124.15, 122.36, 122.15, 121.80, 117.90, 51.62, 51.55, 27.78, 20.24, 18.92, 18.24. IR (cm^{-1}): 3007, 2965, 1679, 1541, 1459, 1210; MALDI-TOF: m/z: 899.49 $[M+H]^+$ Calc $[M+H]^+$: 899.53.

7. Bibliography

1. Lindgard, P. *J. Phys.: Condens. Matter* **2003,** *15*, S1779-S1786.
2. Bowie, J. *Nature* **2005,** *438*, 581-589.
3. Blackburn, G. M. *Nucleic Acids in Chemistry and Biology*, 2nd ed.; Oxford University Press: London, 1996.
4. Hill, D. J.; Mio, M. J.; Prince, R. B.; Hughes, T. S.; Moore, J. *Chem. Rev.* **2001,** *101*, 3893-4011.
5. Gellman, S. H. *Acc. Chem. Res.* **1998,** *31*, 172-180.
6. Haldar, D.; Jiang, H.; Leger, J.-M.; Huc, I. *Angew. Chem., Int. Ed.* **2006,** *45*, 5483-5486.
7. Stryer, L. *Biochemistry*, 4th ed.; W. H. Freeman and Company: New York, 2000.
8. Vermeulen, A.; McCallum, S.; Pardi, A. *Biochemistry* **2005,** *44*, 6024-6033.
9. van Holde, K. E.; Johnson, W. C.; Ho, P. S. *Principles of Physical Biochemistry*, 1st ed.; Prentice-Hall: Upper Saddle River, 1998.
10. Jonker, H.; Wechselberger, R.; Boelens, R.; Folkers, G.; Kaptein, R. *Biochemistry* **2005,** *44*, 827-839.
11. Socolich, M.; Lockless, S.; Russ, W.; Lee, H.; Gardner, K.; Ranganathan, R. *Nature* **2005,** *437*, 512-518.
12. Kelly, J. *Nature* **2005,** *437*, 486-487.
13. Chan, H. S.; Dill, K. *Physics Today* **1993**, 24-32.
14. Sanford, A. R.; Yamato, K.; Yang, X.; Yuan, L.; Han, Y.; Gong, B. *Eur. J. Biochem.* **2004,** *271*, 1416-1425.
15. Cheung, M. S.; Finke, J. M.; Callahan, B.; Onuchic, J. N. *J. Phys. Chem. B* **2003,** *107*, 11193-11200.
16. Zhang, A.; Han, Y.; Yamato, K.; Zeng, X. C.; Gong, B. *Org. Lett.* **2006,** *8*, 803-806.
17. Garric, J.; Leger, J.-M.; Huc, I. *Angew. Chem., Int. Ed.* **2005,** *44*, 1954-1958.
18. Bisson, A. P.; Carver, F. J.; Eggleston, D. S.; Haltiwanger, R. C.; Hunter, C. A.; Livingstone, D. L.; McCabe, J. F.; Rotger, C.; Rowan, A. E. *J. Am. Chem. Soc.* **2000,** *122*, 8856-8868.
19. Nicoll, A. J.; Weston, C. J.; Cureton, C.; Ludwig, C.; Dancea, F.; Spencer, N. S., O. S.; Gunther, U. L.; Allemann, R. K. *Org. Biomol. Chem.* **2005,** *3*, 4310-4315.
20. Baldauf, C.; Gunther, R.; Hofmann, H.-J. *Phys. Biol.* **2006,** *3*, S1-S9.
21. Nelson, J. C.; Saven, J. G.; Moore, J. S.; Wolynes, P. G. *Science* **1997,** *277*, 1793-1796.
22. Tanatani, A.; Mio, M. J.; Moore, J. S. *J. Am. Chem. Soc.* **2001,** *123*, 1792-1793.
23. Zhu, A.; Mio, M. J.; Moore, J.; Drickamer, H. G. *Chem. Phys. Lett.* **2001,** *342*, 337-341.
24. Nishinaga, T.; Tanatani, A.; Oh, K.; Moore, J. S. *J. Am. Chem. Soc.* **2002,** *124*, 5934-5935.
25. Cubberley, M. S.; Iverson, B. L. *J. Am. Chem. Soc.* **2001,** *123*, 7560-7563.
26. Zych, A. J.; Iverson, B. L. *J. Am. Chem. Soc.* **2000,** *122*, 8898-8909.
27. Bushey, M. L.; Nguyen, T.-Q.; Zhang, W.; Horoszewski, D.; Nuckolls, C. *Angew. Chem., Int. Ed.* **2004,** *43*, 5446-5453.

28. Soth, M. J.; Nowick, J. S. *Curr. Opin. Chem. Biol.* **1997,** *1*, 120-129.
29. Violette, A.; Averlan-Petit, M. C.; Semetey, V.; Hemmerlin, C.; Casimir, R.; Graff, R.; Marraud, M.; Briand, J.-P.; Rognan, D.; Guichard, G. *J. Am. Chem. Soc.* **2005,** *127*, 2156-2164.
30. Raguse, T. L.; Lai, J. R.; Gellman, S. H. *J. Am. Chem. Soc.* **2003,** *125*, 5592-5593.
31. Cheng, R. P. *Curr. Opin. Struct. Biol.* **2004,** *14*, 512-520.
32. Semetey, V.; Rognan, D.; Hemmerlin, C.; Graff, R.; Briand, J.-P.; Marraud, M.; Guichard, G. *Angew. Chem., Int. Ed.* **2002,** *41*, 1893-1895.
33. Cuccia, L. A.; Lehn, J.-M.; Homo, J.-C.; Schmutz, M. *Angew. Chem., Int. Ed.* **2000,** *39*, 233-237.
34. Gallant, A. J.; Patrick, B. O.; MacLachlan, M. J. *J. Org. Chem.* **2004,** *69*, 8739-8744.
35. Gallant, A. J.; Yun, M.; Yeung, C. S.; Sauer, M.; MacLachlan, M. J. *Org. Lett.* **2005,** *7*, 4827-4830.
36. Gong, B.; Zeng, H.; Zhu, J.; Yua, L.; Han, Y.; Cheng, S.; Furukawa, M.; PArra, R. D.; Kovalevsky, A. Y.; Mills, J.; Skrzypczak-Jankun, E.; Martinovic, S.; Smith, R.; Zheng, C.; Szypersky, T.; Zheng, X. *Proc. Natl. Acad. Sci. U. S. A.* **2002,** *99*, 11583-11588.
37. Gong, B. *Chem. Eur. J.* **2001,** *7*, 4336-4342.
38. Yuan, L.; Sanford, A.; Feng, W.; Zhang, A.; Zhu, J.; Zeng, H.; Yamato, K.; Li, M.; Ferguson, J.; Gong, B. *J. Org. Chem.* **2005,** *70*, 10660-10669.
39. Hamuro, Y.; Geib, S. J.; Hamilton, A. D. *J. Am. Chem. Soc.* **1996,** *118*, 7529-7541.
40. Hamuro, Y.; Geib, S. J.; Hamilton, A. D. *J. Am. Chem. Soc.* **1997,** *119*, 10587-10593.
41. Berl, V.; Huc, I.; Khoury, R. G.; Krische, M. J.; Lehn, J.-M. *Nature* **2000,** *407*, 720-723.
42. Maurizot, V.; Linti, G.; Huc, I. *Chem. Commun.* **2004,** *2004*, 924-925.
43. Sinkeldam, R. W.; van Houtem, M.; Koeckelberghs, G.; Vekemans, J.; Meijer, E. W. *Org. Lett.* **2006,** *8*, 383-385.
44. van Gorp, J.; Vekemans, J.; Meijer, E. W. *Chem. Commun.* **2004**, 60-61.
45. Tang, H.; Doerksen, R. J.; Tew, G. N. *Chem. Commun.* **2005**, 1537-1539.
46. Corbin, P. S.; Zimmerman, S. C. *J. Am. Chem. Soc.* **2000,** *122*, 3779-3780.
47. Corbin, P. S.; Zimmerman, S. C.; Thiessen, P. A.; Hawryluk, N. A.; Murray, T. J. *J. Am. Chem. Soc.* **2001,** *123*, 10475-10488.
48. Pedersen, C. J. *J. Am. Chem. Soc.* **1967,** *89*, 7017.
49. Hanan, G. S.; Lehn, J.-M.; Kyritsakas, N.; Fischer, J. *J. Chem. Soc., Chem. Commun.* **1995**, 765-766.
50. Baranovski, V. I.; Sizova, O. V. *Chem. Phys. Lett.* **1999,** *315*, 130-134.
51. Katritzky, A. R. *Handbook of Heterocyclic Chemistry*, 1st ed.; Pergamon Press Ltd.: Oxford, 1985.
52. Ribeiro da Silva, M.; Miranda, M. S.; Vaz, C. M. V.; Matos, M. A. R.; Acree, W. E. *J. Chem. Thermodyn.* **2005,** *37*, 49-53.
53. Akochi-K, E.; Alli, I.; Kermasha, S. *J. Agric. Food Chem.* **1997,** *45*, 3368-3373.
54. Pieterse, K.; Vekemans, J.; Kooijman, H.; Spek, A. L.; Meijer, E. W. *Chem. Eur. J.* **2000,** *6*, 4597-4603.

55. Heirtzler, F.; Neuburger, M.; Kulike, K. *J. Chem. Soc., Perkin Trans. 1* **2002,** 809-820.
56. Seneviratne, D. S.; Uddin, J.; Swayambunathan, V.; Schlogel, H. B.; Endicott, J. F. *Inorg. Chem.* **2002,** *41*, 1502-1517.
57. Gallou, I.; Eriksson, M.; Zeng, X.; Senanayake, C.; Farina, V. *J. Org. Chem.* **2005,** *70*, 6960-6963.
58. Hoang, J. B.Sc. Honours, *Towards Chiral Induction of Urea Linked, Pyrimidine-based, Helical Foldamers*, Concordia University, **2005** 47.
59. Saravanakumar, S.; Kindermann, M. K.; Kockerling, M. *Chem. Commun.* **2006,** 640-642.
60. Dolain, C.; Leger, J.-M.; Delsuc, N.; Gornitzka, H.; Huc, I. *Proc. Natl. Acad. Sci. U. S. A.* **2005,** *102*, 16146-16151.
61. Bied, C.; Moreau, J. J. E.; Man, M. W. C. *Tetrahedron: Asymmetry* **2001,** *12*, 329-336.
62. Scortanu, E.; Hitruc, E. G.; Caraculacu, A. A. *Eur. Polym. J.* **2003,** *39*, 1051-1061.
63. Bowser, J. R.; Williams, P. J.; Kurz, K. *J. Org. Chem.* **1983,** *48*, 4111-4113.
64. Oishi, Y.; Kakimoto, M.; Imai, Y. *Macromolecules* **1988,** *21*, 547-550.
65. Oishi, Y.; Kakimoto, M.; Imai, Y. *Macromolecules* **1987,** *20*, 703-704.
66. Lozano, A. E.; de Abajo, J.; de la Campa, J. *Macromol. Theory Simul.* **1998,** *7*, 41-48.
67. Lozano, A. E.; Abajo, J. d.; De la Campa, J. *Macromolecules* **1997,** *30*, 2507-2508.
68. Smith, R. A.; Barbosa, J.; Blum, C. L.; Bobko, M. A.; Caringal, Y. V.; Dally, R.; Johnson, J. S.; Katz, M. E.; Kennure, N.; Kingery-Wood, J.; Lee, W.; Lowinger, T. B.; Lyons, J.; Marsh, V.; Rogers, D. H.; Swartz, S.; Walling, T.; Wild, H. *Bioorg. Med. Chem. Lett.* **2001,** *11*, 2775-2778.
69. Sudha, L. V.; Sathyanarayana, D. N. *J. Mol. Struct.* **1985,** *131*, 141-146.
70. Sudha, L. V.; Sathyanarayana, D. N.; Bharati, S. N. *Magn. Reson. Chem.* **1987,** *25*, 474-479.
71. Lambert, J. B.; Mazzola, E. P. *Nuclear Magnetic Resonance Spectroscopy*, 1st ed.; Pearson Prentice Hall: Upper Saddle River, 2004.
72. Heinz, T.; Rudkevich, D. M.; Rebek, J. *Nature* **1998,** *394*, 764-766.
73. Korner, S. K.; Tucci, F. C.; Rudkevich, D. M.; Heinz, T.; Rebek, J. *Chem. Eur. J.* **2000,** *6*, 187-195.
74. Saito, S.; Nuckolls, C.; Rebek, J. *J. Am. Chem. Soc.* **2000,** *122*, 9628-9630.
75. Amaya, T.; Rebek, J. *J. Am. Chem. Soc.* **2004,** *126*, 6216-6217.
76. McClellan, A. L. *Tables of Experimental Dipole Moments*; W. H. Freeman and Company: San Francisco, 1963.
77. Quesada, R.; Gale, P. A. *Annu. Rep. Prog. Chem., Sect. B: Org. Chem.* **2005,** *101*, 148-170.
78. Petitjean, A.; Cuccia, L. A.; Lehn, J.-M.; Nierengarten, H.; Schmutz, M. *Angew. Chem., Int. Ed.* **2000,** *41*, 1195.
79. Odriozola, I.; Kyritsakas, N.; Lehn, J.-M. *Chem. Commun.* **2004,** *2004*, 62-63.
80. Chang, J. Y.; Do, S. K.; Han, M. J. *Polymer* **2001,** *42*, 7589-7594.
81. Seo, S. H.; Kim, Y.-W.; Chang, J. Y. *Macromolecules* **2005,** *38*, 1525-1527.

82. Xing, L. M.Sc., *Synthesis of Heterocyclic Macrocycles and Folding Oligomers*, Concordia University, **2005** 193.
83. Xing, L.; Ziener, U.; Sutherland Todd, C.; Cuccia Louis, A. *Chem. Commun.* **2005**, 5751-5753.
84. *Personal Communcation (Liyan Xing).*
85. Noelting, E.; Thesmar, G. *Chem. Ber.* **1902**, 628-650.
86. Morgan, G. T. *J. Am. Chem. Soc.* **1902**, 86-100.
87. Peng, X.; Suzuki, H. *Org. Lett.* **2001,** *3*, 3431-3434.
88. Crossley, A. W.; Renouf, N. *Proc. Chem. Soc.* **1908**, 202-215.
89. Noelting, E.; Braun, A.; Thesmar, G. *Chem. Ber.* **1901**, 2242-2253.
90. Kanetani, F.; Yamaguchi, H. *Bull. Chem. Soc. Jpn.* **1981,** *54*, 3048-3058.
91. Norman, R. O. C.; Radda, G. K. *J. Chem. Soc.* **1961**, 3030-3037.
92. Moodie, R. B.; Thomas, P. N.; Schofield, K. *J. Chem. Soc., Perkin Trans. 2* **1977**, 1693-1705.
93. Suzuki, H.; Tatsumi, A.; Ishibashi, T.; Mori, T. *J. Chem. Soc., Perkin Trans. 1* **1995**, 339-343.
94. Voyksner, R. D.; Straub, R.; Keever, J. T. *Environ. Sci. Technol.* **1993,** *27*, 1665-1672.
95. Bermes, R.; Keilhauer, H., BASF Aktiengesellschaft, United States Patent, *5,424,403*, **1995**
96. Furniss, B. S.; Hannaford, A. J.; Smith, P. W. G.; Tatchell, A. R. *Vogel's Textbook of Practical Organic Chemistry*, 5th ed.; Prentice Hall: London, 1996.
97. Majer, P.; Randad, R. S. *J. Org. Chem.* **1994,** *59*, 1937-1938.
98. Albrecht, M.; Witt, K.; Frohlich, R.; Kataeva, O. *Tetrahedron* **2002,** *58*, 561-567.
99. Boehme, F.; Kunert, C.; Komber, H.; Voigt, D.; Friedel, P.; Khodja, M.; Wilde, H. *Macromolecules* **2002,** *35*, 4233-4237.
100. Azad, S.; Kumamoto, K.; Uegaki, K.; Ichikawa, Y.; Kotsuki, H. *Tetrahedron Lett.* **2006,** *47*, 587-590.
101. Mastsumura, Y.; Satoh, Y.; Onomura, O.; Maki, T. *J. Org. Chem.* **2000,** *65*, 1549-1551.
102. Chong, P. Y.; Petillo, P. A. *Org. Lett.* **2000,** *2*, 2113-2116.
103. Kruijtzer, J. A. W.; Lefeber, D. J.; Liskamp, R. M. J. *Tetrahedron Lett.* **1997,** *38*, 5335-5338.
104. Raju, B.; Kassir, J. M.; Kogan, T. P. *Bioorg. Med. Chem. Lett.* **1998,** *8*, 3043-3048.
105. Wiszniewska, A.; Kunce, D.; Chung, N. N.; Schiller, P. W.; Izdebski, J. *Lett. Pept. Sci.* **2003,** *10*, 33-39.